TU Delft

bt projects
innovative renewable energy

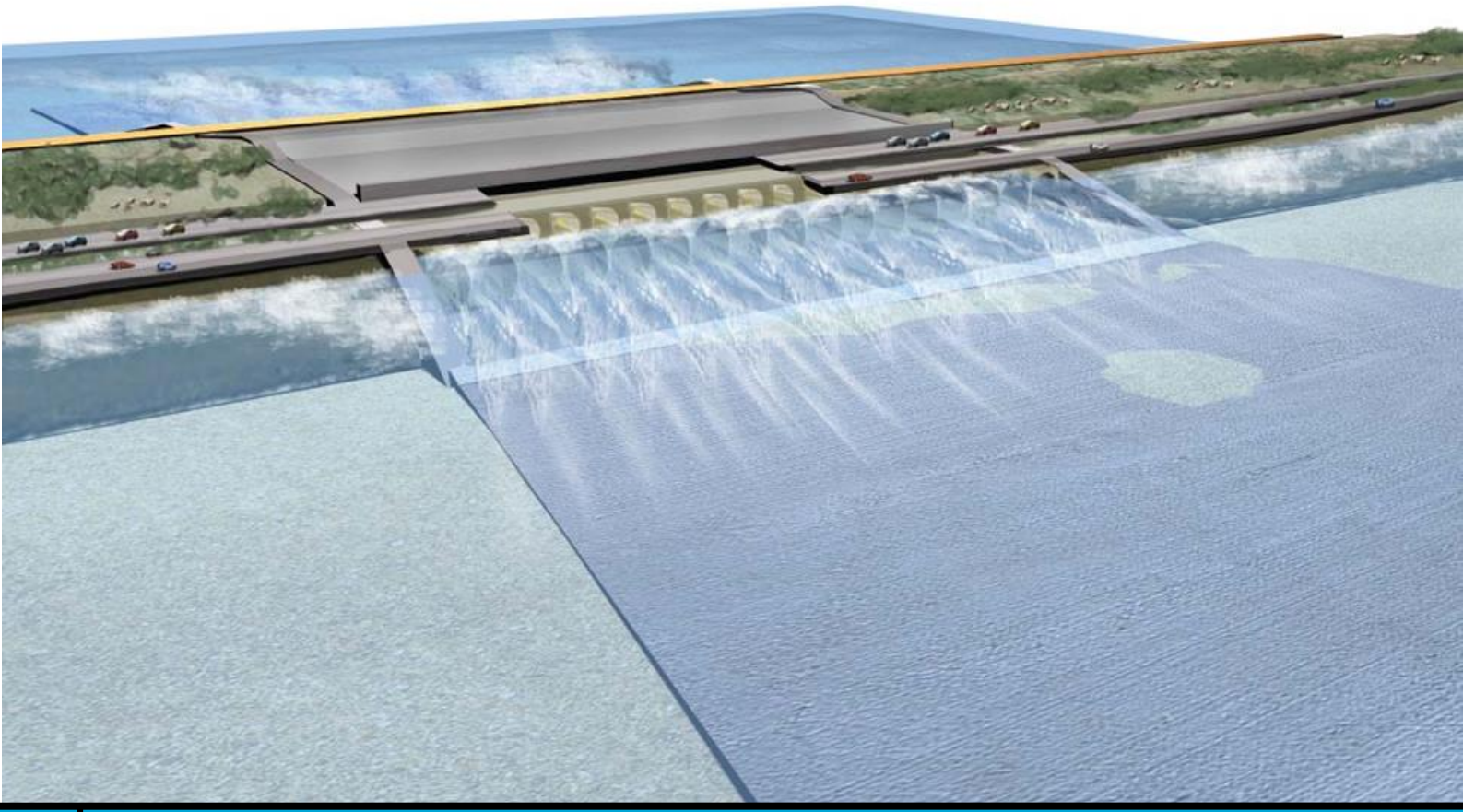

The consideration of constrained flow solutions for the purpose of implementing a tidal power plant in the Brouwersdam reconnecting Lake Grevelingen and the North Sea

R. de Visser

Delft University of Technology
2019

Cover illustration retrieved from Getij Grevelingen (2018)

The consideration of constrained flow solutions for the purpose of implementing a tidal power plant in the Brouwersdam reconnecting Lake Grevelingen and the North Sea

By

R. de Visser

in partial fulfilment of the requirements for the degree of

Master of Science
in Offshore & Dredging Engineering

at the Delft University of Technology,
to be defended publicly on Wednesday August 28th, 2019 at 11:00 AM.

Supervisor:	Dr. ir. A. Jarquin Laguna	
Thesis committee:	Prof. dr. A.V. Metrikine,	TU Delft
	Dr. ir. A. Jarquin Laguna,	TU Delft
	Ir. V.S. Maniyara	BT-Projects

TU Delft

bt projects
innovative renewable energy

This master thesis is dedicated to my father, Hans de Visser, who is no longer with us, who has taught me the first principles of engineering, and to my mother, Karin de Visser, who taught me to keep moving forward, not matter what.

Abstract

After the construction of the Grevelingendam (1965) and Brouwersdam (1971), the tidal movement in Lake Grevelingen disappeared. This caused a deterioration of ecological parameters influencing the surrounding flora and fauna and consequently a decline of the water quality set in. Amongst others, Rijkswaterstaat and the provinces of Zeeland and South-Holland aim to reconnect Lake Grevelingen with the North Sea to infuse oxygen enriched water into the lake and reintroduce an attenuated tide in the lake, thereby improving the quality of the local ecology. To reach the desired water quality, culverts will be installed in the Brouwersdam, thereby restoring the connection between the two water bodies. As part of an integrated approach, Rijkswaterstaat intends to implement turbines into the culverts to not only generate power, but also perform water management.

The conclusion from the literature study is that implementation of constrained flow devices, wherein the entire mass flow is guided through the turbine, is preferred as these turbines are able to modulate discharge through the tidal barrage. Moreover, constrained flow devices have a higher theoretical power output than the other considered hydropower methods applicable in a tidal barrage. In order to broaden the insight into the behaviour of the water level in Lake Grevelingen, due to the construction of the tidal barrage, three hydraulic configurations are evaluated wherein input water level data from the North Sea is used to model the tidal variation in the lake while simultaneously estimating the energy output of the system. Considering a culvert array of 18 culverts, measuring 8 m by 8 m, the first considered case takes into account 11 of the culverts equipped with unidirectional turbines, while the remaining culverts are unequipped. The second case involves all 18 culverts with unidirectional turbines, while the third case is set up with 18 bidirectional devices.

Additionally, to provide a larger view on the possibilities, a multivariable analysis of the three cases is carried out wherein power generation and water management requirements are considered. Herein varying the cross-sectional area of the culverts and their numbers, though, for the configuration consisting of equipped and unequipped culverts, also the number of empty culverts is varied. From these analyses, one can conclude that installing unequipped culverts and unidirectional turbines in the array will diminish the controllability, whereas bidirectional turbines increase the controllability of the flow which is desirable.
Furthermore, full time turbine modulation, wherein the turbines are not generating the optimal amount of power over the full scope of the tidal range for the purpose of water management is preferred over intermittent turbine modulation, wherein turbine modulation only occurs when the water level surpass certain water levels, because the turbines can be altered continuously, which increases the controllability of the discharge.
Nevertheless, for the culvert arrays with bidirectional turbines applies that the required values of the monthly averaged and maximum tidal ranges are insufficient. Even though, the water level in Lake Grevelingen does not exceed the overshoot/undershoot boundaries, established by Rijkswaterstaat, the entire vision of water management is only partially fulfilled due to the lack of amplitude in the tidal range.

The study concludes with the selection of the following culvert array existing of 24 culverts measuring 9 m by 9 m executed with bidirectional turbines. From an economic feasibility study, wherein, amongst other involved parameters, an installed capacity of 36 MW, a market price of electricity of € 0.13 per kilowatt hour for the first 15 years and € 0.049 per kilowatt hour for the second 15 years and a loan period of 15 years, follows a payback period of 15 years and a levelised cost of energy value of € 0.058 per kilowatt hour.

Acknowledgements

Throughout the final part of my education I have received a great deal of support and assistance. First, I would like to thank my corporate supervisor, Vineeth Maniyara, who helped me through the journey of writing my master thesis. Without his expertise, dedication and endurance, I could not have accomplished this.

Secondly, the advice given by my academic supervisors, dr. A. Jarquin Laguna and prof. dr. A.V. Metrikine, during the progress meetings has been a great help and is highly appreciated. Thereafter, my gratitude goes out to Menno Broers and my colleagues at BT Projects for the opportunity they gave me to write my master thesis there and I wish them all the best in the future endeavors of BT Projects.

Also, I cannot thank my friends and family enough, who always had a sympathetic ear, as well as providing happy distraction to rest my mind outside of my research. Finally, my mother deserves a special mention, as she always believed in me. Even when times were rough, she was the anchor in the storm.

R. de Visser
Delft, August 2019

Contents

List of Symbols & Abbreviations

β	*Betz*-factor	[-]
Δh	Hydraulic head, difference between North Sea water level and Lake Grevelingen water level	[m]
Δh_Q	Hydraulic head used for flow	[m]
Δh_T	Hydraulic head extracted by turbine	[m]
Δt	Timestep in water level datafile	[min]
ε	Roughness height of culvert wall	[m]
ϵ	Dimensionless turbine cross-section	[-]
ζ	Ratio between maximal harvestable power of confined free flow and maximal harvestable power of constrained flow	[-]
ν	Kinematic viscosity of fluid	[m^2/s]
ρ	Density of fluid	[kg/m^3]
τ	Time period	[yrs]
a	Acceleration	[m/s^2]
AEY	Annual Energy Yield	
A	Cross-sectional area of flow	[m^2]
A_c	Cross-sectional area of duct	[m^2]
A_{LG}	Superficial area of Lake Grevelingen	[m^2]
A_T	Cross-sectional area of turbine	[m^2]
A_0	Cross-sectional area of culvert	[m^2]
A_1	Cross-sectional area just behind turbine	[m^2]
A_2	Cross-sectional area of bypass flow	[m^2]
BTPP	Brouwersdam Tidal Power Plant	
b	Vertical intersection of degree of reaction graph	[-]
CPB	Netherlands Bureau for Economic Policy Analysis	
C_{sys}	System los coefficient	[-]
$C_{sys,t}$	System los coefficient when accounted for turbine installation	[-]
C_{tot}	Total costs of investment	[€]
$c_{p,CF}$	Coefficient of power in constrained flow scenario	[-]
$c_{p,CFF}$	Coefficient of power in confined free flow scenario	[-]
$c_{p,FF}$	Coefficient of power in free flow scenario	[-]
D_h	Hydraulic diameter	[m]
d_{bp}	Thickness of bottom protection	[m]
ECN	Energy Centre the Netherlands	
E	Energy yield by turbine	[J], [Wh]
E_τ	Electrical energy generated in year τ	[J], [Wh]
E_{kin}	Kinetic energy in the water	[J]

E_{pot}	Potential energy in the water	[J]
FLH	Full Load Hours	
FTM	Fulltime turbine Modulation	
F	Force	[N]
f	Degree of reaction of turbine	[-]
f_f	*Darcy* friction factor	[-]
g	Gravitational acceleration	[m/s^2]
H	Enthalpy	[J]
h	Height of culvert	[m]
h_f	Energy height dissipation term due to friction	[m]
h	Height of culvert floor	[m]
h_L	Energy height dissipation term in *Bernoulli* equation	[m]
h_{max}	Maximum culvert height	[m]
IRR	Internal Rate of Return	
ITM	Intermittent Turbine Modulation	
I_τ	Investment expenditures in year τ	[€]
i	Number of iteration steps	[-]
j	Slope of degree of reaction signal	[1/s]
K_c	Loss coefficient due to culvert entrance dissipation	[-]
K_e	Loss coefficient due to culvert exit dissipation	[-]
K_f	Loss coefficient due to wall friction in culvert	[-]
K_L	Loss coefficients due to dissipation mechanisms	[-]
L	Number of tidal cycles within a month	[-]
l	Length of the culvert	[m]
LCoE	Levelised Cost of Energy	
M	Number of empty culverts	[-]
M_τ	Operation and maintenance expenditures in year τ	[€]
m	Mass	[kg]
$\dot{m}$	Mass flow	[kg/s]
N	Number of culverts	[-]
n	Number of timesteps in data file	[-]
NAP	Amsterdam Ordnance Datum, vertical water level reference datum	
NPV	Net Present Value	
O	Circumference of culverts	[m]
OS	Overshoot percentage	[%]
P	Generated power	[W]
$\bar{P}$	Mean generated power	[W]
P_{CF}	Theoretical harvestable power in constrained flow scenario	[W]

P_{CFF}	Theoretical harvestable power in confined free flow scenario	[W]
P_{FF}	Theoretical harvestable power in free flow scenario	[W]
P_{fluid}	Theoretical power present in the fluid	[W]
P_{max}	Maximum generated power	[W]
PBP	Payback period	
p	Hydraulic pressure	[Pa]
p_0	Free stream pressure	[Pa]
p_2	Pressure in bypass flow	[Pa]
p_3	Downstream pressure	[Pa]
Q	Discharge through culvert	[m^3/s]
Q_e	Discharge through empty culvert	[m^3/s]
Q_t	Discharge through culvert equipped with turbine	[m^3/s]
q	Discount rate	[%]
R	Net cash flow per year	[€/yr]
R_τ	Net cash inflow/outflow in year τ	[€/yr]
Re	*Reynolds* number	[-]
r	Dimensionless turbine velocity	[-]
SDE+	Stimulation arrangement Sustainable Energy	
s	Covered distance	[m]
t	Time	[s]
t_B	Bounding time	[s]
t_c	Duration of one tidal cycle	[s]
T	Number of years	[-]
T_{exp}	Expected lifetime	[yrs]
T_r	Tidal range	[m]
$T_{r,max}$	Maximum tidal range	[m]
$\overline{T_r}$, $T_{r,mean}$	Mean tidal range	[m]
US	Undershoot percentage	[%]
u	Flow velocity in direction of the flow through the culvert	[m/s]
u_0	Free stream velocity	[m/s]
u_1	Flow through the turbine	[m/s]
u_2	By-pass flow velocity around the turbine	[m/s]
u_T	Flow velocity through the turbine	[m/s]
V	Volume	[m^3]
W	Work	[Nm]
w	Width of culvert	[m]
w_{tot}	Total width of tidal power plant	[m]
w_{wall}	Width of culvert wall	[m]

WL_{NS}	Water level in North Sea	[m]
WL_{LG}	Water level in Lake Grevelingen	[m]
$\widehat{WL}_{LG}$	Maximum water level in Lake Grevelingen	[m]
$\widetilde{WL}_{LG}$	Minimum water level in Lake Grevelingen	[m]
$WL_{LG,max}$	Upper limiting water level in Lake Grevelingen	[m]
$WL_{LG,min}$	Lower limiting water level in Lake Grevelingen	[m]
WL_P^+	Upper precautious water level	[m]
WL_P^-	Lower precautious water level	[m]
z	Potential head in *Bernoulli* equation	[m]
Z	Total number of data points in dataset	[-]

List of Figures

List of Tables

1 Introduction

'De zoute zee slaakt een diepe zilte zucht.
Boven het vlakke land trilt stil de warme lucht…'
Aan de kust - Bløf

1.1 Posing of the problem

The former estuary, *Brouwershavensche Gat*, located between the islands of *Schouwen-Duiveland* and *Goeree-Overflakkee*, was isolated from its surrounding waters as part of the famous Delta works. This isolation initially started by constructing the Grevelingendam in 1965, followed by the Brouwersdam in 1971 (Bezuyen, Stive, Vaes, Vrijling, & Zitman, 2011). The lake that came into existence was called Lake Grevelingen and became the largest saltwater lake of Western Europe. Figure 1 depicts a topographical map of the considered area.

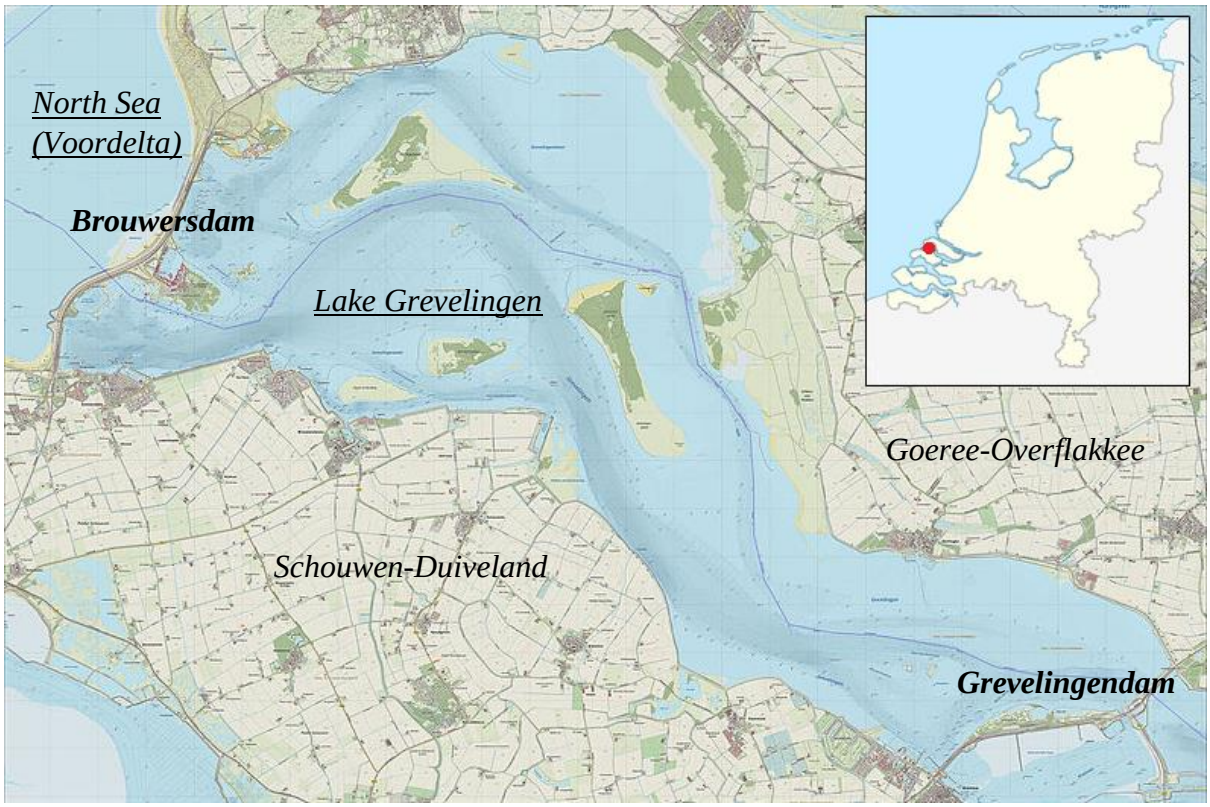

Figure 1: Topographic overview of Lake Grevelingen and its surroundings (Open Topografie Nederland, 2018).

With the isolation of Lake Grevelingen, the tidal effects in the lake disappeared and caused a slow conversion to a freshwater environment. This conversion had a large impact on the local flora and fauna. To counteract this freshwater inflow, installment of a sluice gate was a necessity. The Brouwerssluis was deployed in 1978 in the southern part of the Brouwersdam and Lake Grevelingen was reconnected with the North Sea again.

In the present day, in spite of the Brouwerssluis letting in water, there is still a decline of ecological parameters. To stay in line with the European Water Framework Directive regulations, Rijkswaterstaat, together with municipalities, corporate parties and research institutes, is planning to construct culverts in the Brouwersdam to reintroduce an attenuated tide to Lake Grevelingen and infuse oxygen enriched water into the lake (Tidal Grevelingen

Project, 2018). This tidal movement should result in an improvement of the local ecosystem. To realise this ecological improvement, the attenuated tide is found to be effective at a tidal range oscillating between *-0.45* m NAP and *+0.05* m NAP.
To integrate water level control and energy harness in Lake Grevelingen, initiatives exist to implement turbines in the culverts, which not only harness energy from the water flow, but are also used for controlling the in- and outflow of water into the lake or North Sea (Tidal Grevelingen Project, 2018).

1.2 Brouwersdam

The Brouwersdam is a *6*.5 km long water barrier connecting the island of *Goeree*-Overflakkee in the north and *Schouwen-Duiveland* in the south. The planned location of the tidal power plant is set at the northern part of the Brouwersdam. To distinguish locations along the Dutch coast, the coast is divided into segments by section lines. Tidal Grevelingen Project (2018) states that the tidal power plant needs to be constructed between section lines 2120 and 1975 as depicted in Figure 2. According to the current plans, the tidal power plant will be constructed between section lines 2120 and 2020.

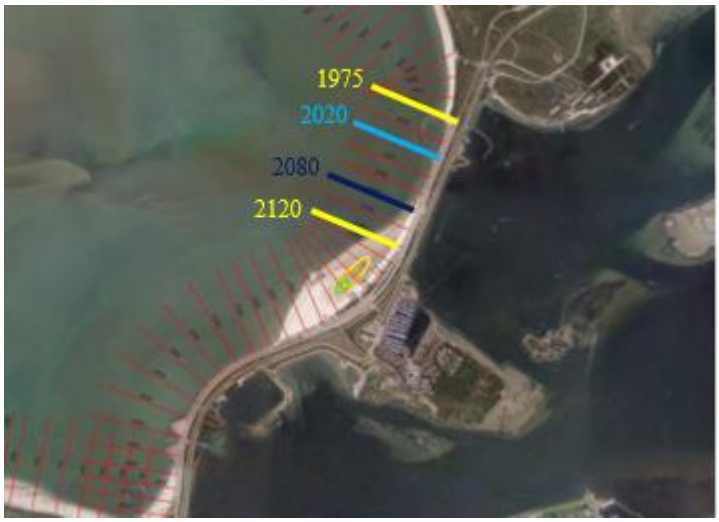

Figure 2: Location of the section lines between which the tidal power plant must be constructed (Tidal Grevelingen Project, 2018).

At the time of the construction, two closure gaps where formed in the northern and southern part of the dam to guide the water in a controllable manner. Later, the southern closure gap was closed with concrete blocks, while the northern closure gap was sealed by concrete passage caissons. These passage caissons are situated within the set section line range. The caissons measure *18* m x *16.2* m x *68* m (*l* x *h* x *w*) each and are submerged at a depth of *-10.00* m NAP on top of a bed consisting of rip-rap filter layers (Mooyaart & van den Noortgaete, 2010). A cross-section of the Brouwersdam at approximately section line *2080* (marked in Figure 2) is depicted in Figure 3.

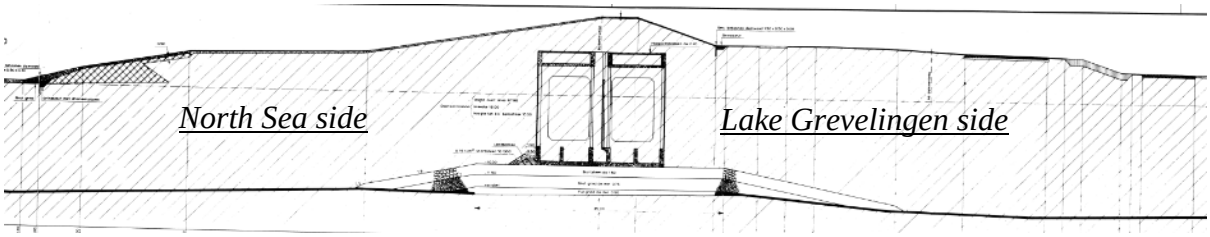

Figure 3: Cross-section of the Northern closure gap at approximately section line 2080 with the North sea on the left and Lake Grevelingen on the right (Rijkswaterstaat, 1971).

Besides the water retaining function of the Brouwersdam, the dam also has infrastructural function. The Brouwersdam provides a connection from the island of *Schouwen-Duiveland* and *Goeree-Overflakkee* through provincial road N57, a bicycle path, pedestrian walkways and a steam tram. Furthermore, Brouwersdam has many recreational purposes, including a beach, a marina and food service industry.

1.3 Surrounding waters

1.3.1 Lake Grevelingen

As mentioned before, Lake Grevelingen arose after the construction of the Deltaworks. The lake is announced to be a Natura 2000 natural reserve. Natura 2000 is a European network of natural reserves. In Natura 2000 areas, species and their natural habitat are protected to conserve the biodiversity. Moreover, the lake has an average water depth of *5.4* m, a maximum water depth of *48* m and a surface area of *110* km^2. The current still water level is at *-0.20* m NAP. At the deeper parts of the lake, oxygen rich water hardly appears, which started the growth of white bacteria mats at the lakebed, as can be seen in Figure 4. These bacteria consume the already scarce amount of oxygen, which deteriorates the current ecological state of the lake (Tidal Grevelingen Project, 2018).

Figure 4: White bacteria colonies caused by lack of oxygen enriched water at the bed of Lake Grevelingen (Tidal Grevelingen Project, 2018).

A number of tidal flats appear in the lake. These tidal flats are an important place for flora and fauna: The tidal flats harbour a variety of special plant species and function as a resting and mating place for seals and a large number of bird species. These tidal flats are also covered by the Natura 2000 legislation. Additionally, Lake Grevelingen is a popular place for boat owners, divers and wind surfers.

1.3.2 Voordelta

The part of the North Sea, where the Brouwersdam borders on, is also known as the Voordelta. The Voordelta is a shallow part of the North Sea containing multiple mud flats. Like Lake Grevelingen, the Voordelta is also entitled as a Natura 2000 area. Also, the mud flats in the Voordelta accommodate different species which must be conserved.

1.4 Research approach

1.4.1 Research questions

Enlisted below, the main research question with its component sub questions is phrased.

‘’How could the bi-directional flow profile at the Brouwersdam be guided through the system in such a way that the water management is satisfied while ensuring critical factors like power generation and economic feasibility are suitably addressed?’’

With the corresponding sub questions:

1. What are the dimensional, hydraulic and environmental constraints which describe the Brouwersdam tidal power plant system?
2. What are the critical markers identified to evaluate each of the three design parameters within the Brouwersdam design process?
3. Which design options can be considered to be viable and what are their disadvantages and advantages?

The first goal that has to be resolved is establishing an evaluation template which outlines the critical physical parameters of the Brouwersdam system and their constraint values. The evaluation template also serves a larger goal when considering design concepts outside of the scope of this master thesis. This evaluation template is envisioned to answer sub questions 1 and 2. The evaluation template also acts as a foundation from which the design methodology can be developed. Furthermore, the state of the art methods of harnessing energy through turbines will be regarded and their differences, application and (dis)advantages are discussed.

The design methodology describes the approach of implementing the elements mentioned in the evaluation template upon a design concept. In order to arrive at concepts that fulfill the constraint parameters of the Brouwersdam tidal power plant project. These design concepts are to be evaluated and concluded upon, thereby fulfilling sub question 3, in the design concept evaluation. These design concepts are chosen to explore a larger area of the design landscape and therefore includes different culvert parameters. With this amassed information of the tidal power plant Brouwersdam, one may draw conclusions on future work.

1.4.2 Process description

The research process is divided into three stages. In stage 1, a literature study will be executed wherein the governing aspects of the construction and environment, water management, power generation and economics with regard to the Brouwersdam tidal power plant is studied in detail. Based on this study, an evaluation template for the Brouwersdam tidal power plant will be built. This evaluation template is envisioned as a framework, which contains critical parameters and physical system constraints. Furthermore, the state of the art will be evaluated, wherein the current technology is considered. The review on the state of the art will produce a number of design concepts that are evaluated. The information gathered in the evaluation template and state of the art review will fuel the design methodology. The design methodology describes the approach of further developing of the design concepts.

In stage 2, the water management and energy extraction of the three design concepts are

considered with a fixed number of culverts and a fixed cross-sectional area of the culvert, better known as the invariant culvert configuration. These concepts are established by first considering a simple case and subsequently add layers of resolution to approach reality. Moreover, the critical parameters are determined to mirror their behaviour to the posed requirements. After that, the multivariable culvert configuration phase starts, wherein the behaviour of the three concepts of the tidal power plant and its surrounding waters are analysed when the number of culverts and their dimensions is varied. Parameters influencing the water management and power generation aspects are considered and an overview of the influence of the variation of culvert numbers and the culvert dimensions can be set up. Then an economical analysis will provide an investment cost report, which will feed into a feasibility study combined with the power generation and energy yield. Finally, in stage 3, the results will be examined and conclusions will be drawn. These conclusions will induce recommendations from which future work can be carried out.

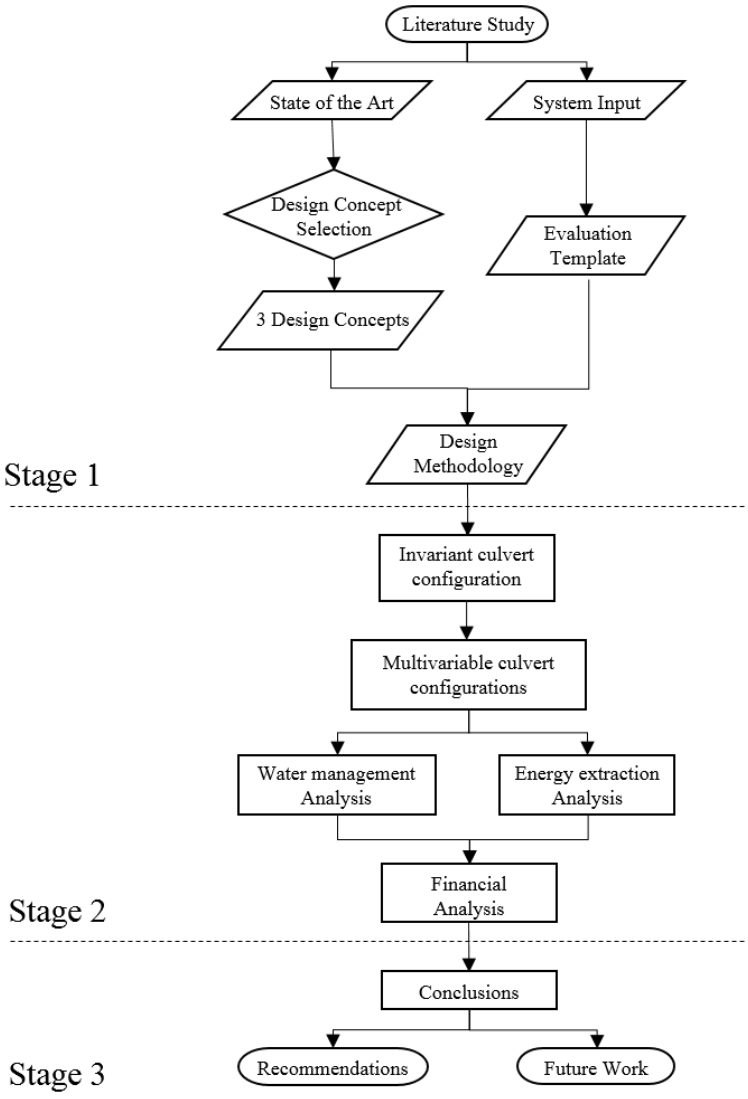

Figure 5: Process flow chart.

1.4.3 Evaluation template

the evaluation template contains criteria to which designs of the culverts in the Brouwersdam tidal power plant should comply with. These criteria are divided into four categories: The Brouwersdam layout, power generation, water management and economics.

1.4.3.1 *Brouwersdam*

Properties of the current Brouwersdam construction are coming from drawings and literature, mostly made available by Rijkswaterstaat. Along with the characteristics at the current Brouwersdam construction. Dimensional properties of the tidal power plant are largely accessed by the most recent market consultation document, research documents and turbine manufacturers.

1.4.3.1.1 Project demarcation with respect to Brouwersdam layout

The location of the Brouwersdam tidal power plant is fixed to the northern part of the Brouwersdam, between island *Goeree-Overflakkee* and *Kabbelaarsbank*. To be precise: between section lines 2120 and 1975.

1.4.3.2 *Water management*

The water management section is separated into two elements: flood risk safety and flow control. Flood risk safety depends on the probability of occurrence of a storm more severe than the design storm of the storm surge barrier. Also, the stability and strength of the Brouwersdam are parameters that have their effect on the flood risk safety.
Regarding flow control, Tidal Grevelingen Project (2018) states that the water level fluctuation at Lake Grevelingen must lie between *-0.45* m NAP and *+0.05* m NAP.Besides, the monthly averaged tidal range and monthly maximum tidal range must have a value of consecutively *0.40* m and *0.50* m. To convey the fluid volume through the passage, the controlling factors are the total discharge area, the discharge time and the discharge velocity which accordingly relies on the water head difference and system resistances to flow. The total discharge area is linked to the height and width of a single culvert and the amount of the culverts to be constructed in the Brouwersdam. The material, length and shape of the culverts also contribute to this. The degree of reaction of the device represents the distribution of energy consumed by the turbine to extract energy and the energy that is used to induce flow rate. Section 2.1.2 elaborates more on the definition of the degree of reaction. By adjusting this degree of reaction, the discharge can be altered. The integration of water management and power generation will be established by varying the degree of reaction.

1.4.3.2.1 Project demarcation with respect to water management

To preserve the water retaining function of the Brouwersdam, the strength and stability of the Brouwersdam must be maintained. The aim of the project has a more hydraulic sense rather than a structural one. Therefor the flood risk safety of the tidal power plant Brouwersdam is not taken into account.

1.4.3.3 *Power generation*

In order to generate energy from flowing water, essentially a pressure difference is a necessity. In this particular case, this pressure difference is caused by a water level height difference i.e. hydraulic head, between the North Sea and Lake Grevelingen. The pressure gradient induces a volumetric flow which follows the pressure gradient from high to low.

In this process, potential energy is converted into kinetic energy, which then is partly harvested by the turbine. Accordingly, the kinetic energy of the turbine is then converted to electrical energy by means of a generator. To improve the energy yield, one can decrease the hydraulic losses generated by e.g. turbulent motions and wall friction. This influence is represented by the system loss coefficient. Furthermore, different turbine concepts will be considered, wherein their impact on the energy yield is evaluated. Further, the power generation aspect must be in line with the flow control function of the tidal power plant. This means the tidal motion control in Lake Grevelingen is classified with higher priority than the power generation aspect. Therefore, the degree of reaction has to be modified over time, to satisfy the flow control criteria.

1.4.3.4 *Economics*

To supply an insight in the financial picture of the Brouwersdam tidal power plant, a cost estimation will be established. In this estimation, global assessments on the construction of the civil structure, turbines and soil and excavation will be regarded. Combined with the energy yield, the costs and revenue can be mapped out. These parameters help to determine the following key numbers, which can evaluate the economic feasibility: A cash flow statement, The Net Present Value (NPV) with a justified discount rate, the Internal Rate of Return (IRR), the Payback Period (PBP) and the Levelised Cost of Energy (LCoE) (Tidal Grevelingen Project, 2018). The net present value sums up the cash flows over the lifetime cycle of the project with due regard for the time value of the money. When the net present value turns out to be positive, the project is, in principle, beneficial. The internal rate of return is determined by equating the net present value to zero and calculating the corresponding discount rate. The payback period is the period until the net value of the project is exactly zero (Vrijling & Verlaan, 2015). Finally, The levelised cost of energy is an economic valuation of the average total costs to build and operate a power-generating asset over its lifetime, divided by the total energy output of the asset over that lifetime. It can also be regarded as the average minimum price at which electricity must be sold in order to break-even over the lifetime of the project.

1.4.3.4.1 Project demarcation with respect to finances

As stated in Tidal Grevelingen Project (2018), to determine the economic feasibility, Rijkswaterstaat expects a cash flow statement and the values of the following feasibility key numbers: Internal Rate of return, Net Present Value, Payback Period and the Levelised Cost of Energy.

2 Energy harvesting methods

"In theory, there is no difference between theory and practice.
But in practice, there is.''
B. Brewster

In order to generate energy from flowing water using turbines, one can primarily distinguish three types: constrained flow, confined free flow and free flow systems. These types have their specific differences concerning, water management, energy extraction, ecology and finance and find their application in particular segments of the working landscape.

In the case of the Brouwersdam tidal powerplant, the energy extraction is initiated by occurrence of a water level difference between Lake Grevelingen and the North Sea, or vice versa. This water level difference is also known as the hydraulic head. This hydraulic head will induce a movement of the water from high water level to low water level. When a turbine is placed in the flow, the volume flow will drive the turbine, which accordingly drives a generator, wherein mechanical energy is transformed to electrical energy.

2.1 Constrained flow

In a constrained flow method, the total volume stream is forced through the turbine. The water is funnelled towards the turbine through a casing, as can be seen in Figure 6. This method formerly found its application in large hydropower dams, where a high hydraulic head regime occurred. These solutions often impacted the local environment largely. because of the absence of a by-pass flow, i.e. a volume flow wherein no energy is dissipated to the turbine, aquatic organisms are prone to be (lethally) injured, because the probability of being struck by one of the turbine blades is rather large. Fortunately, nowadays turbine manufacturers are developing fish-friendly turbines to diminish the rate of animal harm. On the other hand, due to the absence of by-pass flow, one is capable of regulating the discharge through the culvert up to a certain height by modulating the turbine's properties such that the water dissipates more or less energy to the turbine and the flow rate is controlled.

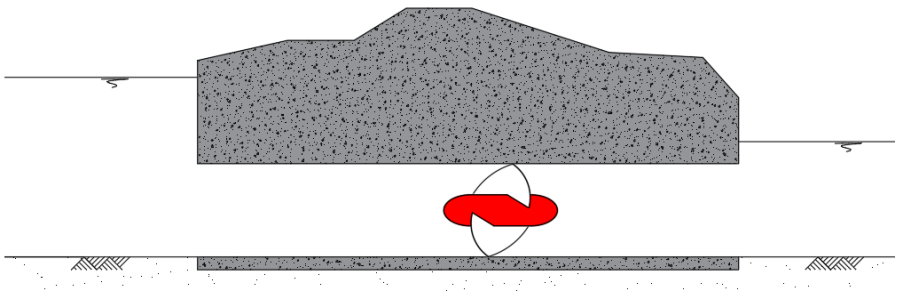

Figure 6: Constrained flow principle.

A well-known example of a constrained flow solution is the La Rance tidal power station. This tidal barrage is located on the estuary of the Rance river, near Saint Malo, Brittany, France and closes of a reservoir with a *22* km^2 surface area. The mean occurring tidal range that occurs is *8.2* m with a maximum of *13.5* m. the maximum flow rate occurring that is created is *9600* m^3/s. The power plant opened in 1966 and has a peak power rating of *240* MW, an average power supply of *96* MW and an annual energy yield (AEY) of approximately *600* GWh. This is established by *24* bulb turbines with a *5.35* m diameter divided over a barrage length of *330* m (Tethys, 2012).

To compare the power extraction capacity of the different principles, the theoretical upper limit of extractable power of the considered types will be determined.

2.1.1 Theoretical upper bound of power generation in a constrained flow device

Fundamentally, power is defined as the rate of doing work per unit time:

$$P = \frac{dW}{dt} = \frac{dFs}{dt} \qquad Eq.\,2.1$$

Assuming force *F* to be constant, this correlates to:

$$P = F\frac{ds}{dt} = Fu \qquad Eq.\,2.2$$

Knowing that force is equal to pressure times area:

$$P = pAu \qquad Eq.\,2.3$$

And cross-sectional area times flow velocity equals discharge:

$$Q = Au \qquad Eq.\,2.4$$

Then, *Bernoulli's* principle is regarded for a streamline through a duct:

$$\rho g z_1 + p_1 + \frac{\rho u_1^2}{2} = \rho g z_2 + p_2 + \frac{\rho u_2^2}{2} \qquad Eq.\,2.5$$

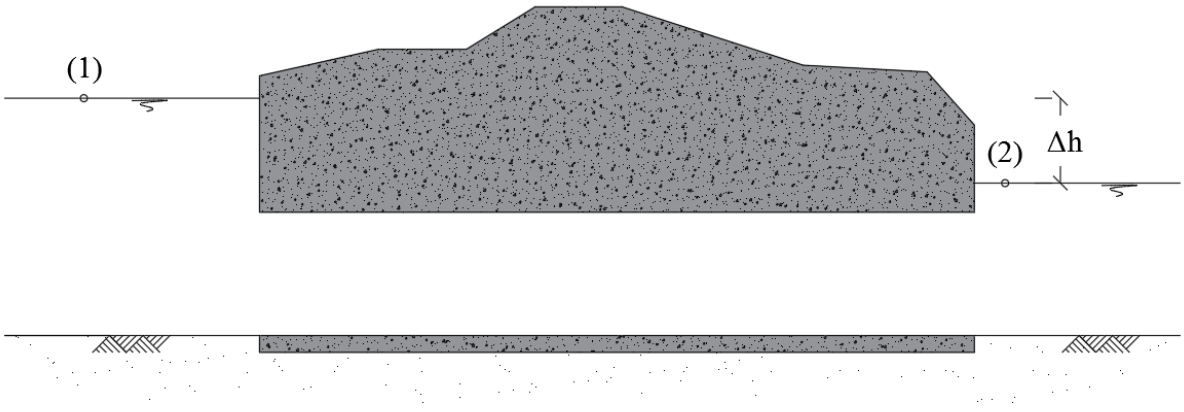

Figure 7: Schematic depiction of a water flow through a duct.

Regarding Figure 7, it is assumed that the water at point *1* is stagnant. Because point *1* lies on the water surface, the pressure is atmospheric. It is assumed that the atmospheric pressure is equal to *0*. Furthermore, the pressure at point *2* is also atmospheric and can therefore be set to *0*. With these assumptions, this converts to:

$$\rho g(z_1 - z_2) = \rho g \Delta h = \frac{1}{2}\rho u_2^2 \qquad Eq.2.6$$

In Eq. 2.6 the one can see the equation between the potential energy on the left hand side and the kinetic energy on the right hand side. From Eq. 2.6, *Torricelli's* theorem can be derived. *Torricelli's* theorem states that the velocity under the force of gravity at a free outflow is equal to the square root of twice the gravitational acceleration times the hydraulic head difference (White, 2011).

$$u = \sqrt{2g\Delta h} \qquad Eq.2.7$$

In Eq. 2.5, *Bernoulli's* principle is expressed in terms of pressure. Therefore, combining Eq. 2.3, Eq. 2.4 and Eq. 2.6:

$$P = pAu = \rho g \Delta h A u = \rho g \Delta h Q \qquad Eq.2.8$$

Then applying *Torricelli's* theorem on Eq. 2.8 to convert *Q* in terms of *Δh*.

$$P = \rho g \Delta h Q = \rho g \Delta h A\sqrt{2g\Delta h} \qquad Eq.2.9$$

Hereby the total theoretical power in the fluid P_{fluid} is established:

$$P_{fluid} = \rho g \Delta h A_c \sqrt{2g\Delta h} \qquad Eq.2.10$$

2.1.1.1 *System loss coefficient*

Considering Eq. 2.6, In this equation the potential energy term ($\rho g \Delta h$) and the kinetic energy term ($1/2\rho u^2$), both expressed in terms of pressure, are equal. This means that the total amount of potential energy is converted to kinetic energy. The ratio between potential and kinetic energy would therefore be equal to *1*. In reality, not all potential energy is converted to kinetic energy. The energy is also converted to e.g. frictional and turbulence losses. When losses are accounted, the ratio between potential and kinetic energy would therefore be greater than *1*. This ratio is better known as the system loss coefficient.

$$C_{sys} = \frac{E_{pot}}{E_{kin}} = \frac{\rho g \Delta h}{\frac{1}{2}\rho u_2^2} \qquad Eq.2.11$$

When *Bernoulli's* equation is considered with a dissipation term h_L:

$$z_1 + \frac{p_1}{\rho g} + \frac{u_1^2}{2g} = z_2 + \frac{p_2}{\rho g} + \frac{u_2^2}{2g} + h_L \qquad Eq.2.12$$

Assuming that the pressure terms p_1 and p_2 are atmospheric and the flow velocity at point *1* is negligibly small (See Figure 7) , Eq. 2.12 can be written as:

$$z_1 - z_2 = \frac{u_2^2}{2g} + h_L \qquad Eq.2.13$$

This can be rewritten as:

$$\rho g \Delta h = \frac{1}{2}\rho u_2^2 + \rho g h_L \qquad Eq.2.14$$

In which the potential and kinetic energy terms can be recognised.
Dividing every term by the kinetic energy yields:

$$\frac{\rho g \Delta h}{\frac{1}{2}\rho u_2^2} = 1 + \frac{\rho g h_L}{\frac{1}{2}\rho u_2^2} \qquad Eq.\,2.15$$

By definition, the loss coefficient K_L is determined by the ratio between the dissipated energy and the kinetic energy. Knowing this, Eq. 2.15 can be written as:

$$C_{sys} = 1 + K_L \qquad Eq.\,2.16$$

Hence, C_{sys} is, by definition, greater than or equal to *1*.

Considering Eq. 2.12 again. As mentioned before, h_L is defined as the ratio between the dissipated energy and the kinetic energy. So, Eq. 2.12 can be rewritten as:

$$\rho g \Delta h = \frac{1}{2}\rho u_2^2 + K_L \frac{1}{2}\rho u_2^2 = (1 + K_L)\frac{1}{2}\rho u_2^2 \qquad Eq.\,2.17$$

The loss coefficient K_L is the sum of the loss coefficients of the dissipation mechanisms and is computed for different kinds of transitions and fittings in pipe flows and can be extracted from literature. Furthermore, Eq. 2.17 is written as:

$$\Delta h = C_{sys}\frac{u_2^2}{2g} \qquad Eq.\,2.18$$

Then, applying Torricelli's theorem and accounting for dissipation due to wall friction, culvert entrance and culvert exit:

$$u = \sqrt{\frac{2g\Delta h}{C_{sys}}} = \sqrt{\frac{2g\Delta h}{1 + \sum K_L}} = \sqrt{\frac{2g\Delta h}{1 + f_f \frac{l}{D_h} + K_e + K_c}} \qquad Eq.\,2.19$$

The values of K_e and K_c are extracted from White (2011) and are valued respectively as *0.50* and *1.00*, because a sharp-edged culvert entrance and exit are assumed.

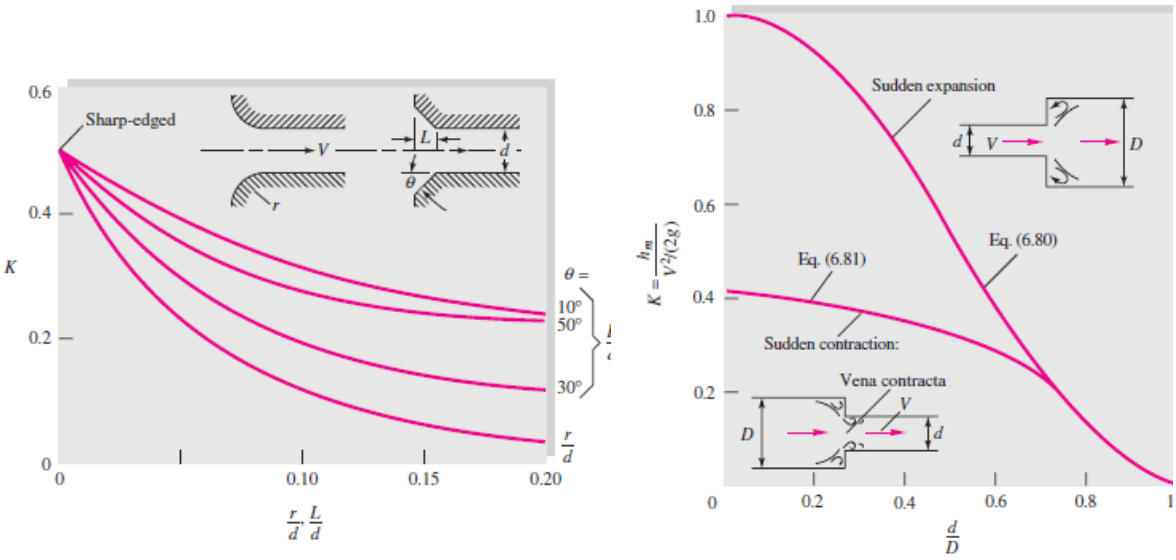

Figure 8: Values of loss coefficients due to duct entrance (left graph) and exit (right graph) (White, 2011).

The loss coefficient due to wall friction is determined by the *Darcy-Weisbach* equation (White, 2011). This equation yields:

$$h_f = K_f \frac{u^2}{2g} = f_f \frac{l}{D_h} \frac{u^2}{2g} \qquad Eq.\,2.20$$

Wherein the *Darcy* friction factor can be determined by the *Colebrook-White* formula:

$$\frac{1}{\sqrt{f_f}} = -2\log\left(\frac{2.51}{Re\sqrt{f_f}} + \frac{\varepsilon}{3.71 D_h}\right) \qquad Eq.\,2.21$$

Wherein, *Re* is the *Reynolds* number. The Reynolds number is the ratio between kinetic forces and viscous forces. A low *Reynolds* number implies that viscous effects are important and inertia effects are negligible, while a high *Reynolds* number indicate predominate kinetic forces. It also depicts if a flow is laminar or turbulent. For *Reynolds* numbers smaller than *2000*, laminar flow will occur and for *Reynolds* numbers larger than *3000*, turbulent flow occurs. In the middle range, so between *Re = 2000* and *Re = 3000*, an unpredictable flow occurs (Elger, Williams, Crowe, & Roberson, 2014). Considering the dimensions of the structure and the occurring flow velocities, the flow will nearly always lie in the turbulent regime. The *Reynolds* number is defined as:

$$Re = \frac{u D_h}{\upsilon} \qquad Eq.\,2.22$$

Where D_h is defined as the hydraulic diameter:

$$D_h = \frac{4A_c}{O} = \frac{4wh}{2(w+h)} \qquad Eq.\,2.23$$

The hydraulic diameter is a quantity that accounts for the fact that the culverts do not have a circular cross-section, but a rectangular one. Returning to the frictional losses. The implicit *Darcy-Weisbach* equation can be estimated by making use of the explicit *Swamee-Jain* approximation:

$$f_f = \frac{0.25}{\left(\log\left(\frac{\varepsilon}{3.7D_h} + \frac{5.74}{Re^{0.9}}\right)\right)^2} \qquad Eq.\,2.24$$

This approximation predicts friction factors that differ by less than *3*% from those calculated by The *Colebrook-White* method for $4 \cdot 10^3 < Re < 10^8$ and $10^{-5} < \varepsilon/D_h < 2\ 10^{-2}$ (Elger et al., 2014).

Moreover, the presence of a turbine in the duct will induce energy dissipation, and hence an extra term in the system loss coefficient equation is required. Because the type of turbine is not known yet and to establish a general insight in the behaviour of the Brouwersdam tidal power plant, the loss coefficient due to the turbine's presence is assumed to be *0*. Therefore, the performed calculation will establish a theoretical upper bound.

2.1.2 Degree of reaction

The energy of flowing fluid exists of three components:
- Kinetic energy due to its velocity;
- Pressure energy by virtue of pressure;
- Internal energy due to its temperature.

Pressure and internal energy together are commonly called the enthalpy of the fluid and is denoted by *H*. In this case, changes in temperature are neglected, because of their minor quantity and according influence on the energy distribution (Dixon, 1998). The degree of reaction *f* is defined as:

$$f = \frac{H}{E_{kin} + H} \qquad Eq.\,2.25$$

So essentially, the degree of reaction denotes a percentage of how much of the total energy is part of the enthalpy. Theoretically, if only static energy and no kinetic energy occurs, the water will be stagnant and the degree of reaction will be equal to *1*. On the other hand, if no static pressure occurs, the degree of reaction will be *0*. Another way to regard the degree of reaction is a distribution of energy consumed by the turbine and used to keep the water running, i.e. discharge. Herein, the pressure energy is consumed by the turbine and the kinetic energy is used for discharge. Hypothetically, If the turbine does not harvest any energy, all the energy is consumed for discharge, and hence the degree of reaction is *0*. And when all the available energy is harvested by the turbine, no energy is left to be used to keep the water running and no flow will occur. In that case the degree of reaction is equal to *1*.

The amount of energy that is potentially present in the water is given by:

$$E_{pot} = \rho g \Delta h \qquad Eq.\,2.26$$

One can see immediately that the potential energy is thus dependent on the water level difference between the North Sea and Lake Grevelingen assuming the density of the fluid and the gravitational acceleration to be constant. From Eq. 2.9 follows that the generatable power depends on the hydraulic head and the discharge, that consequently also depends on the hydraulic head. If we distinguish a part of the hydraulic head consumed by the turbine and a part of the hydraulic head used for discharge (Meijnen & Arnold, 2015), one can say:

$$\Delta h_T = f\Delta h \qquad Eq.2.27$$

And automatically:

$$\Delta h_Q = (1-f)\Delta h \qquad Eq.2.28$$

This distribution of energy is schematically depicted in Figure 9.

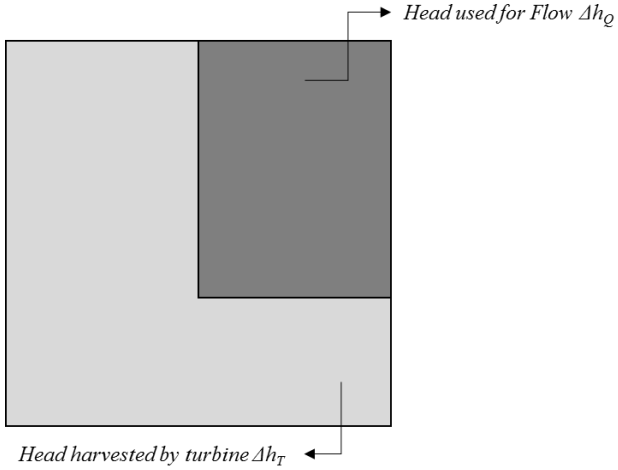

Figure 9: Schematic depiction of energy distribution in the tidal power plant.

First, considering Eq. 2.9 to calculate the power due to flowing water. With this in mind, Eq. 2.9 can be expanded with the distribution of the energy, i.e. hydraulic head, from Eq. 2.27 and Eq. 2.28. the equation for the discharge through the culvert and the power generation for constrained flow devices is then as follows:

$$Q_{CF} = A_c\sqrt{\frac{2g\Delta h_Q}{C_{sys,t}}} = A_c\sqrt{\frac{2g(1-f)\Delta h}{C_{sys,t}}} \qquad Eq.2.29$$

And:

$$P_{CF} = \rho g\Delta h_T A_c\sqrt{\frac{2g\Delta h_Q}{C_{sys,t}}} = \rho g f\Delta h A_c\sqrt{\frac{2g(1-f)\Delta h}{C_{sys,t}}} \qquad Eq.2.30$$

Which can be written as:

$$P_{CF} = f\sqrt{1-f}\rho g\Delta h A_c\sqrt{\frac{2g\Delta h}{C_{sys,t}}} \qquad Eq.2.31$$

The ratio between P_{CF} and P_{fluid} can be defined as the constrained flow power coefficient $c_{p,CF}$.

$$c_{p,CF} = \frac{P_{CF}}{P_{fluid}} \qquad Eq.2.32$$

To establish a theoretical upper bound of harvestable power, it is assumed that no energy dissipation occurs and that the turbines perform at their optimal degree of reaction. And thus, is assumed that the system loss coefficient C_{sys} is equal to *1* and the degree of reaction *f* is

equal to *2/3*. The derivations of these values can be found in respectively section 2.1.1.1 and section 2.1.2.1. Thereupon, Eq. 2.32 is filled in:

$$c_{p,CF} = \frac{f\sqrt{1-f}\,\rho g \Delta h A_c \sqrt{\frac{2g\Delta h}{C_{sys,t}}}}{\rho g \Delta h A_c \sqrt{2g\Delta h}} = f\sqrt{\frac{1-f}{C_{sys,t}}} = \frac{2}{3}\sqrt{1-\frac{2}{3}} \cong 0.385 \qquad Eq.\,2.33$$

This means that, under constrained flow conditions, maximally *38.5%* of the power present in the fluid can be harvested by the turbine.

2.1.2.1 *Derivation of optimal degree of reaction*

When Eq. 2.30 is rearranged and the degree of reaction *f* is isolated, it yields:

$$P = \rho g \Delta h A_c \sqrt{\frac{2g\Delta h}{C_{sys,t}}} \cdot f\sqrt{1-f} \qquad Eq.\,2.34$$

To calculate the optimal value of *f*, the derivative of *P* with respect to *f* needs to be equal to *0*.

$$\frac{\partial P}{\partial f} = \rho g \Delta h A_c \sqrt{\frac{2g\Delta h}{C_{sys,t}}} \cdot \frac{2-3f}{2\sqrt{1-f}} = 0 \qquad Eq.\,2.35$$

This results in:

$$\frac{\partial P}{\partial f} = 0 \quad \text{for} \quad f = \frac{2}{3} \quad \text{for } f \in (0,1)$$

Looking at the graph where the power *P* is plotted against the degree of reaction *f* in Figure 10, the power output is at its greatest at *f = 2/3*.

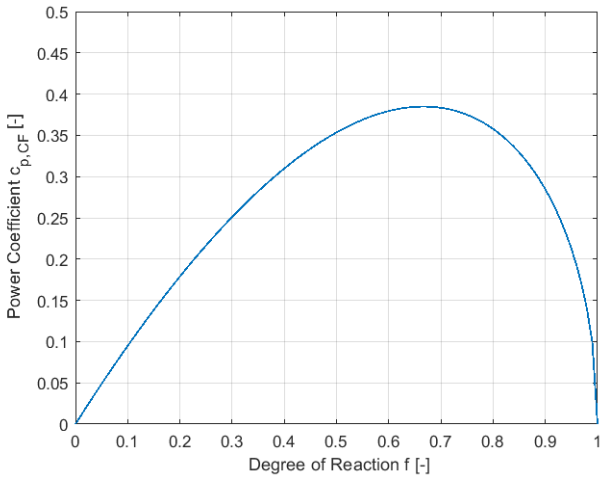

Figure 10: Power coefficient of constrained flow versus degree of reaction.

2.2 Free flow

Free flow devices are commonly placed at the sea bed at locations with a high flow velocity regime. For example in headlands, inlets and straits. The turbines can be placed both solitairy as in a group, which is called a tidal array. Free flow devices are the under water equivalent of a traditional windturbine and the theoretical upper bound is calculated in an identical manner. Caused by the higher water density , the dimensions of the blades can be decreased and the blades can rotate in a lower frequency and at the same time produce a significant power output. To improve the flow and subsequently the power energy harvest, concentrators may be used around the blades to concentrate and streamline the flow towards the rotors (European Marine Energy Centre, n.d.).

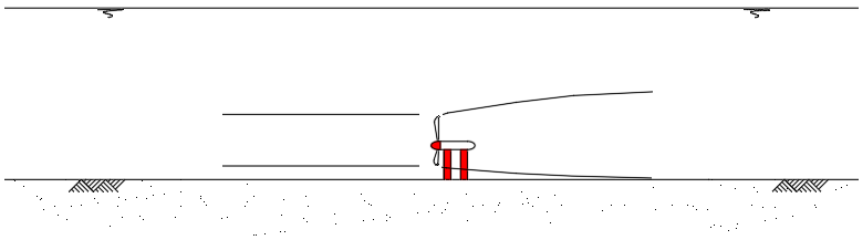

Figure 11: Free flow principle.

A well known location where free flow devices are installed is the Pentland Firth, a strait between the Scottish mainland and the Orkney Islands. Hidden under the water surface, four *1.5* MW turbines are placed on the seabed to convert the kinetic energy of the tides into electricity. The capacity to supply electricity to *2600* homes across Scotland is classed as the world's largest tidal stream array project in the world. Plans are in the pipeline to potentially install *265* additional (Maynard, 2018).

2.2.1 Theoretical upper bound of power generation in a free flow device

Considering a turbine placed in an infinitely large channel, so that the flow is not influenced by the presence of any kind of boundaries, such as walls or shores. Furthermore, the turbine is modelled as an actuator disc. This actuator disc is assumed to be an ideal energy converter and does not induce a drag resistance to the water flowing through it. In addition, uniform flow is assumed over the whole area of the actuator disc and the approach velocity u_0 is assumed to be axial (Ragheb & Ragheb, 2011). The extraction of energy occurs by reducing the kinetic energy of the fluid stream from upstream to downstream. In this case, the velocity in the turbine is smaller than the approach velocity:

$$u_1 < u_0$$

Mass conservation yields:

$$\rho A_T u_T = \rho A_1 u_1 \qquad Eq.2.36$$

To satisfy the law of conservation of mass, it means that:

$$A_T < A_1$$

Where A_1 is the cross-sectional area of the wake behind the turbine.
From Newton's second law of motion follows:

$$F = ma$$

$$F = m\frac{du}{dt} = \dot{m}(u_0 - u_1)$$

$$F = \rho A_T u_T (u_0 - u_1) \qquad Eq.\,2.37$$

Already mentioned in Eq. 2.2:

$$P = Fu$$

Combining Eq. 2.2 and Eq. 2.37:

$$P = \rho A_T u_T^2 (u_0 - u_1) \qquad Eq.\,2.38$$

The power as the rate of change of kinetic energy from upstream and downstream is given by:

$$P = \frac{\Delta E}{\Delta t}$$

$$P = \frac{\frac{1}{2}mu_0^2 - \frac{1}{2}mu_1^2}{\Delta t} = \frac{\frac{1}{2}m(u_0^2 - u_1^2)}{\Delta t}$$

This is equal to:

$$P = \frac{1}{2}\dot{m}(u_0^2 - u_1^2) = \frac{1}{2}\rho A_T u_T (u_0^2 - u_1^2) \qquad Eq.\,2.39$$

Equating Eq. 2.38 and Eq. 2.39 yields:

$$u_T = \frac{1}{2}(u_0 + u_1) \qquad Eq.\,2.40$$

Filling in Eq. 2.40 in into Eq. 2.39:

$$P = \frac{1}{4}\rho A_T (u_0 + u_1)(u_0^2 - u_1^2) \qquad Eq.\,2.41$$

Introducing the dimensionless interference factor *r*:

$$r = \frac{u_1}{u_0}$$

And applying to Eq. 2.41:

$$P = \frac{1}{4}\rho A_T u_1^3 (1 + r)(1 - r^2) \qquad Eq.\,2.42$$

The power present in a flowing fluid can be determined by:

$$P_{fluid} = Fu$$

From Bernoulli's theorem follows:

$$P_{fluid} = \frac{1}{2}\rho A u^2 u = \frac{1}{2}\rho A u^3 \qquad Eq.\,2.43$$

The ratio between the extractable power in free flow scenario's and the power present in the fluid is defined as:

$$c_{p,FF} = \frac{P}{P_{fluid}} = \frac{\frac{1}{4}\rho A_T u_1^3 (1+r)(1-r^2)}{\frac{1}{2}\rho A_T u_1^3} = \frac{1}{2}(1+r)(1-r^2) \qquad Eq.\,2.44$$

To determine the maximum value of $c_{p,FF}$, differentiation with respect to r is executed:

$$\frac{dc_{p,FF}}{dr} = \frac{1}{2}(1-3r)(1+r) = 0 \qquad Eq.\,2.45$$

This results in:

$$\frac{dc_{p,FF}}{dr} = 0 \quad \text{for} \quad \mathrm{r} = \frac{1}{3} \quad \text{for} \quad r \in (0,1)$$

Filling in this value in Eq. 2.44:

$$c_{p,FF} = \frac{1}{2}\left(1+\frac{1}{3}\right)\left(1-\left(\frac{1}{3}\right)^2\right) = \frac{16}{27} \cong 0.59 \qquad Eq.\,2.46$$

This value is better known as the *Betz*-limit β.

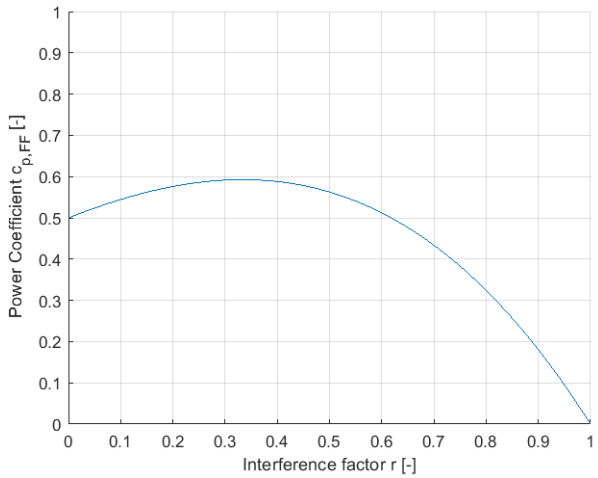

Figure 12:Power coefficient $c_{p,FF}$ for varying interference factor r.

2.3 Confined free flow

In confined free flow situations, a free flow device is placed in a confined region, such as culverts or narrow sea straits. The presence of a solid boundary, like the culvert wall, sea bed, or shore, influences the power output of the energy generation device, as can be seen in Section 2.3.1. Also, the fact that the flow is not entirely guided through the turbine and thereupon a by-pass flow is created, has its consequences on the energy harnessing capacity. Moreover, discharge modulation in a confined free flow situation is not as easy as in a constrained flow condition, because of the by-pass flow. On the other hand, the presence of the by-pass flow provides a passage for fish and aquatic mammals to go by the turbine without coming into contact with the turbine blades. As a reference, Leopold & Scholl (2018) researched the possible cause of death of harbour- and grey seals and porpoises caused by confined free stream devices placed in the nearby Eastern Scheldt Barrier. The result of the postmortal research on seals and porpoises indicate that the number of animals diagnosed with blunt trauma, as a result of being struck by a turbine blade, is small.

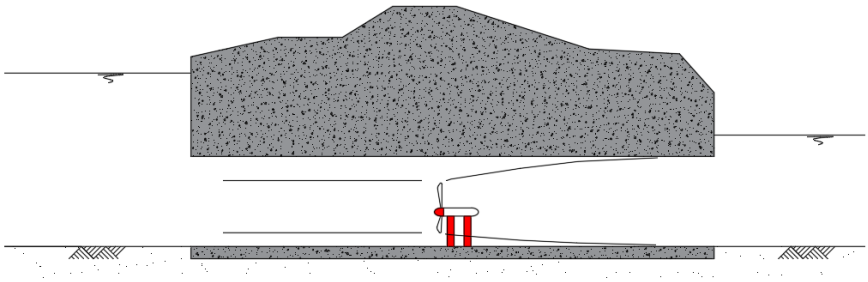

Figure 13: Confined free flow method

2.3.1 Theoretical upper bound of power generation in a confined free flow device

Garrett & Cummins (2004) considered a scenario of a turbine occupying a fraction of the cross section of a channel, which is schematically depicted in Figure 14. When the principle of mass conservation is applied, it yields:

$$A_c u_0 = A_T u_1 + A_2 u_2 \qquad Eq.\,2.47$$

Wherein the first term on the right-hand side depicts the wake flow and the second term the bypass flow. Introducing parameter ϵ, which is the ratio between the turbines cross-sectional area and the cross-sectional area of the duct:

$$\epsilon = \frac{A_T}{A_c} \qquad Eq.\,2.48$$

Eq. 2.47 then converts to:

$$u_0 = \epsilon u_1 + (1-\epsilon) u_2 \qquad Eq.\,2.49$$

From which follows:

$$u_2 = \frac{u_0 - \epsilon u_1}{1-\epsilon} \qquad Eq.\,2.50$$

Assuming that pressure p_2 downstream of the turbine is continuous laterally from the free stream into the wake of the turbine so as not to drive significant transverse flow, one can pose:

$$p_0 - p_2 = \frac{1}{2}\rho(u_2^2 - u_0^2) \qquad Eq.\,2.51$$

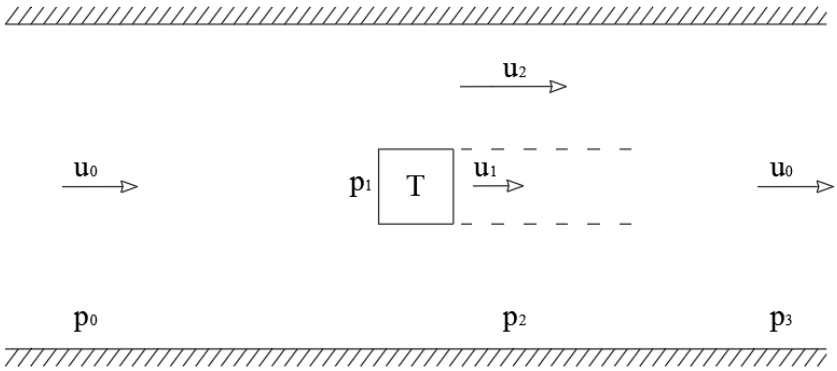

Figure 14: Schematical depiction of a confined free flow scenario.

From *Bernoulli's* theorem, the pressure drop $p_1 - p_2$ across the turbine can be written as:

$$p_1 - p_2 = \frac{1}{2}\rho(u_2^2 - u_1^2) \qquad Eq.\,2.52$$

The power generated for confined free flow scenario's is then:

$$P_{CFF} = \frac{1}{2}\rho\epsilon A_c(u_2^2 - u_1^2) \qquad Eq.\,2.53$$

Considering the flow through the culvert well down stream, the wake flow and the by-pass flow are assumed to have mingled to a uniform flow with velocity u_0. Then, applying the conservation of momentum principle between cross-sections 2 and 3, pressure p_3 can be obtained by:

$$p_3 + \rho u_0^2 = p_2 + \rho\epsilon u_1^2 + \rho(1-\epsilon)u_2^2 \qquad Eq.\,2.54$$

Where it is necessary to note that the values of p_3 and p_0 do not have the same value, since some head is lost due to lateral mixing. With Eq. 2.51 and Eq. 2.54 the following equation can be established:

$$p_0 - p_3 = \frac{1}{2}\rho(u_0^2 + u_2^2) - \rho\epsilon u_1^2 - \rho(1-\epsilon)u_2^2 \qquad Eq.\,2.55$$

With this equation, an equation for the power that is generated by a turbine occupying the full cross-sectional area of the duct can be set up. Occupying the full cross-sectional area of the duct means that a constrained flow scenario is established. The power of the constrained flow scenario can be written as:

$$P_{CF} = (p_0 - p_3)A_c u_0 \qquad Eq.\,2.56$$

The ratio between the power generated by the confined free flow scenario, mentioned in Eq. 2.53 and the constrained flow scenario in Eq. 2.56 is defined as:

$$\zeta = \frac{P_{CFF}}{P_{CF}} \qquad Eq.2.57$$

And can be reduced to:

$$\zeta = \frac{r(1 + r - 2\epsilon r)}{2r + \epsilon(1 - 3r)} \qquad Eq.2.58$$

In which:

$$r = \frac{u_1}{u_0}$$

In Figure 15, one can see that if the velocity in front of the turbine is equal to the velocity behind the turbine, the dimensionless turbine velocity *r* is equal to *1*, and accordingly the dimensionless turbine cross-sectional area is equal to *1*. When these values are reached, a constrained flow scenario is established and ζ has a value equal to *1*. For other values of *r* and ϵ, ζ is smaller than *1* as can be seen in Figure 15.

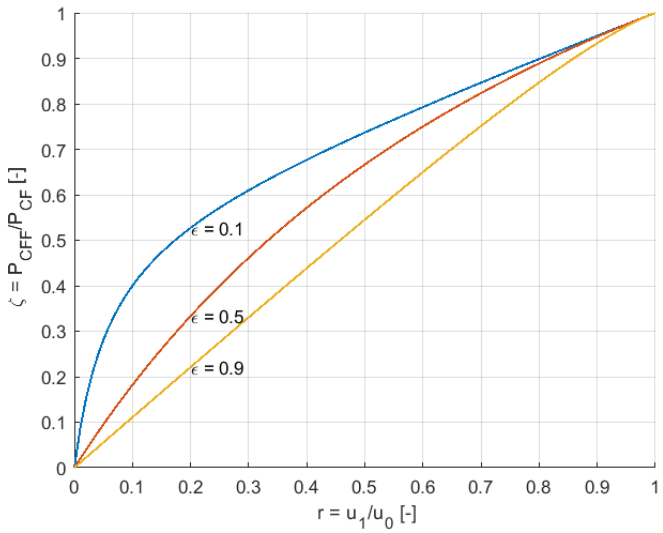

Figure 15: Relation between dimensionless turbine velocity and confined free flow power coefficient.

Regarding Eq. 2.57 again, the maximal harvestable power for confined free flow devices with respect to constrained flow solutions is:

$$P_{CFF} = \zeta P_{CF}$$

From Eq. 2.32, one can see that:

$$P_{CF} = c_{p,CF} P_{fluid}$$

Therefore, one can state that the following yields:

$$P_{CFF} = \zeta c_{p,CF} P_{fluid} = c_{p,CFF} P_{fluid} \qquad Eq.2.59$$

From Eq. 2.59 can be concluded that the maximum theoretical power extracted by constrained flow devices is always larger than confined free stream solutions, as can be seen in Figure 16. The theoretical upper bound for confined free flow scenarios depends on the value of ζ, which accordingly depends on the ratio's ϵ and r.

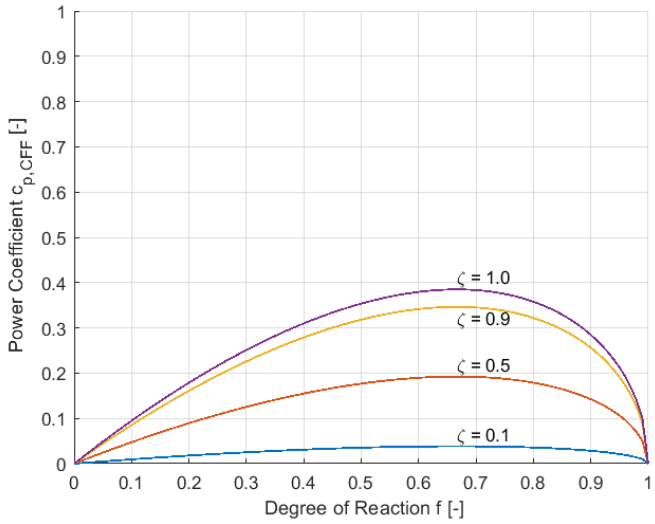

Figure 16: Graphical representation of the confined free flow power coefficient against varying degree of reaction for different ζ-values.

3 Methodology

"The cure for anything is salt water:
sweat, tears or the sea''
K. Blixen

3.1 Water level modelling & energy harness methodology

Considering the three energy extraction methods described in the previous chapter and the desire to regulate the discharge by modulation of turbines, one can say that constrained flow devices are clearly advantageous compared to the confined free flow and free flow solutions because of the volume flow totally passing through the turbine. Given this, discharge can be controlled easier than confined free flow turbines, where the occurrence of by-pass flow, which is more difficult or even impossible to control, throws a spanner in the works. Besides, the theoretical generated power of a confined free flow device is always a fraction of the theoretical power of a constrained flow device, which is also not in the favour of the confined free flow solution. Because of the high priority of the water level control in Lake Grevelingen, it is decided to exclusively consider constrained flow solutions.

To increase the understanding of the influence of the tidal power plant on Lake Grevelingen, a storage basin model is established. With this model the water level in Lake Grevelingen is simulated. The model is used to examine the proposed Protide design by Tidal Grevelingen Project (2018). Three possible turbine configurations, including the Protide design, are regarded and their influence on the lake and power extraction is investigated. The considered amount of culverts is *18*, with a cross-sectional area of *8* m by *8* m and a culvert length of *49* m. For this investigation, water level data of the North Sea is necessary. Provided by Rijkswaterstaat (2019), a *10* minute interval measurement water level data is used as an input of the model. The water level data spans an interval of three years, from 2016 to 2018 and is measured at measuring station *Brouwershavensche Gat 08.*

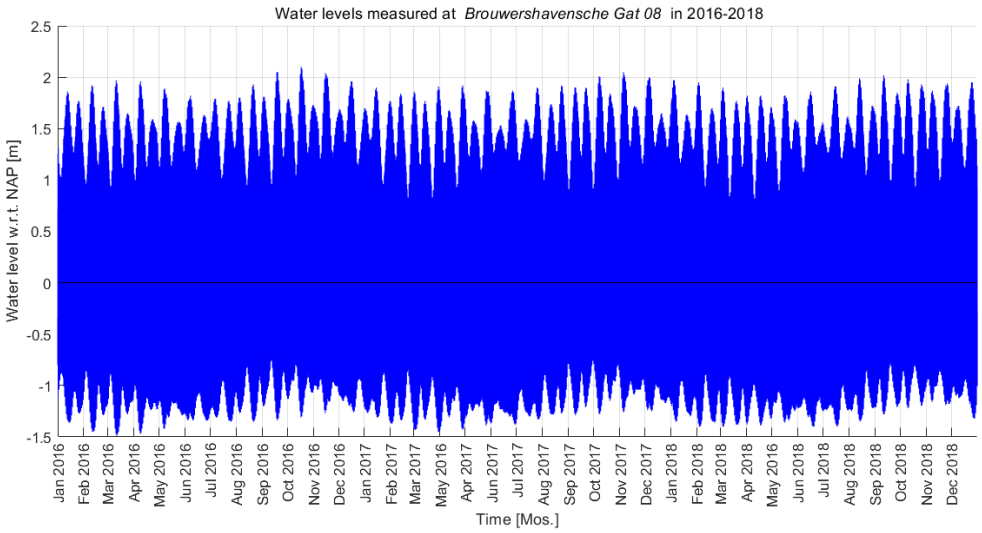

Figure 17: North Sea water level data measured at Brouwershavensche Gat 08.

Regarding the measurements in Figure 17, one can conclude that a semi-diurnal tide with a tidal period of approximately *12.5* hours occurs. In addition, twice a month, spring and neap tides occur. The water level roughly varies between *+2.00* m NAP and *-1.50* m NAP. The

high water peaks generally occur approximately around October, while the minimum low water level mainly occur around June. This can be clarified by a higher wind set up and higher river discharges due to melt water and higher precipitation during winter months (Rijkswaterstaat, n.d.).

The data from the measuring station in the North Sea is truncated at the begin of the data to ensure the signal starts at the beginning of a flood period. In this case, this means that *74* from *157824* water level values are removed from the dataset. The dataset used in the algorithm therefore counts *157750* elements.

3.1.1 Model assumptions

It is assumed that Lake Grevelingen has vertical banks and is therefore modeled as a cuboidal basin, as can be seen in Figure 18. This vertical bank assumption ascertains that the lake's surface area does not change with variation of the water level. From this, one can say that the volume in the lake is proportional to the total water depth. The lake's surface area is assumed to be *110* km^2 according to Tidal Grevelingen Project (2018).

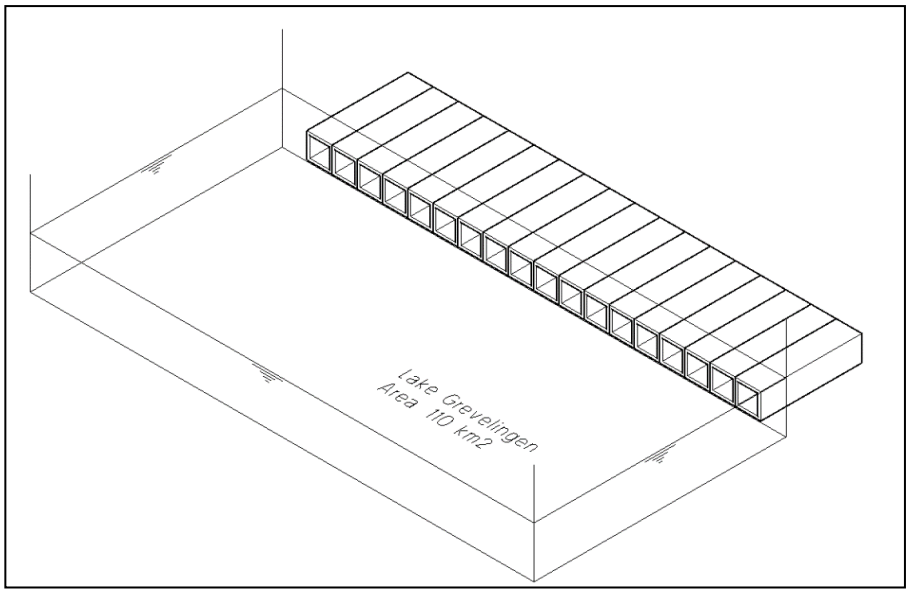

Figure 18: Three-dimensional visualisation of the model.

For simplicity reasons, it is also assumed that no water can flow in or out of the lake other than through the Tidal Power Plant. Thereupon, water exchange through sluice gates, boat locks, precipitation and evaporation is assumed to be *0*.This assumption is reasonable, because the order of magnitude of the water mass flowing in or out of the lake through the tidal power plant is much higher than the order of magnitude of the beforementioned discharge mechanisms. Additionally, the following hydraulic constants are assumed:

Table 1:General hydraulic constants.

Parameter:	**Symbol:**	**Quantity:**
Density of salt water [kg/m^3]	ρ	1025
Gravitational acceleration [m/s^2]	g	9.81
Kinematic viscosity [m^2/s]	ν	10^{-6}
Roughness height culvert [m]	ε	0.0003

From a hydraulic perspective, the flow is assumed to be steady state, stationary at every considered point of time, inviscid and incompressible. With these assumptions, *Bernoulli's* principle can be applied. The incompressibility of the fluid is valid as long as the flow velocity does not exceed *3/10* of the speed of sound in the fluid, i.e. the Mach-number is smaller than *0.3* (Elger et al., 2014), which can be expected. Assuming that the flow velocity upstream of the culvert is negligibly small and the ambient pressure at the water surface both upstream and downstream is assumed to be the same, *Torricelli's* law can be used, as derived in Section 2.1.1. Moreover, the system loss coefficient valid for empty culverts is used as the system loss coefficient for equipped culverts cannot be extracted from literature and experimental or numeric methods are needed to determine these.

As regards to the culverts, it is assumed that every culvert has the same properties and thus has the same contribution in influencing the flow. The turbines are assumed to all behave in the same manner along the culvert array. Moreover, it is assumed that the turbines are able to adjust immediately to changes in the hydraulic regime and are not subject to inertial resistance.

3.1.2 Algorithm description

The change in water level in Lake Grevelingen is dependent on the amount of water volume that flows through the total amount of culverts per unit of time, i.e. the total discharge. Because the vertical bank assumption is applied, the change in volume in the lake in time is proportional to the total discharge *NQ(t)*. Therefore, the change in water level in time is proportional to $NQ(t)/A_{LG}$, and one can state the following:

$$\frac{dWL_{LG}(t)}{dt} = \frac{NQ(t)}{A_{LG}} \qquad Eq.\,3.1$$

Which is described as a differential equation of the first order. *Torricelli's law*, as derived in Section 2.1.1, states that the discharge through a duct, subject to energy dissipation and the presence of a turbine, can be described as:

$$Q(t) = A_c\sqrt{\frac{2g(1-f(t))\Delta h(t)}{C_{sys}(t)}} = A_c\sqrt{\frac{2g(1-f(t))(WL_{NS}(t)-WL_{LG}(t))}{1+f_f(t)\frac{l}{D_h}+K_e+K_c}} \qquad Eq.\,3.2$$

In the case no energy dissipation occurs, one can state:

$$C_{sys}(t) = 1$$

Which means:

$$f_f(t) = K_e = K_c = 0$$

And if no turbine is placed in the culvert:

$$f(t) = 0$$

Because the input data of the water level in the North Sea is a discrete signal with a measurement interval of *10* minutes, Eq 3.1 can be discretised:

$$\frac{\Delta WL_{LG}(t)}{\Delta t} = \frac{NQ(t)}{A_{LG}} \qquad Eq.\,3.3$$

This can be written as:

$$\frac{WL_{LG,n+1} - WL_{LG,n}}{t_{n+1} - t_n} = \frac{NQ_n}{A_{LG}} \qquad Eq.\,3.4$$

By rewriting Eq. 3.4 , one can determine the water level in Lake Grevelingen for the next time step. This is also known as the *Forward Euler* method:

$$WL_{LG,n+1} = WL_{LG,n} + \frac{NQ_n}{A_{LG}}(t_{n+1} - t_n) = WL_{LG,n} + \frac{NQ_n}{A_{LG}}\Delta t \qquad Eq.\,3.5$$

In which Q_n is described as:

$$Q_n = A_c u_n = A_c \sqrt{\frac{2g(1-f_n)(WL_{NS,n} - WL_{LG,n})}{1 + f_{f,n}\frac{l}{D_h} + K_e + K_c}} \qquad Eq.\,3.6$$

In Eq. 3.6, the *Darcy* friction factor is determined with the *Swamee-Jain* approximation. The *Swamee-Jain* approximation depends on the *Reynolds* number, which consequently depends on the flow velocity u_n, as can be seen in Section 2.1.1.1. This means that the flow velocity depends on the flow velocity itself. By making use of the iterative process described below, a converged value of the *Darcy* friction factor for every timestep is determined.

$$u_{n,i} = \sqrt{\frac{2g(1-f_n)(WL_{NS,n} - WL_{LG,n})}{C_{sys,n,i-1}}}$$

$$Re_{n,i} = \frac{u_{n,i} D_h}{\nu}$$

$$f_{f,n,i} = \frac{0.25}{\left(\log\left(\frac{\varepsilon}{3.7D_h} + \frac{5.74}{Re_{n,i}^{0.9}}\right)\right)^2} \qquad Eq.\,3.7$$

$$C_{sys,n,i} = 1 + f_{f,n,i}\frac{l}{D_h} + K_e + K_c$$

In which the initial value for $C_{sys,\,n,\,0}$ is set to *1*.

To apply the *Forward Euler* method, first the discharge should be calculated. The order of computation for every timestep in the numerical code is then:

$$Q_n = A_c \sqrt{\frac{2g(1-f_n)(WL_{NS,n} - WL_{LG,n})}{1 + f_{f,n}\frac{l}{D_h} + K_e + K_c}} \qquad Eq.\,3.8$$

$$WL_{LG,n+1} = WL_{LG,n} + \frac{NQ_n}{A_{LG}}\Delta t$$

The water level signal of the North Sea is already provided, so an initial value the water level in Lake Grevelingen is required to compute the rest of the water level in the Lake for the time duration of three years. This initial water level is stated at the current still water level of *-0.20* m NAP. The initial North Sea water level value starts at the beginning of a flood period at *-1.13* m NAP. Worth mentioning is that when the water level in Lake Grevelingen is greater than the water level in the North Sea, which physically means that Lake Grevelingen is being drained, a negative argument under the square root appears, which result in undesirable imaginary numbers. This is solved by implementing an if-statement in the numerical code, that states that when the water level in the lake is greater than the water level in the North Sea, a negative discharge must take place:

$$Q_n = \begin{cases} A_c \sqrt{\dfrac{2g(1-f_n)\Delta h_n}{C_{sys,n}}} & \text{if } \Delta h \geq 0 \\ -A_c \sqrt{\dfrac{2g(1-f_n)|\Delta h_n|}{C_{sys,n}}} & \text{if } \Delta h < 0 \end{cases} \qquad Eq.\,3.9$$

This numerical scheme to determine the water level in Lake Grevelingen acts as a spine for the more resolute schemes that are being considered. For cases where no discharge modulation occurs, the degree of reaction is constant at its optimal value to generate the largest amount of energy. To control the water flow through the culverts, the degree of reaction is modulated in order to satisfy the set water management requirements.

3.1.2.1 *Turbine modulation*

In cases wherein the turbines are not modulated, exceedances of the limiting water levels are possible to occur. To counteract this surpassing, the degree of reaction of the turbines can be varied and subsequently the discharge and water level can be modulated. The water level in Lake Grevelingen is bounded by an upper and lower limiting water level, where the water level should lie in between. To determine the necessity of turbine modulation, an upper and lower precautious water level is introduced, WL_P^+ and WL_P^-. When the water level in the lake exceeds the precautious water level, modulation of the turbines sets in.

To determine the value of the degree of reaction per timestep, the time to reach the maximum or minimum water level from the previous water level, defined as the bounding time, is computed first. Here is assumed that the hydraulic head and consequently the discharge do not change within the bounding time, as depicted in Figure 19. The gradient of the water

level is defined as the discharge calculated with the hydraulic head from the previous timestep divided by the superficial area of the lake. Knowing the rate of change of the water level, the bounding time can be calculated per timestep:

$$t_{B,n} = \frac{(WL_{LG,max} - WL_{LG,n-1})A_{LG}}{NQ_{n-1}} \qquad Eq.3.10$$

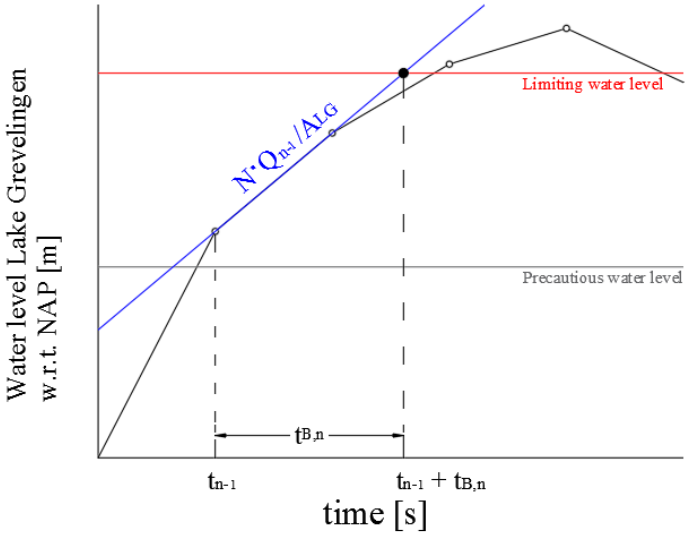

Figure 19: Visual definition of bounding time t_B.

Elaborating on the alteration of the degree of reaction. Once the lakes water level reaches the limiting water level, the degree of reaction should be equal to *1*, because no water can be let in during inflow conditions or let out in outflow conditions. The discharge therefore must be *0*. This limiting water level will be reached in the time $t_{B,n}$. With this information, a linear relation between degree of reaction and time can be established for every timestep. This linear equation is defined as:

$$f_n = j_n t_n + b_n \qquad Eq.3.11$$

In which:

$$j_n = \frac{1 - f_{n-1}}{t_{B,n}} \qquad Eq.3.12$$

$$b_n = 1 - \frac{1 - f_{n-1}}{t_{B,n}}(t_{n-1} + t_{B,n}) \qquad Eq.3.13$$

In the numerical code, the maximum value of *f* is set to *0.999999*. When the value of *f* is equal to *1*, the discharge will be *0*. When the discharge is equal to *0*, the bounding time t_B is not defined. Further more, Figure 20 illustrates j_n and b_n geometrically.

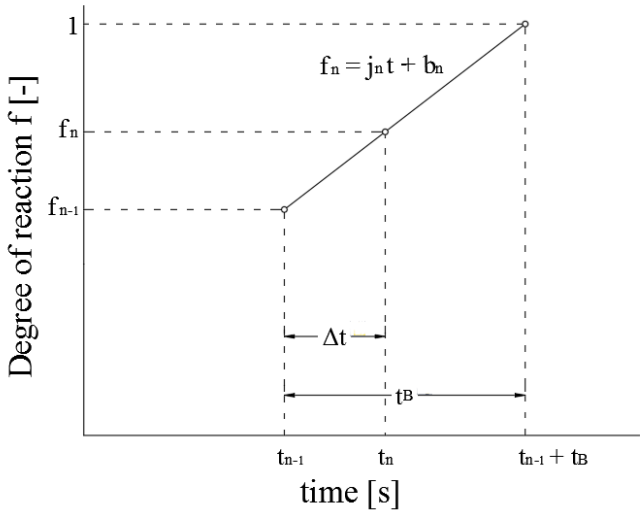

Figure 20: Determination of degree of reaction value per timestep Δt.

This algorithm is performed every timestep as long as the current water level surpasses the upper precautious water level during inflow and surpasses the lower precautious water level during outflow. Mathematically seen, inflow occurs when the gradient of the water level signal is greater than *0.* Subsequently, outflow occurs when the gradient of the water level becomes negative. Thus, if the upper precautious water level is surpassed, only at inflow conditions modulation of the turbines occurs. Because at outflow, the water level is already diminishing and modulation of the turbine is redundant. If the lower precautious water level is exceeded, no modulation of the turbines takes place during inflow, because the water level rises already and therefore modulation is redundant as well.

Moreover, two kinds of turbine modulation can be distinguished: Intermittent Turbine Modulation (ITM) and Fulltime Turbine Modulation (FTM). ITM is activated when a specific precautious lower or upper water level is surpassed. FTM, on the contrary, is turbine modulation that sets in as soon as inflow or outflow starts, thereby modulating over the full range of the water level signal. FTM has the advantage that the discharge is altered any time, while ITM increases the energy yield because the turbines are performing at their optimal degree of eaction for a longer time. If ITM already suffices, implementing FTM is unnecessary.

This algorithm is applied to three design options, all supplied with *18* culvertswith a cross-sectional area of *8* m by *8* m. One design option is equipped with all culverts filled with bidirectional turbines, so energy is harvested during both in- and outflow. The second design option that is considered is an array fully equipped with unidirectional turbines. In this array, no energy is extracted during outflow conditions. The last option that is considered is the Protide design: this design is proposed by Tidal Grevelingen Project (2018) and uses only *11* of *18* culverts to generate power. The remaining *7* culverts are left empty. Aditionally, unidirectional turbines are installed to generate power only during inflow stages. In this case, the algorithm in Eq. 3.8 can be expanded to:

$$Q_{e,n} = A_c \sqrt{\frac{2g(WL_{NS,n} - WL_{LG,n})}{1 + f_{f,n}\frac{l}{D_h} + K_e + K_c}}$$

$$Q_{t,n} = A_c \sqrt{\frac{2g(1 - f_n)(WL_{NS,n} - WL_{LG,n})}{1 + f_{f,n}\frac{l}{D_h} + K_e + K_c}} \qquad Eq.\,3.14$$

$$WL_{LG,n+1} = WL_{LG,n} + \frac{(N - M)Q_{t,n}}{A_{LG}}\Delta t + \frac{MQ_{e,n}}{A_{LG}}\Delta t$$

The results of these options considered can be found in Chapter 5. A brief summary of the used methodology is given in Table 2.

Table 2: Calculation method synopsis.

	Calculation method
1	Iteratively determine discharge.
2	Calculate water level.
3	Check if water level exceeds precautious water level.
4	If so, perform turbine modulation.
5	Update discharge with updated degree of reaction.
6	Calculate modulated water level.

3.1.3 Determination of paramount parameters

With the water level being artificially modified and to inquire if the design options satisfy the posed standards, key numbers are established. The majority of these key numbers are posed by Tidal Grevelingen Project (2018) and are summarised in Table 3:

Table 3: Key numbers posed by Tidal Grevelingen Project (2018).

Parameter:	**Symbol:**	**Quantity:**
Desired mean annual energy yield [GWh]	E	60
Overshoot per year [%]	OS	1
Undershoot per year [%]	US	10
Monthly averaged tidal range [m]	$\overline{T_r}$	0.40
Monthly maximum tidal range [m]	$T_{r,\,max}$	0.50

From a energy extracting point of view, the power that can be harvested by the turbine can be determined directly from the water level difference signal that is established from the algorithm in the previous section. To calculate the power that is extracted by the turbine at every timestep, the following expression, derived in Section 2.1, yields:

$$P_n = \rho g f_n \Delta h_n Q_n = \rho g f_n \Delta h_n A_c \sqrt{\frac{2g(1 - f_n)\Delta h_n}{C_{sys,n}}} \qquad Eq.\,3.15$$

The mean annual energy yield can be determined by integrating the extracted power signal:

$$E = \frac{1}{T}\int_{t_1}^{t_2} P(t)\,dt \qquad Eq.\,3.16$$

The integral from Eq. 3.16 can be approximated by a trapezoidal numerical integration scheme:

$$E \cong \frac{1}{T}\sum_{n=1}^{Z} \frac{P_{n-1} + P_n}{2}\Delta t \qquad Eq.\,3.17$$

For turbine selection purposes, the mean and maximum extrable power are of importance. The mean power can be calculated by:

$$\bar{P} = \frac{1}{Z}\sum_{n=1}^{Z} P_n \qquad Eq.\,3.18$$

The maximum power can be established by determining the maximum value in the collection of the extracted power P_n:

$$P_{max} = \max P_n \qquad Eq.\,3.19$$

Parameters that are of interest for the water management requirements are the monthly averaged tidal range, monthly maximum tidal range and the under- and overshoot percentages. The monthly averaged tidal range is calculated by determining the total distance between the flood and ebb water level per tidal cycle and averaged this over the amount of occurrence within a month:

$$\overline{T_r} = \frac{1}{L}\sum_{k=1}^{L}\left(\left|\widehat{WL}_{LG,k}\right| + \left|\widetilde{WL}_{LG,k}\right|\right) \qquad Eq.\,3.20$$

Wherein L is the number of tidal cycles within a month, which can deviate depending on the days in a month. The monthly maximum tidal range is determined by finding the maximum value within the tidal range collection of a month. For the monthly averaged and monthly maximum tidal range and a water level signal of a duration of three years, this delivers *36* values for both quantities.

$$T_{r,max} = \max_{k=1}^{L}\left(\left|\widehat{WL}_{LG,k}\right| + \left|\widetilde{WL}_{LG,k}\right|\right) \qquad Eq.\,3.21$$

The over- and undershoot percentages are defined as the ratio of the amount of data points surpassing the upper of lower limiting water level versus the amount of data points within a year:

$$OS = \frac{Z_{WL_{LG} > WL_P^+}}{Z_{year}} \qquad Eq.\,3.22$$

$$US = \frac{Z_{WL_{LG} < \bar{WL_P}}}{Z_{year}} \qquad Eq.\,3.23$$

The over- and undershoot will deliver three values each for every considered year in the data file.

3.1.4 Investigation on different culvert arrays

To broaden the view on the implementation possibilities of the tidal power plant, not only an array of *18* culvert of of *8* m by *8* m is considered, but also different culvert numbers and cross-sections. These different configurations are executed in three variants: the first variant implements bidirectional turbines, while the second variant accounts for unidirectional turbines, which are active only in inflow situations. The third variant accounts for empty culverts as well, just like the Protide design, described in Section 3.1.2. To determine if an array can be implemented into the Brouwersdam, it has to satisfy the posed requirements mentioned in Table 3. Concerning the dimensional constraints, the width of the tidal power plant may not exceed *400* m. Additionally, other constraints can be established, such as reducing the total width will result in less civil structure and soil- and excavation costs, while reducing on the number of culverts will reduce the costs of machinery and civil structure costs. Additionally, increasing the energy yield, will have a positive effect on the feasibility (Roberts & Mosey, 2013).

To define a range of culvert numbers and dimensions to consider, constraints from the environment have to demarcate the length and values of the culvert arrays to consider. Vrijling, van Duivendijk and Jonkman (2008) proposes to maintain the bottom protection that is present in the core of the Brouwersdam lying under the caissons. This bottom protection is placed at *-12.75* m NAP. This means that the maximum foundation depth is determined. Spengen, Reijneveld, Wit and Tieleman (2014) assumes a culvert floor height of *2* m, while from Figure 17 one can see that the minimum water level retrieved from Rijkswaterstaat (2019) is approximately *-1.5* m NAP. To prevent the ceiling of the duct to stick out of the low water level, which results in a decreased discharge area, the height of the culvert must be constrained. The maximum height of the duct is then:

$$h_{max} = \left|d_{bp}\right| - h_{floor} - WL_{NS,min} = 12.75 - 2.00 - 1.50 = 9.25\,m \qquad Eq.\,3.24$$

This is schematically illustrated in Figure 21.

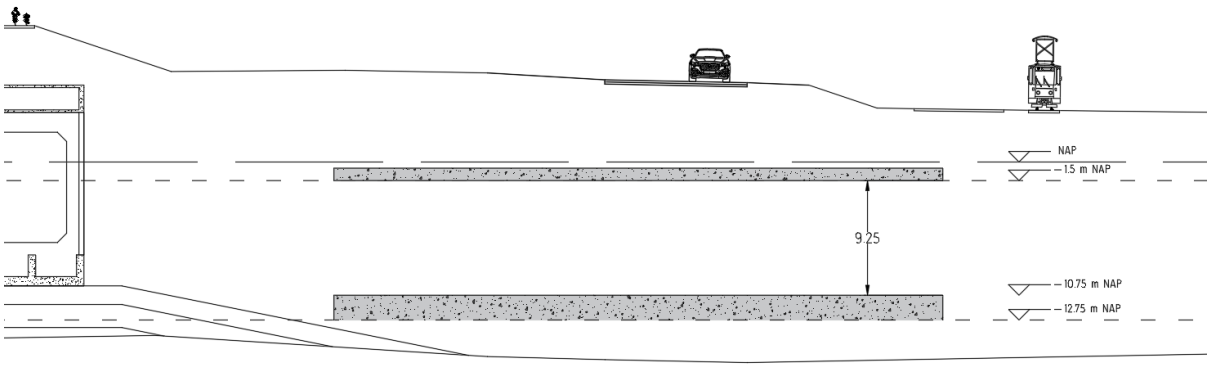

Figure 21: Partial cross-section of the Brouwersdam and a schematical depiction of the maximum height to consider.

Because square cross-sections are considered, the maximum width of the culvert is likewise *9.25* m. For the sake of convenience, this value will be truncated to *9.0* m. Taking into account the culvert width and the width of the walls between the culverts, the total width of the culvert array can be determined by:

$$w_{tot} = Nw + (N+1)w_{wall} \qquad Eq.3.25$$

As posed by Tidal Grevelingen Project (2018), the total width of the culvert array may not exceed *400* m and Spengen et al. (2014) assumes a width of the culvert walls of *1.0* m. Assuming a maximum culvert width of *9.0* m, the maximum amount of culverts to consider can be determined from:

$$Nw + (N+1)w_{wall} \leq 400 \qquad Eq.3.26$$

From Eq. 3.26 follows that the maximum number of culverts to consider is *39*.

To determine the lower limit of the range of the culvert widths, Renewables First (2015) states that low head hydropower sites with a maximum wattage of *25* kW require a turbine house footprint of *16* m^2, which can be translated to a duct width and height of *4* m. Additionally, the lower limit of the amount of culverts can be established. Roughly, one can say that per half tidal cycle (*6* hours and *12.5* minutes) an amount of fluid of *55 000 000* m^3 has to be transported through the culverts. This value of derived from:

$$V = A_{LG}T_r = 110 \cdot 10^6 \cdot 0.5 = 55 \cdot 10^6\ m^3 \qquad Eq.3.27$$

On average, this comes down to an average flow rate of:

$$Q = \frac{V}{t_c} = \frac{55 \cdot 10^6}{6 \cdot 60 \cdot 60 + 12.5 \cdot 60} = 2461\ m^3/s \qquad Eq.3.28$$

From this, the amount of ducts required can be determined, assuming the largest duct dimensions of *9* m by *9* m and a maximum hydraulic head difference of *2.00* m*+0.45* m, which is established by adding the highest North Sea level and the lowest Lake Grevelingen water level.

$$N = \frac{Q}{A_c\sqrt{2g\Delta h}} = \frac{2461}{81\sqrt{2 \cdot 9.81 \cdot 2.45}} = 4.38 \qquad Eq.3.29$$

This value is rounded off to the value of *5*.

The ranges of the width and height and the number of culverts are therefore defined as:

$$N = [5; 39]$$

$$h = [4; 9] \qquad Eq.3.30$$

$$w = [4; 9]$$

For these different configurations, the same algorithm as described in Section 3.1.2 is used. These established ranges will be applied to the three variants. In the third variant, where a number of culverts is left empty, an extra parameter comes into play: the amount of empty culverts *M* in the culvert array. To establish an understanding of the influence of unequipped culverts, the following values of *M*, which are within the range of *N*, are considered:

$$M = [5, 11, 17, 23, 29, 35] \qquad Eq. 3.31$$

3.2 Financial methodology

First an investment costs estimate is established based on a cost estimate published by Mooyaart & van den Noortgaete (2010). The prices of the cost items are scaled down to the price per meter dam width of price per culvert. After that, the considered barrage width and number of culverts can be filled in. With estimate of the investment costs, key numbers to check the feasibility. The considered key numbers are the Net Present Value, Internal Rate of Return, Payback Period and the Levelised Cost of Energy.

The NPV is defined as:

$$NPV = \sum_{\tau=1}^{T_{exp}} \frac{R_t}{(1+q)^{\tau}} \qquad Eq. 3.32$$

The IRR is determined by setting the NPV equal to 0 and solve for discount rate q.

$$\sum_{\tau=1}^{T_{exp}} \frac{R_t}{(1+q)^{\tau}} = 0 \qquad Eq. 3.33$$

The LCoE determines how much money must be made per unit of energy to regain the lifetime costs. This ratio can help to assess the costs of the energy generation compared to other energy generation methods.

$$LCoE = \frac{\sum_{\tau=1}^{T_{exp}} \frac{I_\tau + M_\tau}{(1+q)^{\tau}}}{\sum_{\tau=1}^{T_{exp}} \frac{E_\tau}{(1+q)^{\tau}}} \qquad Eq. 3.34$$

The payback period is the duration required to recover the cost of an investment. The payback period of an investment is an important determinant of whether to undertake the project, as longer payback periods are typically not desirable for investment positions (Vrijling & Verlaan, 2015). The payback period can be calculated by:

$$PBP = \frac{C_{tot}}{R} \qquad Eq. 3.35$$

4 Invariant analysis - water management & power generation

"…De stroom van een rivier, hou je niet tegen
het water vindt er altijd een weg omheen…''
De steen – A.G. Vermeulen

To integrate water management and energy extraction, one must understand the behaviour of the flow under different circumstances. Therefore, three different configurations are regarded first. All consisting of *18* culverts measuring *9* m by *9* m, but the installed turbines are different. The first case considers the Protide design, wherein *11* of *18* are installed with unidirectional turbines, while the remaining culverts are left unequipped. The second case, regards an array with *18* unidirectional turbines. Subsequently, a case with *18* bidirectional turbines is looked into. Finally, a sensibility study to the influence of the assumed culvert wall roughness is considered.

4.1 Case 1 – Tidal Grevelingen Project proposal

This case is proposed by the Tidal Grevelingen Project, a cooperation of, amongst others, Rijkswaterstaat, Province of Zeeland and Province of South Holland. It is also known as the Protide design. This proposal states that *11* of the *18* ducts are equipped with unidirectional turbines, while the remaining *7* are empty. Unidirectional turbines are turbines that only extract energy when the water flows in a specific direction. In this case, no power is generated during outflow conditions. In Case 1a, optimal performance of the turbines is modelled, followed by Case 1b where the turbines are modulated to satisfy the water management standards. In outflow, no energy extraction will occur, according to the proposal from Tidal Grevelingen Project (2018).

4.1.1 Case 1a – Optimal turbine performance

At first, the model is started with the turbines performing optimally, i.e., the degree of reaction is fixed at *2/3* during inflow circumstances. In outflow conditions the degree of reaction is lowered to *0*, illustrated in Figure 24. As can be seen in Figure 22 and Figure 23, both the lower and upper limiting water level are surpassed frequently. The over- and undershoot percentages are depicted in Table 4.

Table 4:Over- and undershoot percentages for Case 1a.

3a	Overshoot OS [%]	Undershoot US [%]
2016	4.4	8.6
2017	4.6	8.6
2018	4.8	8.4

From this can be concluded that modulation of the turbines is required. The modulation of the turbine will be treated in Case 1b. Furthermore, the monthly averaged tidal range varies from *0.44* m to *0.61* m. the monthly maximum tidal range ranges from *0.49* m to *0.94* m. where the tidal range of *0.94* m is presumably an outlier.

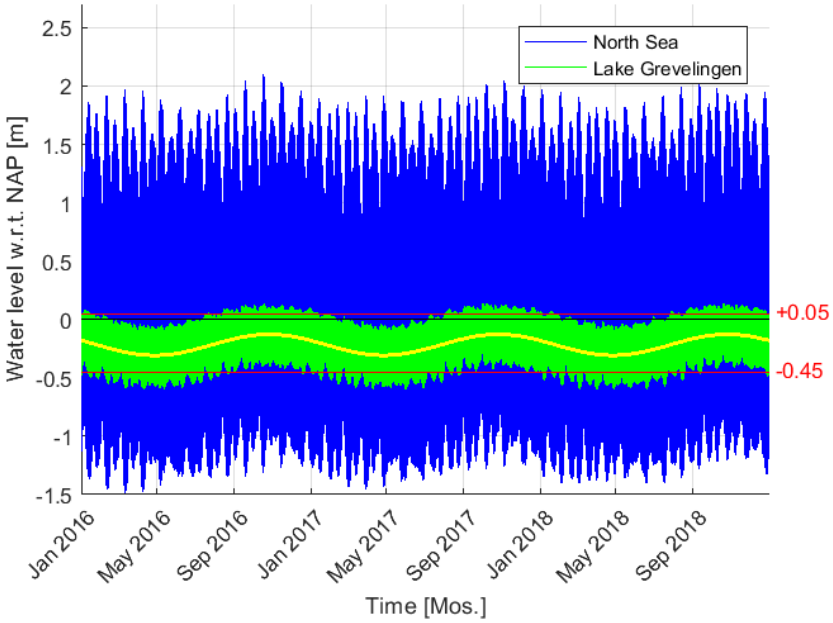

Figure 22: Water level signal for the Tidal Grevelingen Project proposal.

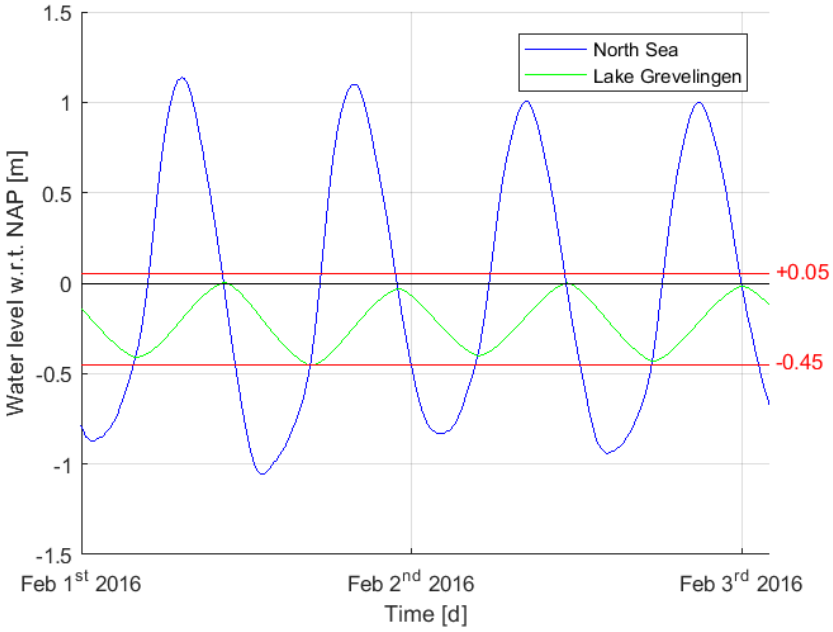

Figure 23: Water level signal for the tidal Grevelingen Project proposal.

The degree of reaction, showed in Figure 24, in Case 1a only varies during transition from inflow regime to outflow regime and vice versa. The empty culverts are not influenced by the turbines and therefore their discharge only depends on the appearing hydraulic head and system loss coefficient.

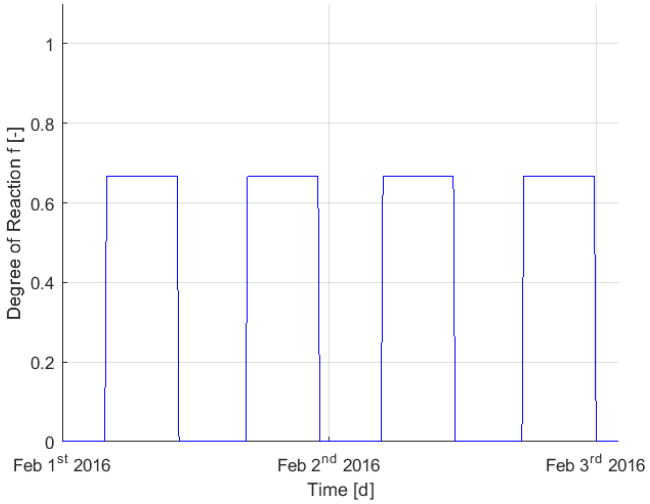

Figure 24: Degree of reaction varying from 2/3 and 0 for Case 3a.

Although it seems that the degree of reaction in Figure 24 alternates instantly, this is not the case. When the signal is considered more closely, as depicted in Figure 25, the degree of reaction jumps from *2/3* to *0* within *1* timestep, which is equivalent to *10* minutes.

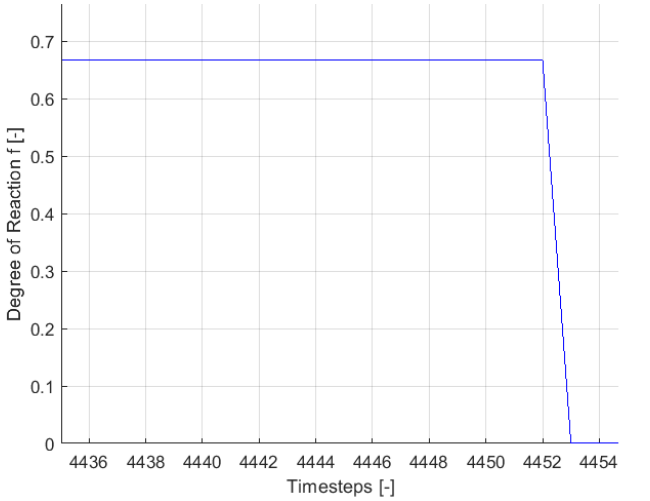

Figure 25: Close-up of the degree of reaction signal depicted in Figure 24.

The power that is extracted by the turbine over time is displayed in Figure 26.

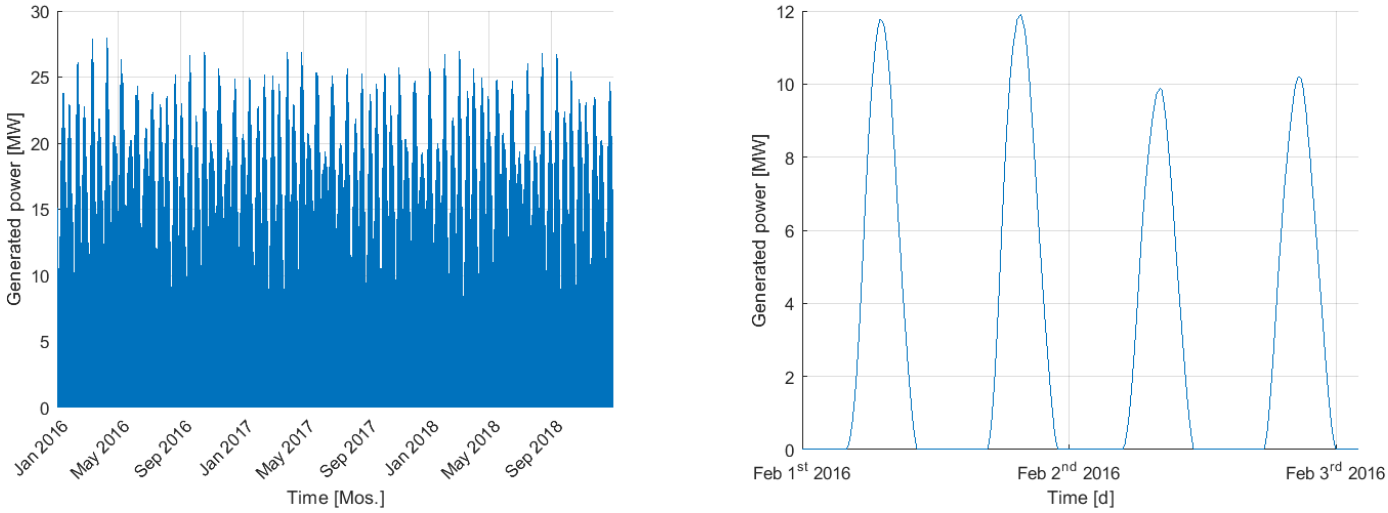

Figure 26: Power signal based on the Tidal Grevelingen project proposal

In Table 5 the mean and maximum generated power and the mean annual extracted energy can be found.

Table 5: Mean and maximum power output and mean annual energy yield for Case 1a.

	Mean power $\bar{P}$ [MW]	Maximum power P_{max} [MW]	Annual mean energy yield E [GWh]
Extracted by turbine	4.02	27.98	35.26

4.1.2 Case 1b – Modulated turbine performance

Because the overshoot percentage and the mean and maximum tidal range in Case 1a are not according to the set requirements, turbine modulation has to take place. Modulation of the turbines can only occur in inflow conditions due to the turbines not extracting energy from the fluid in outflow situations. The extent to which the water level behaves depends on the value of the upper precautious water level. Regarding different values of the upper precautious water level result in different values of the over- and undershoot exceedance percentages. Based on the North Sea water level dataset from 2016-2018, in Figure 27 can be seen that the precautious water level should lie in the interval between -*0.18* m NAP and -*0.09* m NAP. If a higher precautious water level is assumed, the limiting overshoot exceedance percentage of *1* % is surpassed, while assuming upper precautious water levels lower than -*0.18* m NAP will surmount the constraining undershoot exceedance percentage of *10* %.

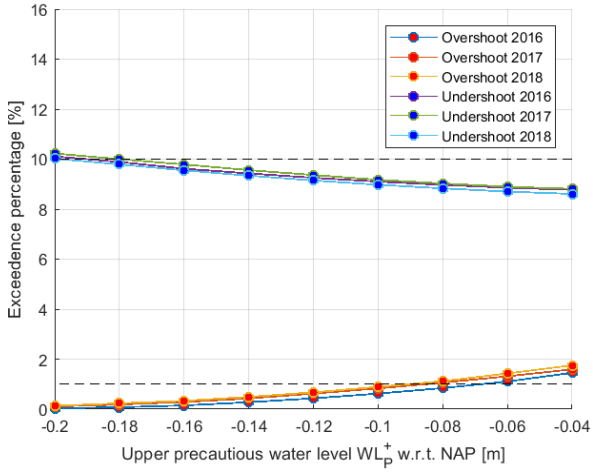

Figure 27: Exceedance percentages for different upper precautious water levels.

The influence of varying the upper precautious water level on the average $\overline{T_r}$ and maximal tidal range $T_{r,\,max}$ is of minor influence looking at Figure 28. In this graph, the monthly averaged and maximum tidal range of June 2018 and December 2018 are illustrated. By varying the upper precautious water level, the tidal range values are not affected in a significant amount.

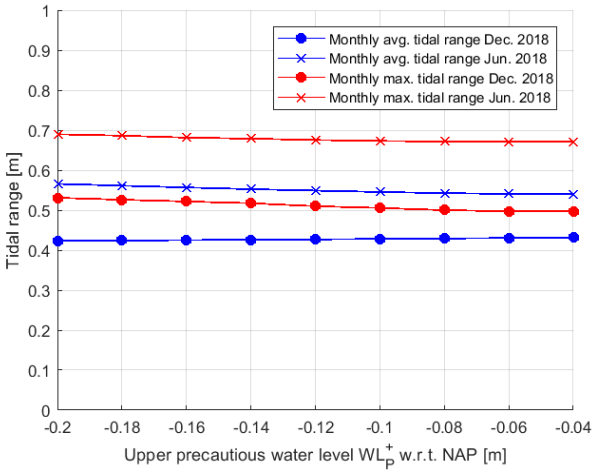

Figure 28: Average and maximum tidal ranges for different values of the upper precautious water level.

As far as the power and energy extraction concerns, the impact of varying the upper precautious water level is small, which can be seen in Figure 29.

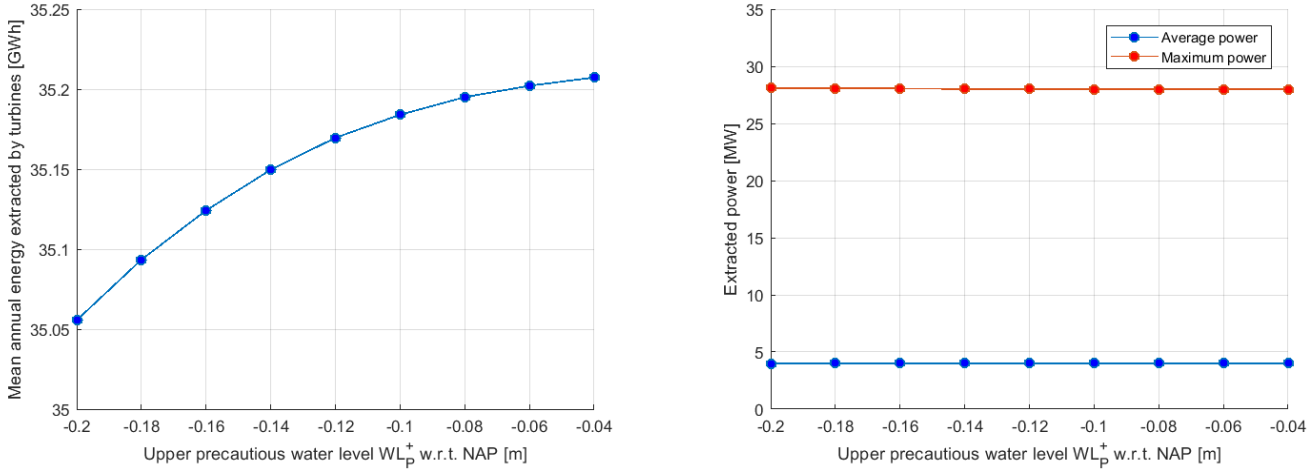

Figure 29: Mean and maximum power for different upper precautious water levels.

Assuming an upper precautious water level in the middle of the upper precautious water level interval. At WL_P^+ = *-0.14* m, the water level signal is calculated and depicted in Figure 30 and Figure 31:

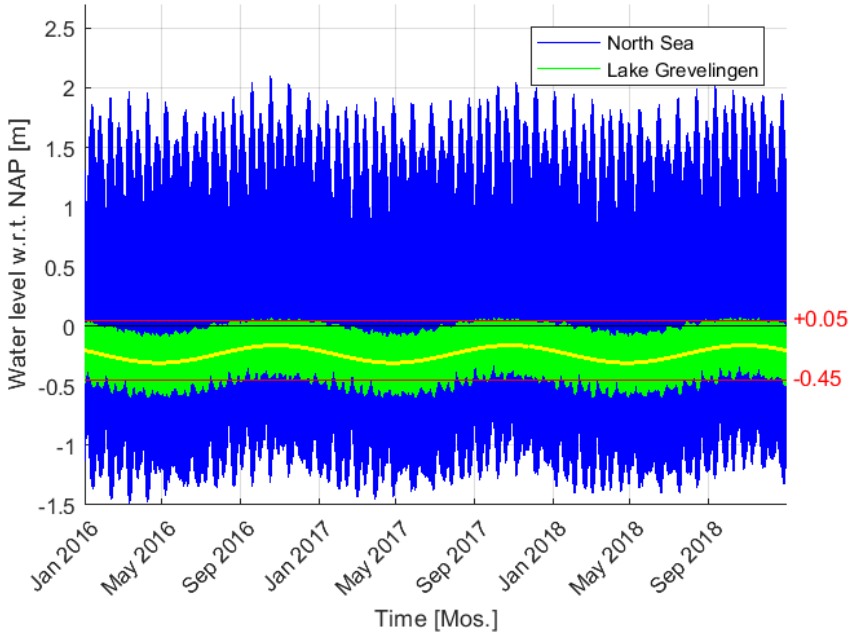

Figure 30: Water level signal for Case 1b.

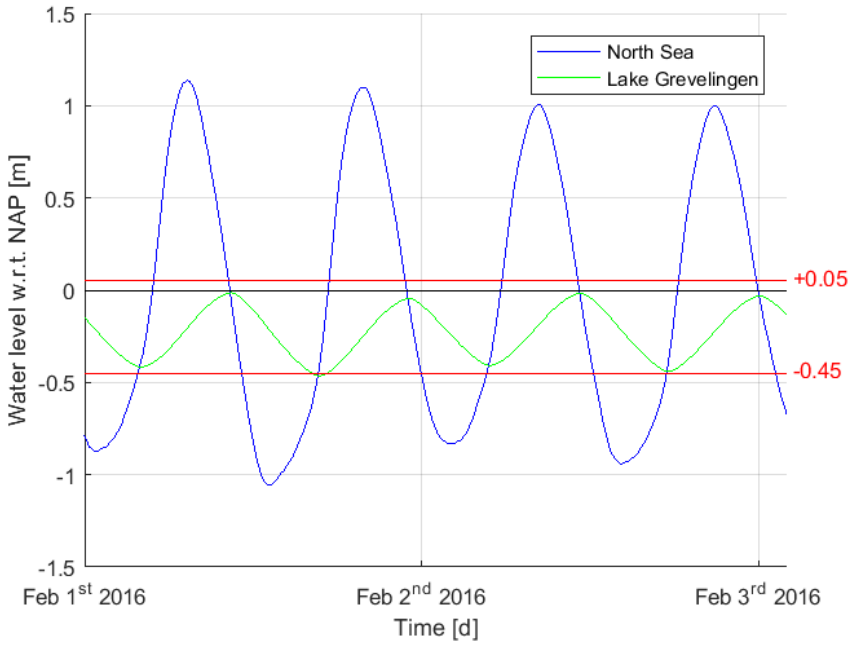

Figure 31: Water level variation for Case 3b assumptions for two days.

In Figure 30 one can see that the upper limiting water level is surpassed less frequent than Case 1a and satisfying the overshoot standards. The exceedance percentages of the upper limiting water level are depicted in Table 6. The undershoot values are increased compared to Case 1a due to the turbine modulation, but are still within the posed boundary.

Table 6:Under- and overshoot percentages for Case 1b.

3b	Overshoot OS [%]	Undershoot US [%]
2016	0.3	9.4
2017	0.4	9.6
2018	0.5	9.3

The monthly averaged and maximum tidal range vary respectively from *0.41* m to *0.61* m and *0.48* m to *0.94* m. Where the last value is still presumably an outlier. The monthly averaged and maximum value per month considered in the dataset are attached in Appendix 1.

The mean and maximum power generated and the mean annual energy yield are depicted in Table 7. The behaviour of the generation of power is depicted in Figure 32.

Table 7: Mean and maximum power output and mean annual energy yield for Case 3b.

	Mean power $\bar{P}$ [MW]	Maximum power P_{max} [MW]	Annual mean energy yield E [GWh]
Extracted by turbine	4.01	28.03	35.15

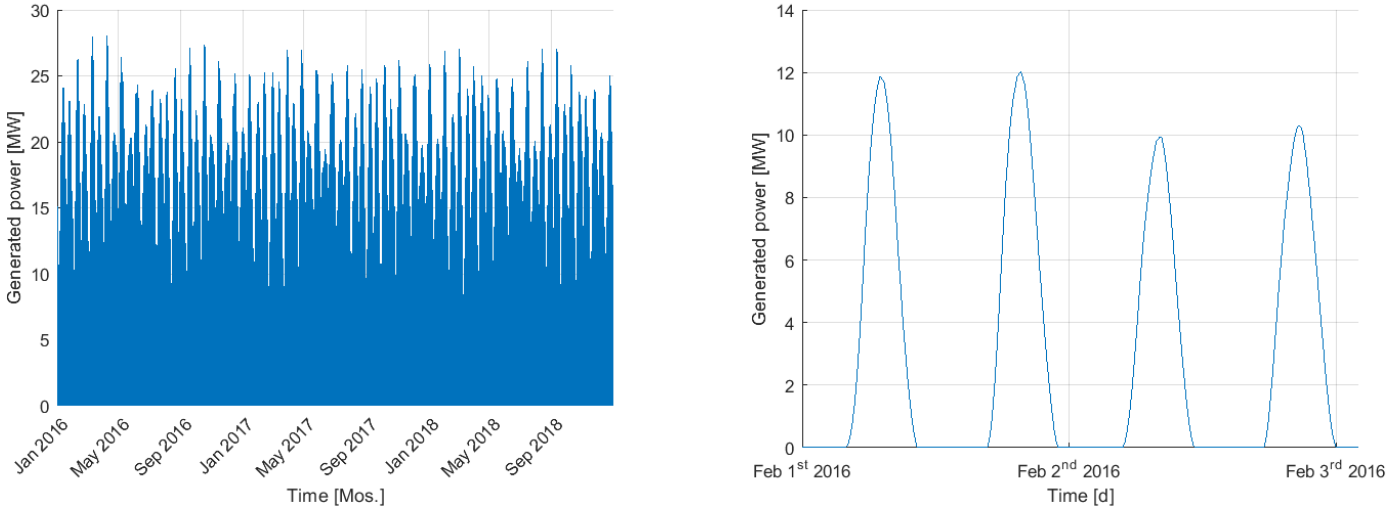

Figure 32: Power signals for Case 3b for full data set and two days of data.

Considering the degree of reaction signal of Case 33b, one can see in the right-hand side graph of Figure 33 that the turbines are less modulated during the periods around May. This is caused by the lower high water levels during these months, causing the turbines to less influence the discharge. Furthermore, the turbines are only modulated during inflow intervals, which explain the increased degree of reaction values at the end of the inflow cycles.

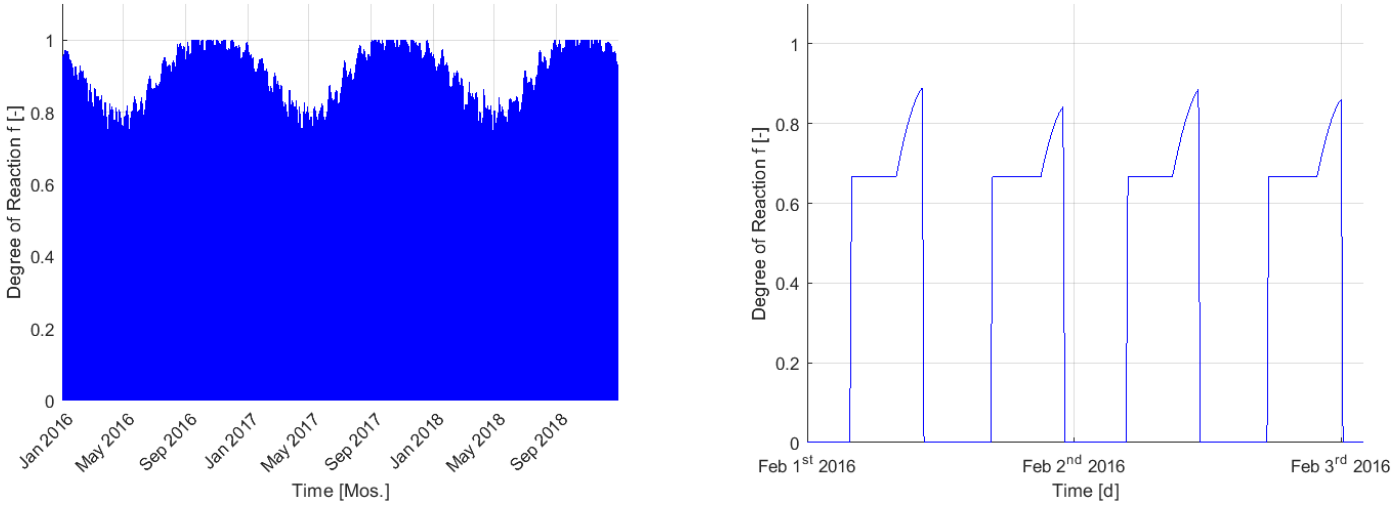

Figure 33: Degree of reaction signal for Case 3b.

4.1.3 Discussion on the results

Considering the problem from a power generating point of view and comparing Case 1a and 3b, the decrease of *0.3* % in mean annual energy yield seems plausible. From water management point of view, the under- and overshoot requirements are also met. Nevertheless, regarding the expected sea level rise in the coming future and the fact that only three years of data is considered, the undershoot exceeding the threshold value is probable. Besides, the tidal range throws a spanner in the works. For the period of August to December, the values are very close to the desired values. But in the remaining months, where the undershoot occurs the most, the tidal range values increase to values which cannot accepted. To decrease the tidal ranges in these periods, it seems wise to perform turbine modulation to

increase the low water level and subsequently decrease the tidal range. Therefore, in the next case, a setup is regarded wherein no empty culverts occur, while the turbines are still functioning unidirectionally.

4.2 Case 2 – Flow through culverts equipped with unidirectional turbines

Case 2 considers a scenario of *18* culverts, all equipped with unidirectional turbines, wherein no energy is generated during the period where the water level is Lake Grevelingen is higher compared to the water level in the North Sea i.e., the situation where water flows out of Lake Grevelingen. The turbines will be rotating freely or are raised from the water according to the Tidal Grevelingen Project (2018) and do not influence the flow during drainage of the lake. To account for zero power generation during outflow, the degree of reaction is set to *0* and, because it is still assumed that the turbines perform at optimal degree of reaction, *2/3* during inflow. Due to the degree of reaction equal to *0* at outflow conditions, no energy is extracted by the turbines and the discharge subsequently increases. Case 2b will account for modulation of the turbines in order to comply to the set water level boundaries.

4.2.1 Case 2a – Optimal unidirectional turbine performance

In this case, the discharge is calculated according to the algorithm stated below:

$$Q_n = A_c \sqrt{\frac{2g(1-f_n)\Delta h_n}{C_{sys,n}}} = A_c \sqrt{\frac{2g(1-f_n)(WL_{NS,n} - WL_{LG,n})}{1 + f_{f,n}\frac{l}{D_h} + K_e + K_c}} \qquad Eq.\,4.1$$

$$WL_{LG,n+1} = WL_{LG,n} + \frac{NQ_n}{A_{LG}}\Delta t$$

With:

$$f = \begin{cases} 0 \; for \; \Delta h \leq 0 \\ \frac{2}{3} \; for \; \Delta h > 0 \end{cases}$$

Figure 34 and Figure 35 show the water level variation of Lake Grevelingen in according to the above mentioned numerical scheme. Note that the signal is shifted down compared to Case 1a. This can be explained by the fact that the discharge out of the lake is greater than the discharge into the lake, because no energy is extracted from the water in outflow conditions.

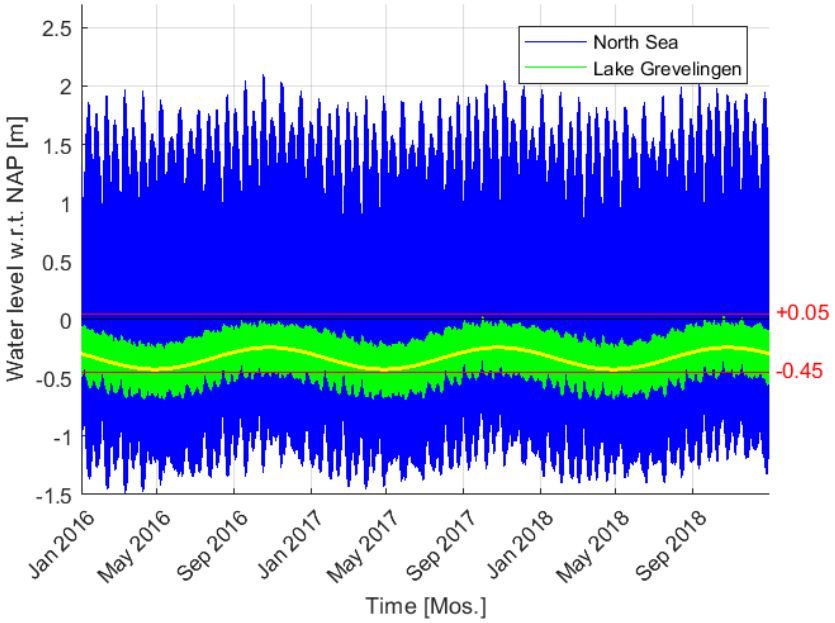

Figure 34: Water levels in Lake Grevelingen according to the Case 2a scenario for 2016-2018.

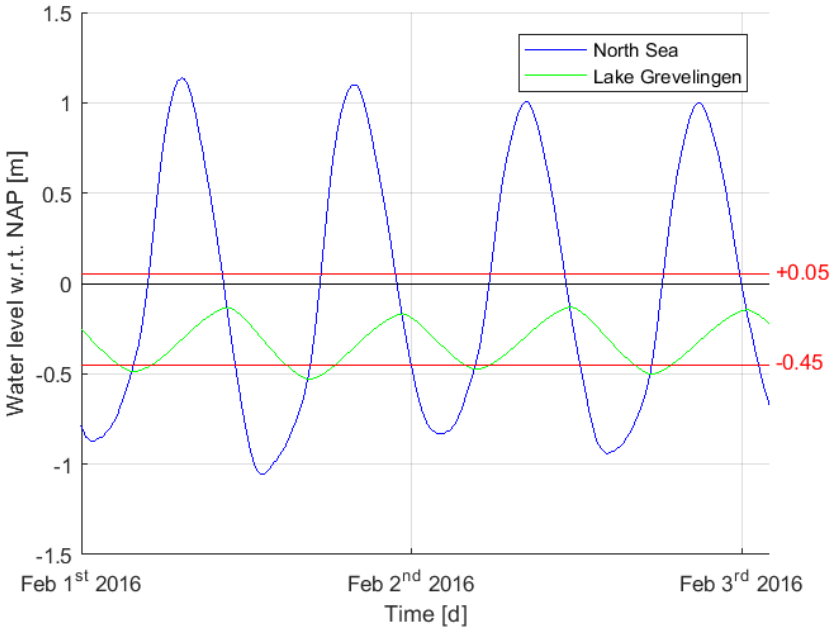

Figure 35: Water levels in Lake Grevelingen according to the Case 2a scenario.

This results in an excessive exceedance of the lower limiting water level, as can be seen in Table 8. The upper limiting water level is not exceeded.

Table 8: Annual over- and undershoot percentages for Case 2a.

	Overshoot OS [%]	Undershoot US [%]
2016	0	23.6
2017	0	23.8
2018	0	23.6

The monthly averaged and maximum tidal range are in the order of *0.65* m and *0.81* m. The monthly values of the monthly averaged and maximum tidal range are attached in Appendix 1. The extracted power is depicted in Figure 36. One can see that the number of peaks is reduced due to the absence of power generating capacity during outflow.

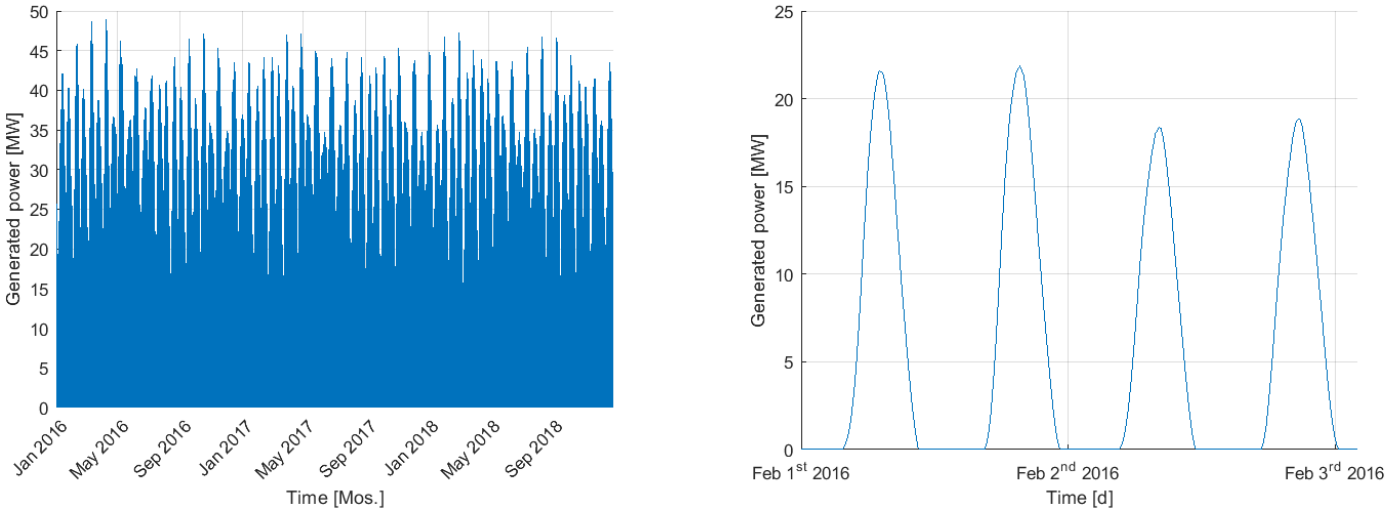

Figure 36: Power graphs according to the Case 2 scenario.

The parameters describing the power output and mean annual energy yield are displayed in Table 9.

Table 9: Mean and maximum power output and mean annual energy yield for Case 2a.

	Mean power $\bar{P}$ [MW]	Maximum power P_{max} [MW]	Annual mean energy yield E [GWh]
Extracted by turbine	7.64	48.90	66.94

4.2.2 Case 2b – Modulated unidirectional turbine performance

Because the lower limiting water level is exceeded too frequently and the tidal ranges are not according to the standards, alteration of the turbines is required. But because the turbines are not functioning during outflow periods, the turbines are unable to extract energy from the water during those periods. This means that nothing changes compared to Case 2a. The turbines are unable to extract energy from the water because they are free spinning i.e., the degree of reaction is equal to *0*. Therefore, the water level signal in Figure 37 and Figure 38 is identical to the water level signal considered in Case 2a.

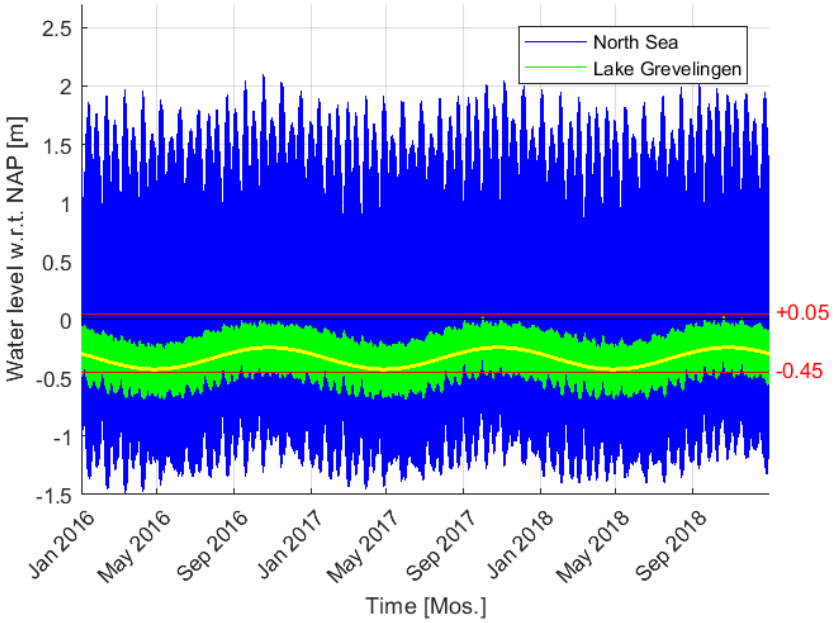

Figure 37: Water levels according to Case 2b scenario.

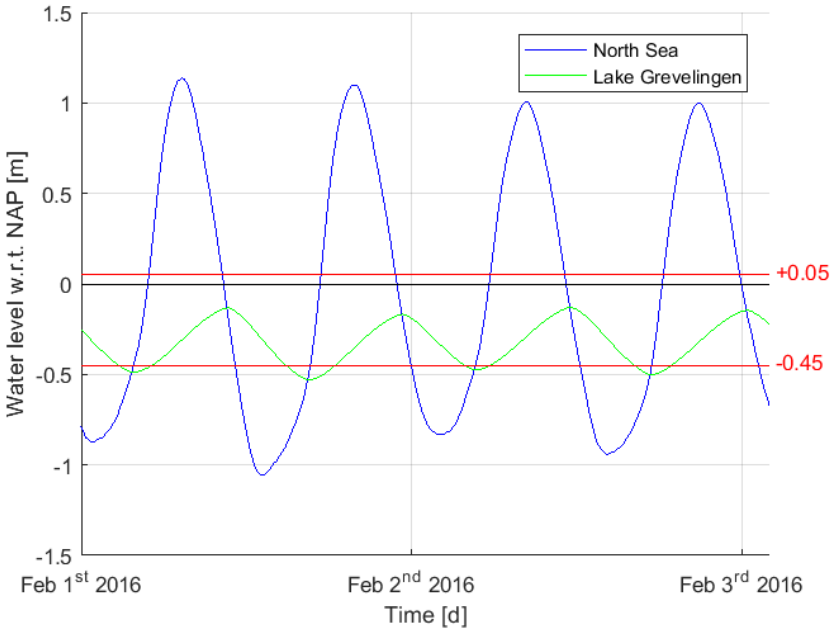

Figure 38: Water levels according to Case 2b scenario.

Not only the water level signal and the hydraulic key numbers stay unaffected, also the extracted energy and the generated power are not changing compared to Case 2a.

4.2.3 Discussion on the results

Comparing Case 2a and Case 2b, no difference in water level and power generation occurs due to the turbines being unable to perform measures for the purpose of water management, because they are set to a non-extracting mode during outflow. The turbines cannot harness energy from the water and therefore, the discharge and additionally the water level in the lake is not influenced. This comparison proves that if the lower limiting water level is surpassed, energy extraction has to occur to enable water level regulation during outflow conditions. Besides, the tidal range is also not affected, which results in a value that is too high. To offer a solution to the outflow problem, the next case will implement bidirectional turbines.

4.3 Case 3 – Flow through culverts equipped with bidirectional turbines

In Case 3, the *18* culverts in the array are implemented with *18* bidirectional turbines. As a result of that, power will be generated during inflow and outflow. At first, the turbines are modelled to perform at their optimal power generation capacity, where the degree of reaction is equal to *2*/3. Moreover, Case 3b takes into account a modulated degree of reaction which feeds the water management requirements.

4.3.1 Case 3a – Optimal bidirectional turbine performance

The numerical time integration scheme of Case 3a is depicted in eq. 4.2:

$$Q_n = A_c\sqrt{\frac{2g(1-f_n)\Delta h_n}{C_{sys,n}}} = A_c\sqrt{\frac{2g(1-f_n)(WL_{NS,n}-WL_{LG,n})}{1+f_{f,n}\frac{l}{D_h}+K_e+K_c}} \qquad Eq.\,4.2$$

$$WL_{LG,n+1} = WL_{LG,n} + \frac{NQ_n}{A_{LG}}\Delta t$$

The corresponding water level signal, determined by the algorithm in Eq 5.3 is depicted in Figure 39 and Figure 40.

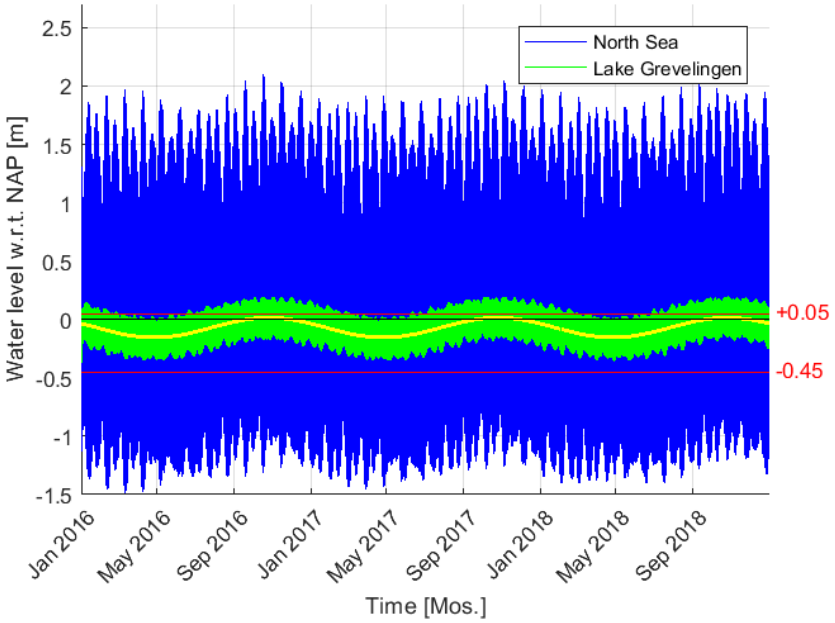

Figure 39: Water level variation in Lake Grevelingen with turbines implemented in the culverts.

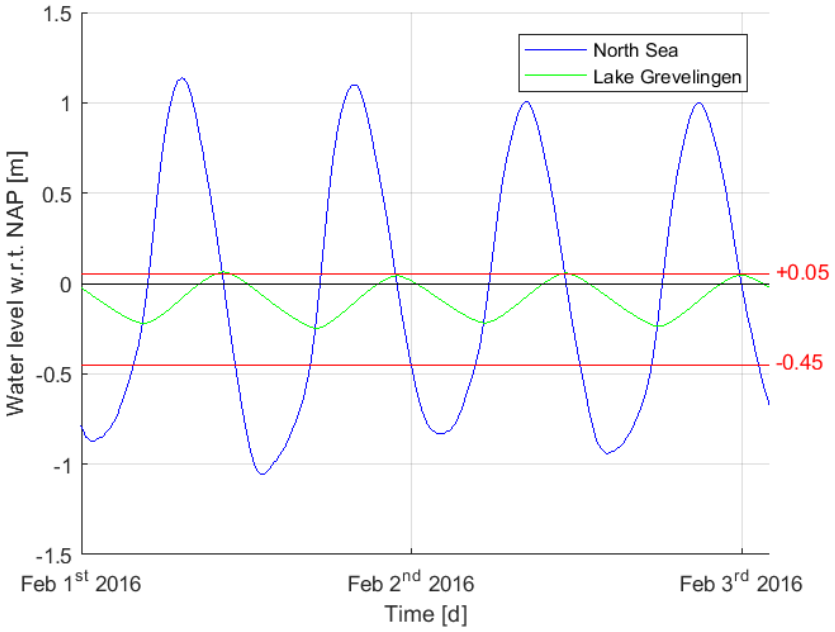

Figure 40: Water level variation in Lake Grevelingen with turbines implemented in the culverts for February 1st and February 2nd 2016.

As can be seen in Figure 39, the amplitude of the tidal range is decreased caused by the turbines extracting energy from the water. Because of the energy extraction, less water is transported through the ducts per unit of time. This decrease of the tidal range subsequently results in a reduced over- and undershoot percentage, as can be seen in Table 10.

Table 10: Annual over- and undershoot percentages.

	Overshoot OS [%]	Undershoot US [%]
2016	17.9	0
2017	18.3	0
2018	18.4	0

Because the overshoot percentage depicted in Table 10 are not satisfying the posed overshoot requirements. Therefore, modulation of the turbines can influence the discharge through the culverts such that the overshoot requirement is satisfied.

The monthly averaged and maximum tidal range are in the order of *0.31* m and *0.36* m. The values per month in the considered dataset can be found in Appendix 1.
Regarding the energy extraction of the turbines, Figure 41 depicts the generated power during the considered water level data set. By integrating the power signal, the energy yield can be determined. Statistical parameters of the power data set are shown in Table 11.

Table 11: Power generation key numbers of Case 1a.

	Mean power $\bar{P}$ [MW]	Maximum power P_{max} [MW]	Mean annual energy yield E [GWh]
Extracted by turbine	9.18	40.36	80.45

Furthermore, it is assumed that the turbines do not have a power value that can maximally be achieved. Thus, the turbines are not restrained by so-called 'Power capping'. Power capping truncates the power generation of a turbine to a specific value, when that value is exceeded. If power capping is not performed, turbines are manufactured to generated large peak power, which increases the turbine costs, while these peaks hardly occur. From an economical point of view, it is often more feasible to perform power capping and release large power peaks and install a turbine that is more suitable for the power values that occur in a larger quantity.

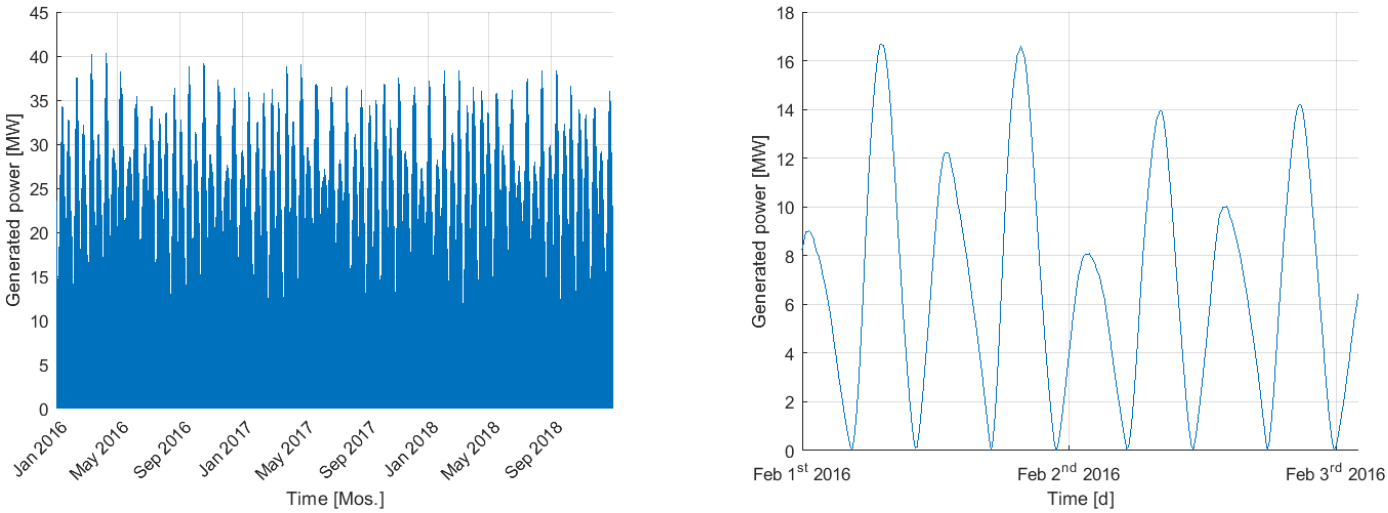

Figure 41: Power generation graph for Case 1a.

4.3.2 Case 3b –Modulated bidirectional turbine performance

Regarding Case 3a, from which Case 3b originates, the lower limiting water level is not reached. Therefore, the undershoot percentage does not need to be reduced. Consequently, the lower precautious water level can be set closer to the lower limiting water level to establish optimal turbine performance. To satisfy the overshoot requirement, turbine modulation has been executed to reduce the overshoot percentage. In this case, the lower precautious water level is set to *-0.40* m NAP. After analysing the numerical algorithm, it appeared that setting the upper precautious water level to *-0.045* m NAP, result in an overshoot percentage of *0* % and a larger region of optimal turbine behaviour. Table 12 depicts the annual under- and overshoot percentages.

Table 12: Annual over- and undershoot percentages for Case 1b.

	Overshoot OS [%]	Undershoot US [%]
2016	0	0
2017	0	0
2018	0	0

The water level signal in Case 3b is depicted in Figure 42 and Figure 43. Note the water level not exceeding the upper limiting water level anymore. The monthly averaged and maximum tidal range are in the order of *0*.30 m and *0*.35 m. The values of the monthly averaged and maximum tidal range per month in the considered data set are depicted in Appendix 1.

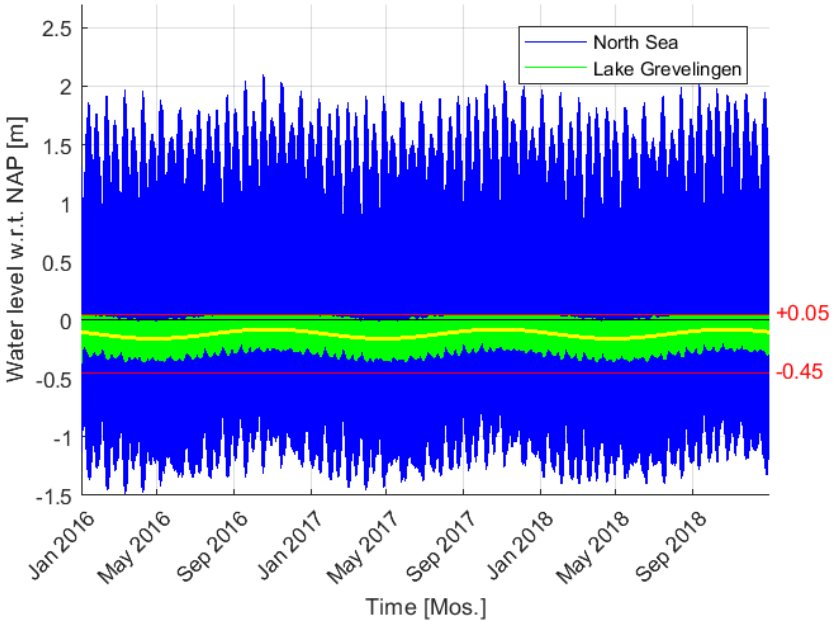

Figure 42: Water levels during 2016-2018 for Case 1b scenario.

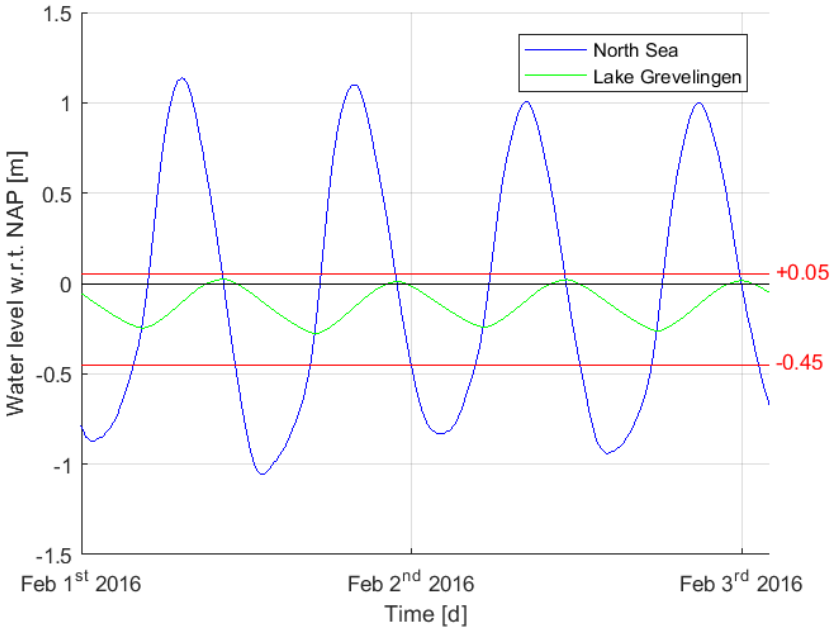

Figure 43: Case 1b scenario water levels for water level data from February 1st 2016 to February 3rd 2016.

Considering the graphs of the altering degree of reaction in Figure 44, the month May in every year catches the eye. The graphs depict global throughs around the month May, this is because the precautious water level is not surpassed frequently and therefore the modulation of the turbines is less urgent. As can be seen in the right graph of Figure 44, the degree of reaction jumps back to the value of *2/3*. At these time moments, the water level in the North Sea is greater than the water level in the lake which means a water flow out of Lake Grevelingen. This means that the water level in the lake is already retreating without the turbines modulating. For energy harvesting purposes, the degree of reaction goes back to its optimal degree of reaction.

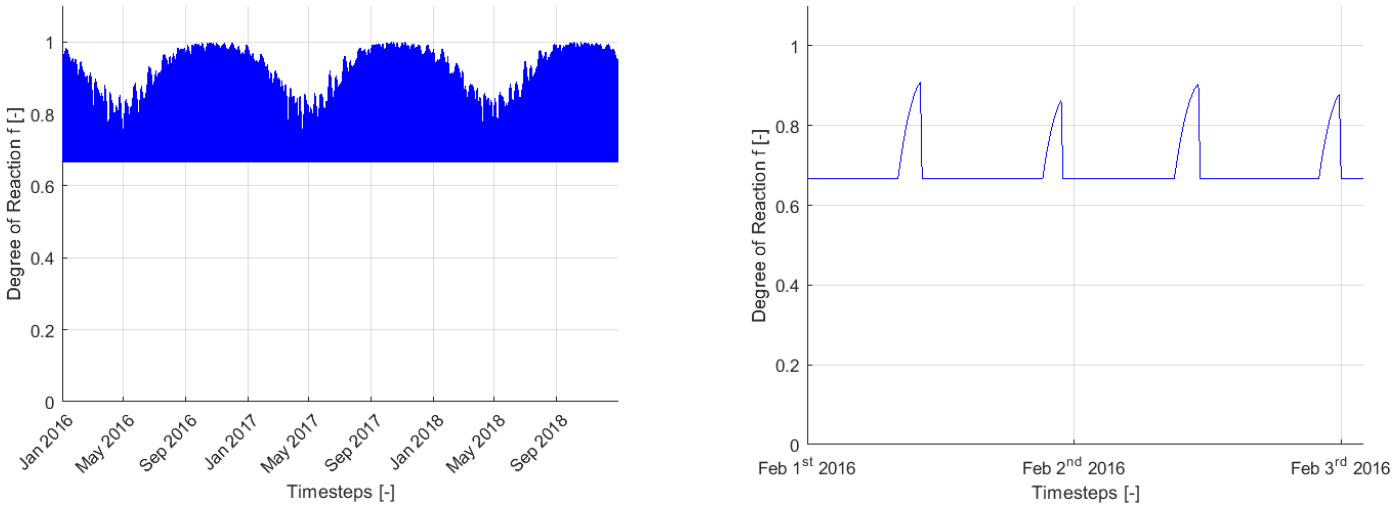

Figure 44: Variation of degree of reaction over time for Case 1b.

Although the degree of reaction seems to instantaneously change back to the value of *2/3* in Figure 44, this is not the case. When the ‘’*Shark-fin*’’-signal is regarded more closely, one can see that the degree of reaction shifts back to the value of *2/3* after the peak of the ‘’*Shark-fin*’’ is reached. This is illustrated in Figure 45. At this point, the local maximum of the water

level signal is reached and outflow sets in again. The degree of reaction changes from its peak value to the value of *2/3* within the duration of one timestep, in this case *10* minutes.

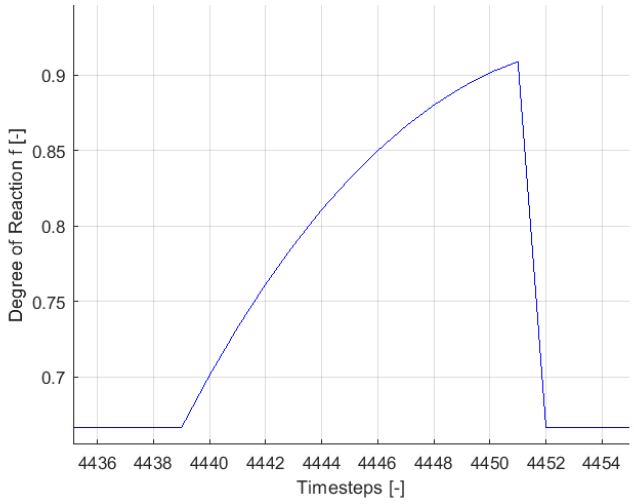

Figure 45: Close-up of the "Shark-fin" signal for Case 3b.

With the modulated degree of reaction signal, the modulated power signal can be derived, as can be seen in Figure 46. The corresponding mean power output, maximum power output and mean annual energy yield is depicted in Table 13.

Table 13: Energy parameters for the situation in Case 3b.

	Mean power $\bar{P}$ [MW]	Maximum power P_{max} [MW]	Mean annual energy yield E [GWh]
Extracted by turbine	8.97	41.71	78.58

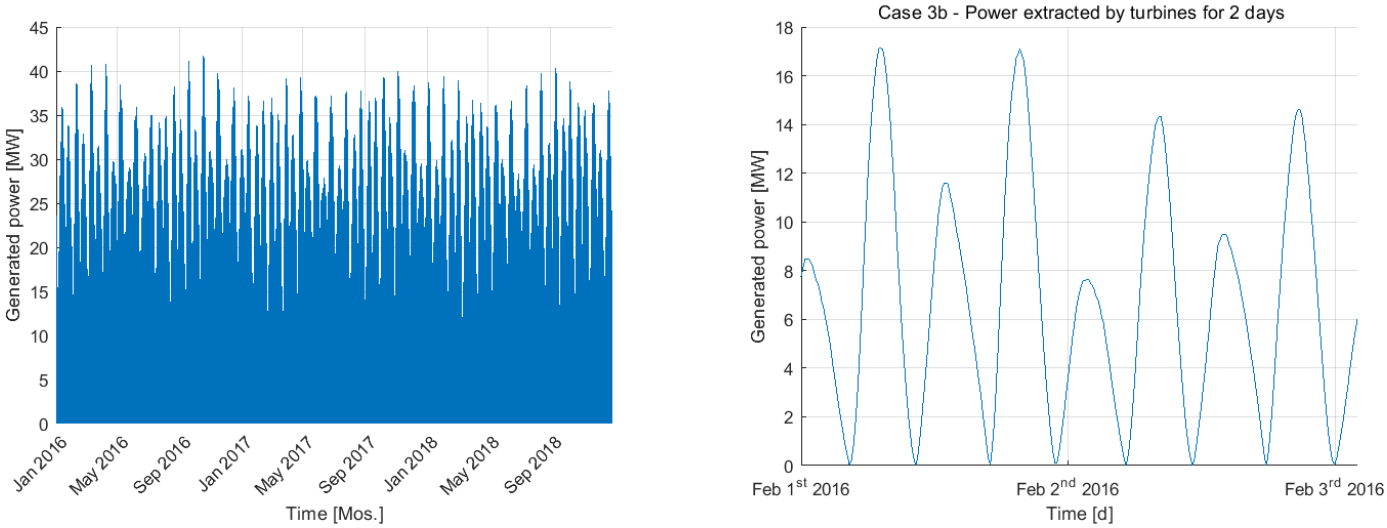

Figure 46: Power graphs according to the Case 3b scenario.

4.3.3 Discussion on the results

Considering Case 3a and Case 3b, the main difference can be seen in the overshoot. Without turbine modulation, the upper limiting water level is exceeded too frequent, wherein the modulated case, the upper limiting water level is not exceeded anymore.

On the contrary of Case 2, the tidal range values in Case 3 are smaller than requested. To increase these values, lowering the degree of reaction from its optimal point during outflow will increase the outflow discharge, further draining the lake, which lowers the lower water and increases the tidal range.
Regarding the mean annual energy yield, the energy harvest that is dissipated to enhance the water management criterion is relatively small compared to the mean annual energy yield of Case 3b: *2.3* %. The energy yield in both Case 3a and 5b is higher than desired by Tidal Grevelingen Project (2018). Although, this research displays an upper limit, because the loss due to mechanical and electrical losses are not accounted for. Also, the presence of the turbine is not considered in the system loss coefficient, which will increase the system loss coefficient more.

4.4 Sensitivity study of the culvert wall roughness height

To investigate the systems sensitivity to the roughness height of concrete culverts walls, a sensitivity study is executed. In this study the impact of the roughness height on a culvert's discharge is examined. Herein, Case 3a will be considered to examine the influence of the roughness height. According to Elger et al. (2014) the roughness height of concrete can be valued from *0.3* mm to *3* mm, depending on the concrete's composition and treatment. The *Darcy* friction factor is determined for the beforementioned range of the roughness height according to the *Swamee-Jain* approximation and is depicted in Figure 47. Herein, the hydraulic diameter is set on *8* m and the flow is considered to be fully turbulent, i.e. the *Reynolds* number is assumed to be high, such that the *Darcy* friction factor does not vary much with the increase of the *Reynolds* number. This occurs approximately at *Reynolds* numbers of 10^7 and higher, as can be seen in the *Moody*-diagram in Figure 48.

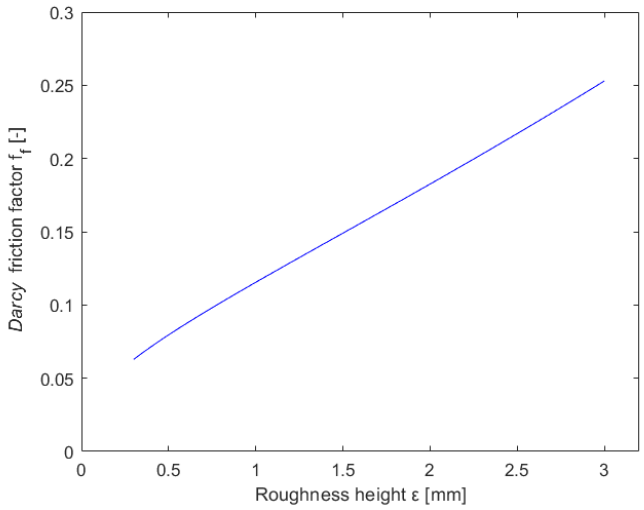

Figure 47: Relation between the Darcy friction factor and the culvert roughness height according to the Swamee-Jain approximation.

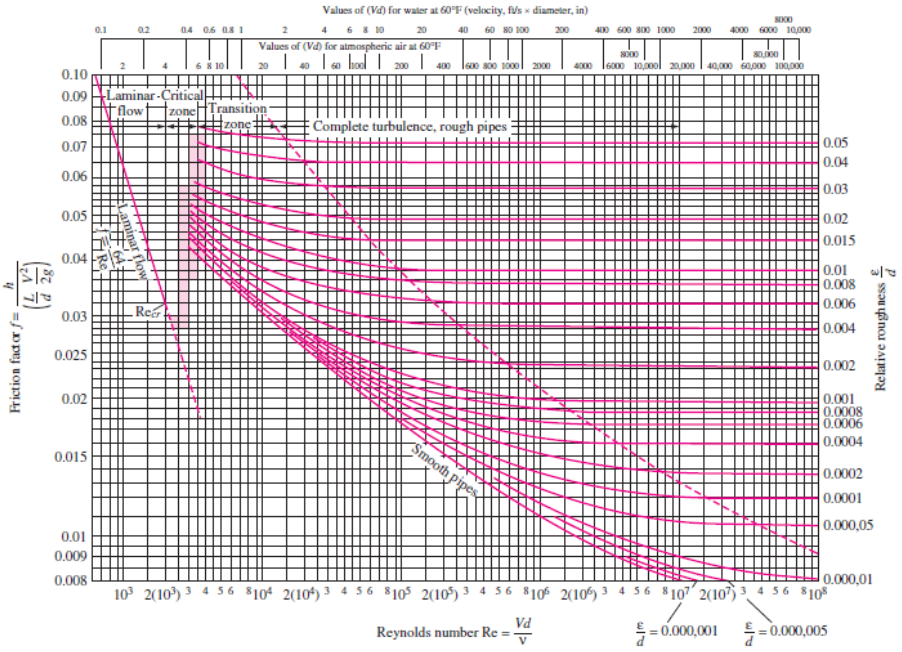

Figure 48:Moody diagram retrieved from White (2014).

To Evaluation of the sensibility of the Brouwersdam tidal power plant system on the *Darcy* friction factor and its influence on the discharge, five equally spaced roughness height values within the set boundaries of *0.3* mm and *3* mm are regarded and the most commonly occurring discharge is calculated for fully turbulent flow through a single duct and an optimal degree of reaction of the turbine. Figure 49 depicts the development of the discharge as the roughness height of the culvert walls increases.

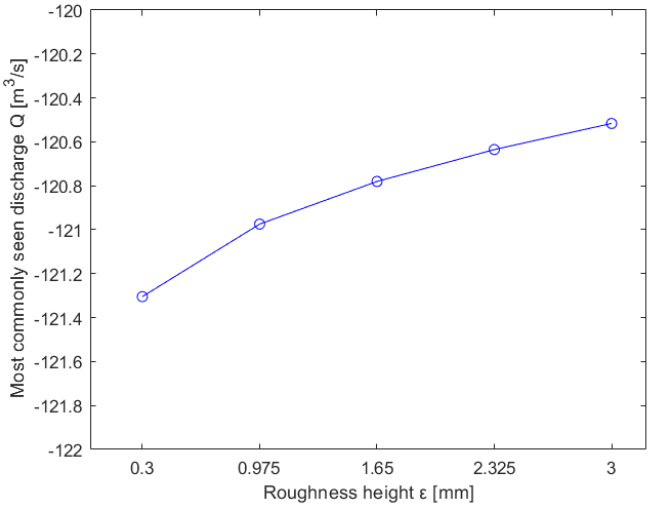

Figure 49: The most commonly occurring discharge for different culvert wall roughness heights.

As can be seen in Figure 49 is the system not very sensible to the increase of the roughness height. The discharge increase over the whole roughness height interval amounts approximately *0.64* %. Physically, this can be explained by the fact that the total cross-sectional area of the culvert is relatively large compared to the cross-sectional area of the culvert that is disturbed due to the presence of the culvert walls.

The undisturbed cross-sectional area remains relatively large compared to the disturbed part of the cross-sectional area when the roughness height is increased. Thereupon, the discharge is not noticeably influenced by the increase of the roughness height.

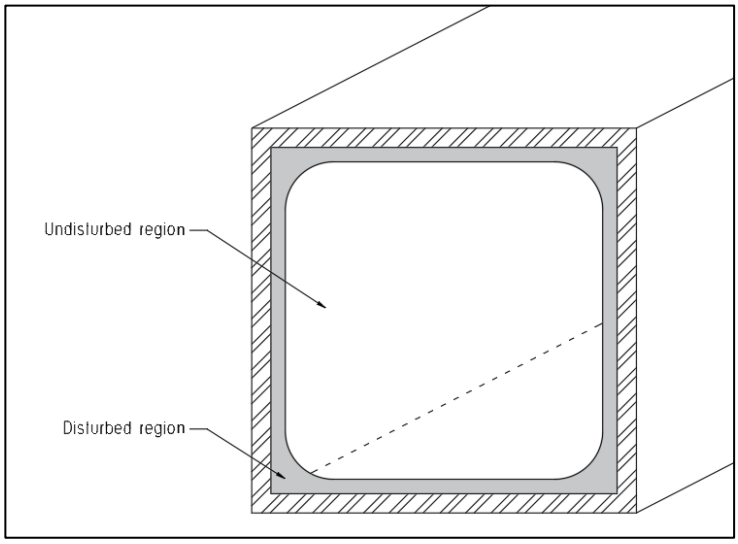

Figure 50: graphical representation of the disturbed and undisturbed regions in the culverts cross-section.

5 Multivariable analysis – water management & power generation

"No man ever steps in the same river twice,
for it is not the same river and he is not the same man''
Heraclitus

To further evaluate the three regarded culvert configurations, variable values of the culvert cross-sectional area and number of culverts is regarded.

5.1 Unidirectional turbines combined with unequipped culverts

In the earlier analysed Protide design in Paragraph 4.1, a combination of equipped and unequipped culverts is regarded. To investigate the influence of these empty culverts on the water management and power generation standards, six cases will be considered wherein a different number of empty culverts is examined. The number of the unequipped culverts lie within the range of the considered number of culverts in the array *N*. The considered numbers of unequipped culverts are:

$$M = [5, 11, 17, 23, 29, 35]$$

When the value of *M* is larger than the total amount of culvert in an array, it is assumed that no equipped culverts occur and that the value of *M* is equal to the total amount of culverts in the array. Therefore, the discharge cannot be controlled and the energy extraction is non-existent. Furthermore, in this case, fulltime turbine modulation is applied as it appeared that intermittent turbine modulation is not sufficient.

5.1.1 Energy yield

Self-evident, for energy generation yields that the number of equipped culverts will increase the annual energy yield. As can be seen in Figure 51, the energy yield for situations where the amount of empty culverts is greater or equal to the total amount of culverts, which implies that no culvert with turbines installed are present in the array. Subsequently, no power is generated and the annual energy yield is zero. Moreover, the greater the number of non-generating culverts, the lower the energy yield. Figure 51 depicts the decrease of the energy yield at *N, w = (39, 9)*. Appendix 2 depicts the results of the other combinations of *N* and *w*.

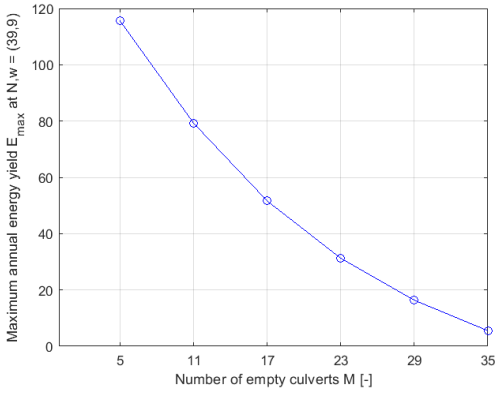

Figure 51: Plot of maximum energy output at N, w = 39,9.

5.1.2 Under- and overshoot

As part of the water management criteria, the over- and undershoot are examined. Considering the undershoot. As the number of empty culverts increases, the undershoot percentage decreases. Figure 52 depicts the undershoot percentages for different culvert dimensions, culvert configurations and number of empty culverts for 2018. The graphs of the undershoot in 2016 and 2017 show a similar behaviour and are therefore not shown.

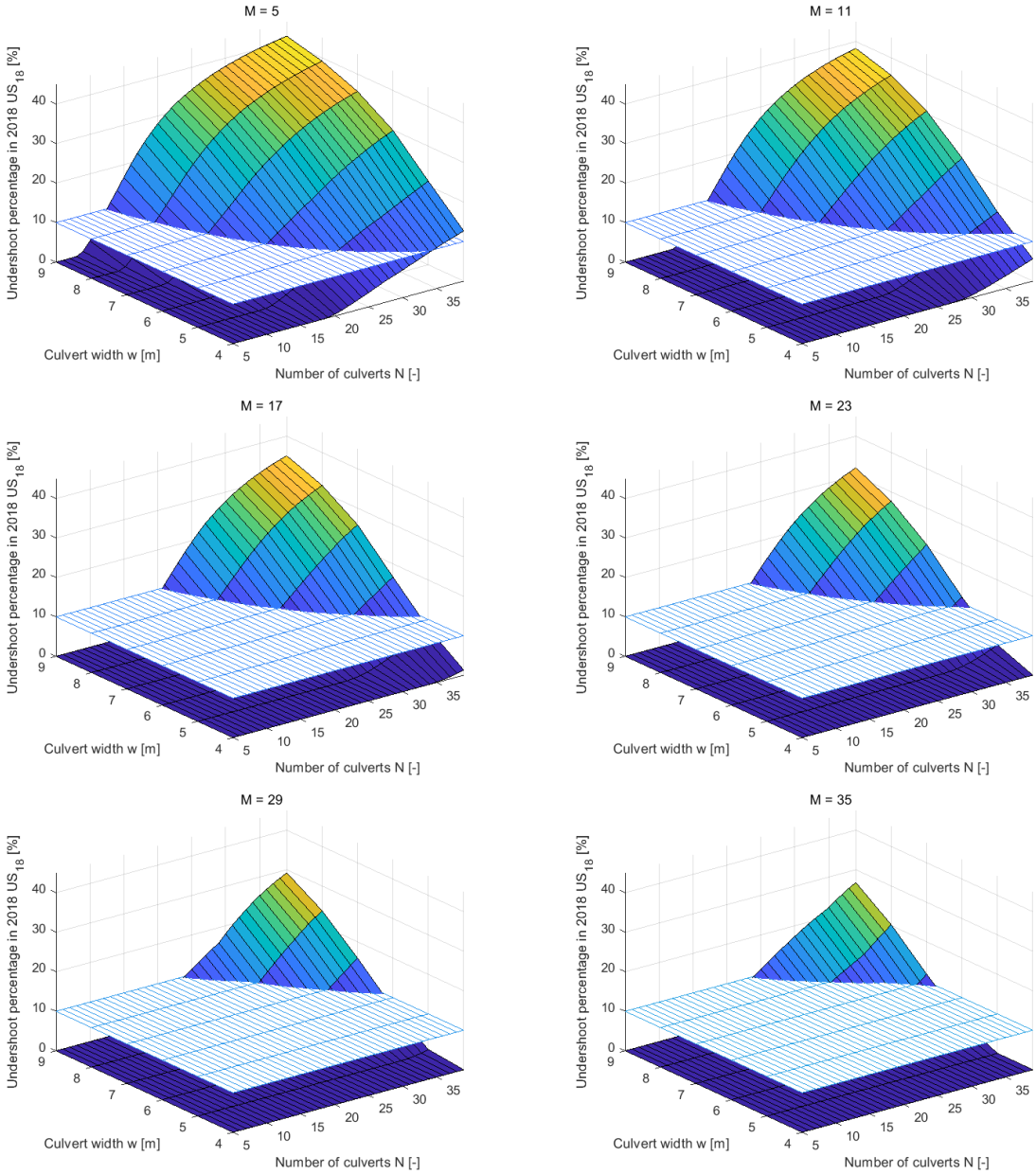

Figure 52: Undershoot behaviour for different numbers of unequipped culverts.

Suppose an array wherein all culverts are equipped with unidirectional turbines. The inflow will be smaller than the outflow due to the turbines not extracting energy in outflow conditions. Consequently, the lower limiting water level will be surpassed in a higher frequency increasing the undershoot value. Now, assuming a part of the culverts in the array are left empty, causing the inflow to increase caused by the higher discharge through the empty culverts. Because of the turbines not performing in outflow, the outflow discharge does not change compared to the fully equipped culvert array situation. The higher discharge

in inflow will result in a higher water level in Lake Grevelingen. When the water flows out of the lake again, the low water levels will be higher than in the fully equipped situation caused by the higher high water level and the unchanged outflow discharge thereby decreasing the undershoot. Examining the overshoot behaviour, in Figure 53 one can observe that the overshoot is bounded for any culvert width at the line where the total amount of culverts is equal to the considered amount of empty culverts. For *N*-values smaller than the considered *M*-value, an array with only empty culverts is regarded and therefore the overshoot increases when *W* and *N* increase. Once *N* is greater than *M*, the culvert array consists of both equipped culverts and empty culverts. This causes a reduction of the overshoot due to the turbines reducing the discharge. Only placement of turbines does not solve the full problem. When the total amount of culverts further increases, the overshoot will increase again, due to the total cross-sectional area of the array increasing the discharge.

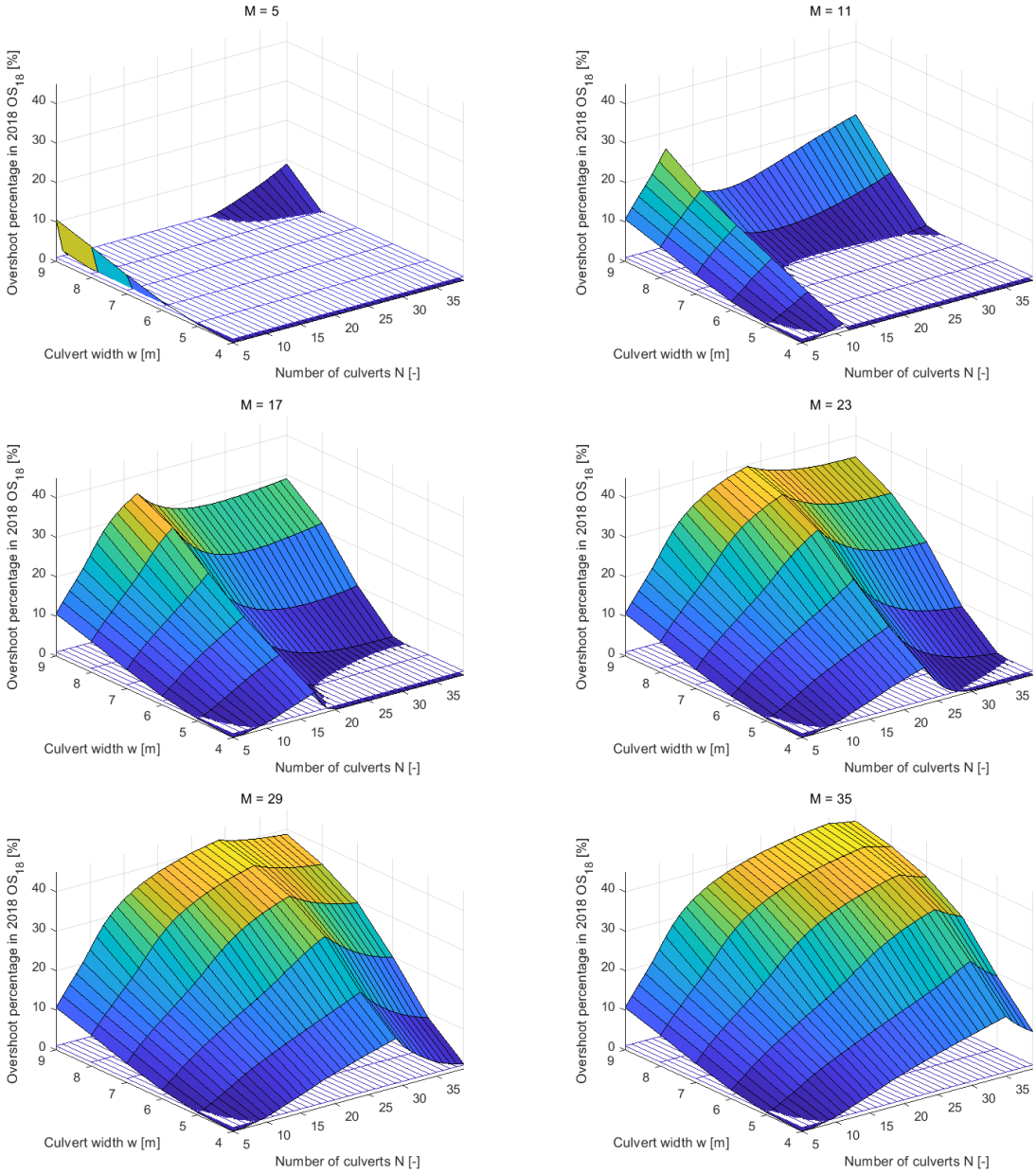

Figure 53: Overshoot values for different tidal power plant configurations.

5.1.3 Tidal range

Another part of the water management requirements is the tidal range. To satisfy the requirements stated by Tidal Grevelingen Project (2018), the monthly averaged tidal range should be *0.40* m and the monthly maximum tidal range should be *0.50* m. because the data retrieved from the three-year data set hardly changes on a yearly base and displaying the data of every month is an unnecessary overload of information, only the data of the most recent typical winter and summer months, June 2018 and December 2018, are depicted.

First, the development of the monthly averaged tidal range of June 2018 is considered. In Figure 54, the intersection of the tidal range graph and the horizontal plane depicts the combination of amount of culverts and the culvert cross-section where the monthly averaged tidal range is at its desired value. As the number of unequipped culverts increases, the value of *N* where the desired monthly averaged tidal range value is reached, shifts up.

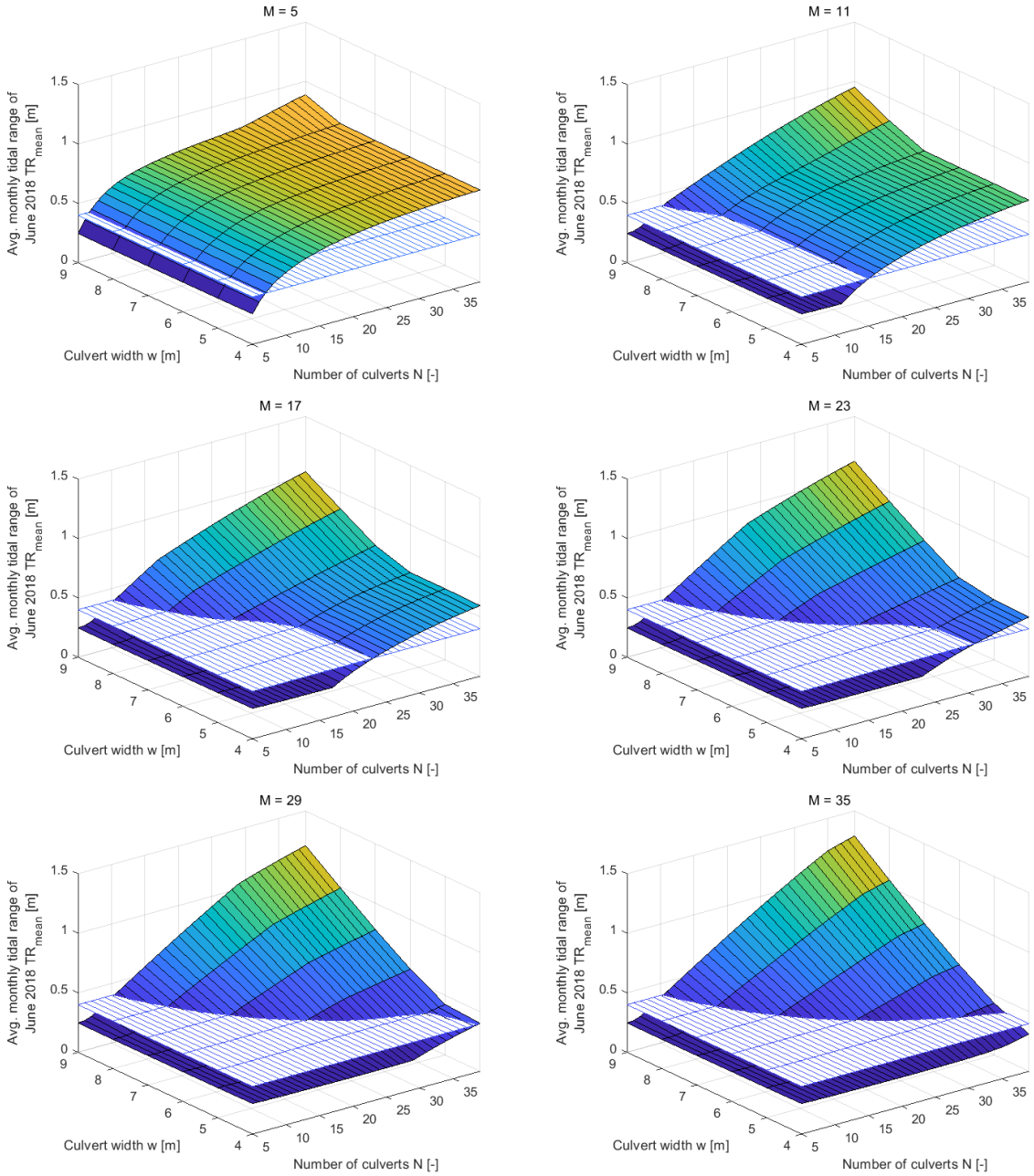

Figure 54: Monthly averaged tidal range of June 2018 for different unequipped culvert values.

If each culvert in the array would be left unequipped, the desired values of the tidal range would not be achieved as can be seen in Figure 54 at *N*-values smaller than the considered *M*-value. In this scenario the monthly averaged tidal range reaches a value of approximately *0.25* m. As soon as turbines are installed, the inflow is obstructed whereas the outflow stays unaffected due to turbines degree of reaction equal to *0*. This means that the high water level does increase but in a smaller rate compared to adding an unequipped culvert. The outflow is still proportional to the number of culverts and will enhance accordingly, further draining the lake and hereby increasing the tidal range. To generate enough blockage in inflow, the amount of equipped culverts need to be increased as the number of unequipped culvert increases. The same theory can be applied on the monthly averaged tidal range of the month December 2018, which can be observed in Figure 55.

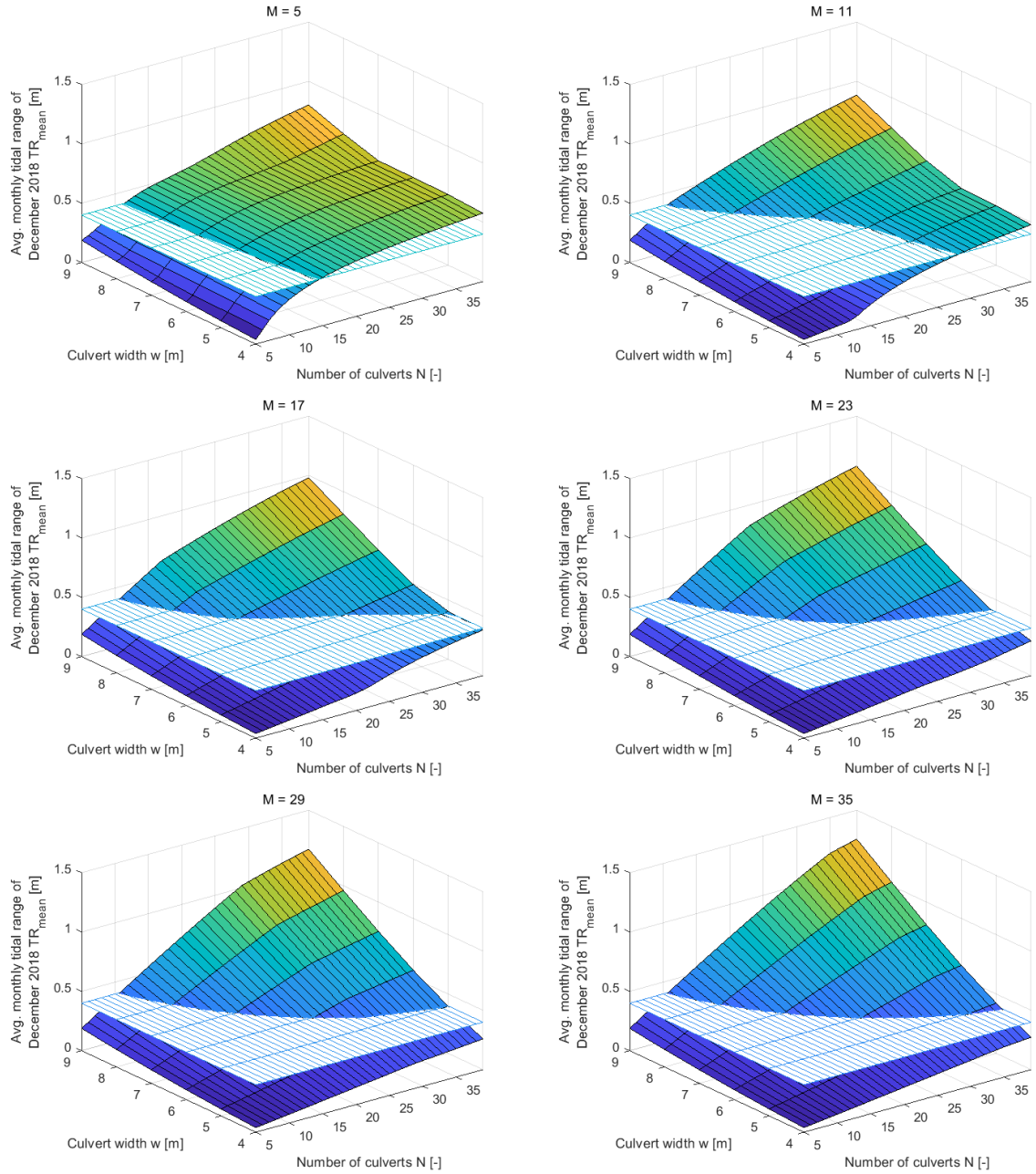

Figure 55: Monthly averaged tidal range for December 2018 dependent on varying values of M.

Regarding the data from June 2018 and December 2018, the intersections with the *0.40* m plane take place at different *N*,*w*-coordinates. This means that the months both have different optimal array dimensions. In practice, only one configuration can be built and this means that additional turbine modulation is required to synchronise the monthly averaged tidal ranges each month to the desired tidal range value. Examining the monthly maximum tidal range values of June 2018 and December 2018, similar monthly behaviours can be regarded, except the values are higher. Still, the same problem as with the monthly averaged tidal range occurs: the desired monthly maximum tidal range value in June 2018 occurs at different culvert configurations than the monthly maximum tidal range value of December 2018. Figure 56 and Figure 57 depict the monthly maximum tidal ranges of June 2018 and December 2018.

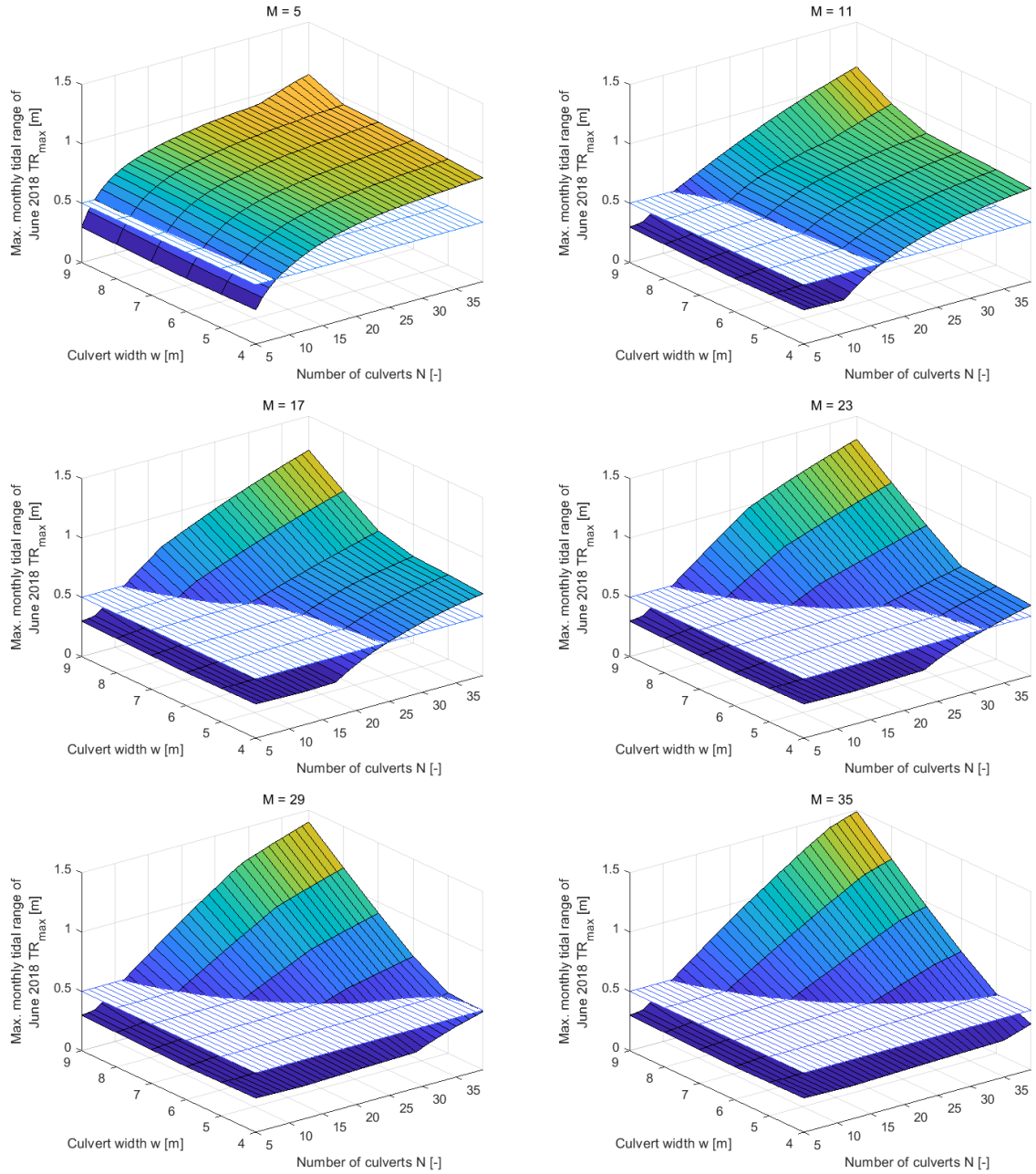

Figure 56: Monthly maximum values of the tidal range in the month June 2018.

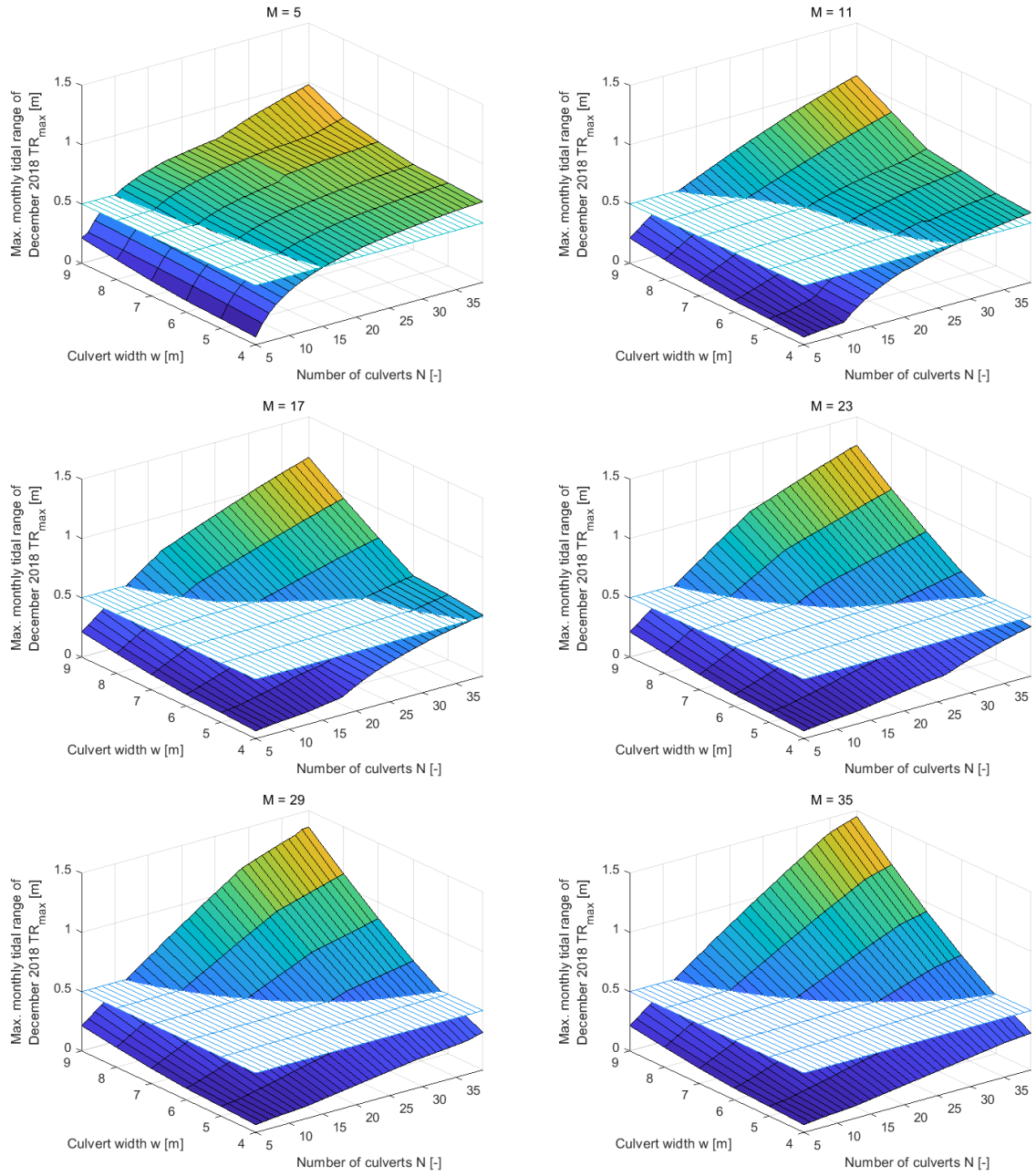

Figure 57: Monthly maximum tidal range values for December 2018.

5.1.4 Discussion on the results

Regarding the overshoot percentages, one can conclude that only in cases with *M = 5*, *M = 11* and *M = 17* configurations occur wherein the overshoot criterion is met. Unfortunately, the possible configurations with *17* empty culverts do not satisfy the energy output of *60* GWh on an annual base. Regarding the rest of the water management parameters, it can be concluded that no configuration immediately satisfies all posed requirements. Therefore, additional turbine modulation could offer a solution to synchronise the water management standards to the energy yield requirements. Because the uni-directionality of the turbines, because of the empty culverts and the bidirectionality of the turbines, it is difficult to fully control the discharge through the tidal power plant. Nevertheless, the implementation of empty culverts can help increase the ecology factor of

the structure, as fish and aquatic mammals can pass the tidal barrage without being possibly harmed by the turbines.

5.2 Unidirectional turbine scenario

In this configuration every culvert is equipped with a unidirectional turbine which extracts energy during inflow conditions. Subsequently no discharge modulation can occur during outflow. In this case, only the surpassing of the upper limiting water level can be modulated and this can be prevented by applying intermittent turbine modulation wherein the precautious upper water level is set to *-0.20* m NAP. Looking at the under- and overshoot, due to the absence of discharge modulation in outflow, the limiting undershoot percentage is exceeded in a large quantity for many considered combinations, as can be seen in Figure 58. As the culvert width increases, the number of culverts to combine with decreases. The limiting upper water level will be hardly surpassed and when this exceedance occurs, it is low frequent, causing the overshoot to stay under the posed overshoot standard.

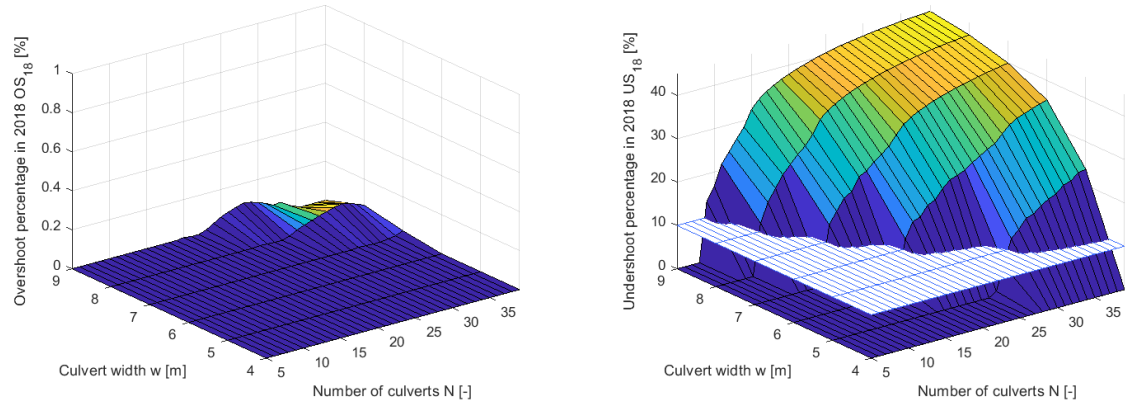

Figure 58: Under- and overshoot percentages for the unidirectional turbine scenario.

Looking at the monthly averaged tidal ranges in Figure 59, one can see that the intersections where the monthly averaged tidal range and monthly maximum tidal range (Figure 60) of June 2018 and December 2018 satisfy the posed requirements are not at the same (*N*, *w*)-coordinates. Besides, depending on the time of year, different optimal culvert combinations occur per month. Given these facts, additional turbine modulation should offer a solution to assure that the tidal range values are in line every month.

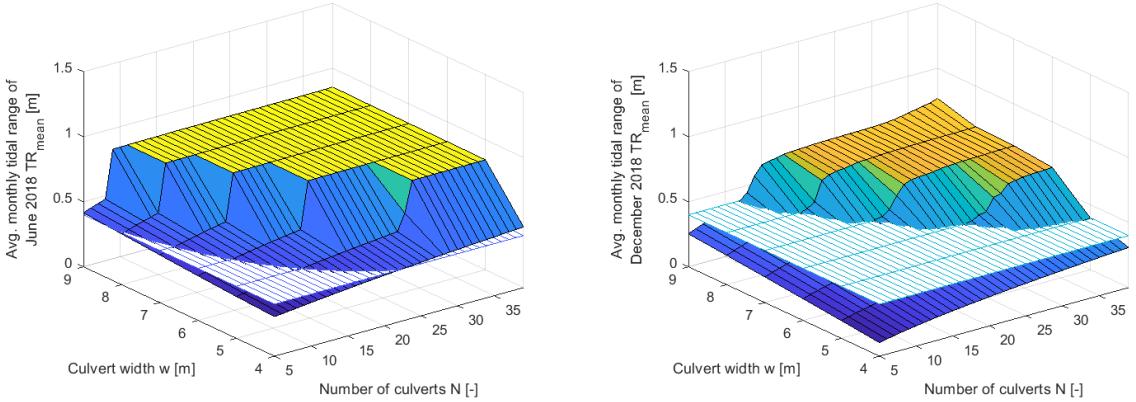

Figure 59: Average monthly tidal range for June 2018 and December 2018.

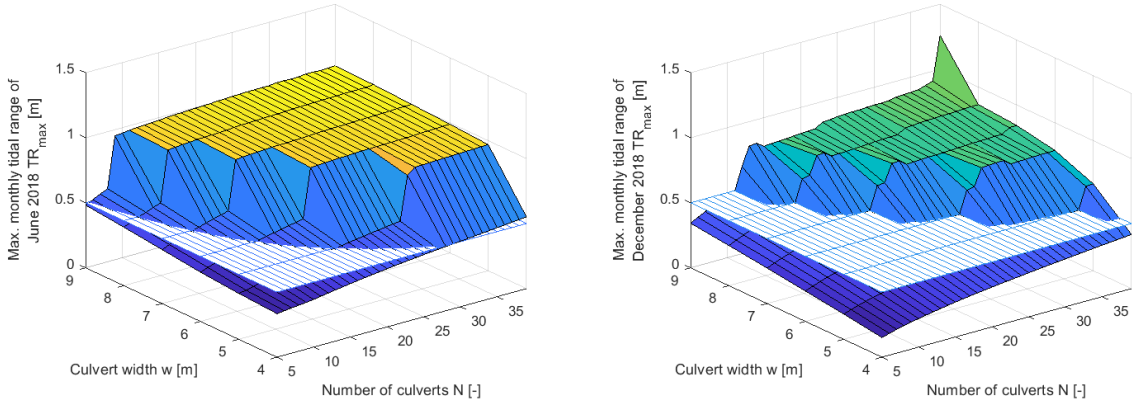

Figure 60: Maximum monthly tidal range for June 2018 and December 2018.

Furthermore, the mean annual energy extracted by the turbines increases with the increase of the cross-sectional area and the number of culverts, which is also the case in the unidirectional scenario combined with empty culverts.

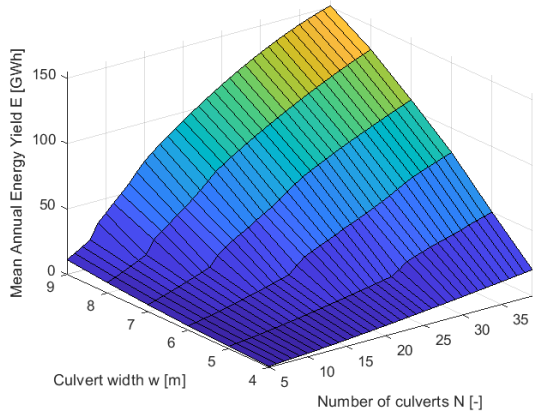

Figure 61: Mean annual energy extracted by turbines for unidirectional turbine solution.

5.2.1 Discussion on the results

When the turbines do not modulate the discharge through the ducts, the water level cannot be controlled during outflow. Thereupon, in many configurations, an exceedance of the lower limiting water level will occur and the lake's water level will become too low, which will have its influence on the surroundings. In the case of the arrays that do satisfy to the lower limiting water level exceedance requirement, another problem emerges: these compositions are not in compliance with the monthly averaged and maximum tidal range requirements. At configurations where the monthly averaged tidal range satisfies, the monthly maximum tidal range does not and vice versa. Also monthly differences occur. Therefore, concessions need to be made, preferably in the form of additional turbine modulation. Herein, sacrificing a part of energy yield to control the discharge through the gates. Regarding the energy yield, it increases as the dimensions and the amount of the culvert also increase. Configurations that approximate the water managements standards, do not approach the posed mean annual energy yield of *60* GWh. To optimally control the discharge, a bidirectional scenario is considered.

5.3 Bidirectional turbine scenario

The considered configuration will account for square culverts, all equipped with bidirectional turbines. These bidirectional turbines are able to perform water management measures in both inflow and outflow conditions. In this model it is assumed the full time turbine modulation is applied. In this case, both in- and outflow turbine modulation sets at *-0.45* m NAP in inflow and *+0.05* m NAP in outflow.

Regarding the development of the mean annual energy yield for varying number and dimensions of the culverts, increasing the number and dimensions of the culvert will result in a higher discharge. This consequently increases the generated power and extracted energy, as can be seen in Figure 62.

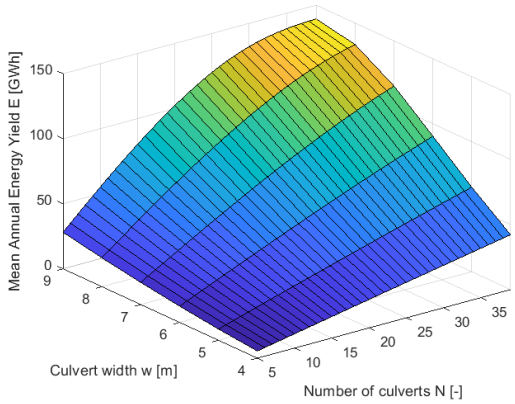

Figure 62: Mean annual energy yields for different number of culverts and culvert dimensions.

Concerning water level management, the under- and overshoot of the considered cases is depicted in Figure 63. The majority of the combinations do not surpass the lower limiting water level and therefore the undershoot is *0*. Except for culvert widths of *9* m and a culvert number greater than 33, an occasional exceedance of the lower limiting water level appears, but this frequency lies well within the tolerance of *10* %.

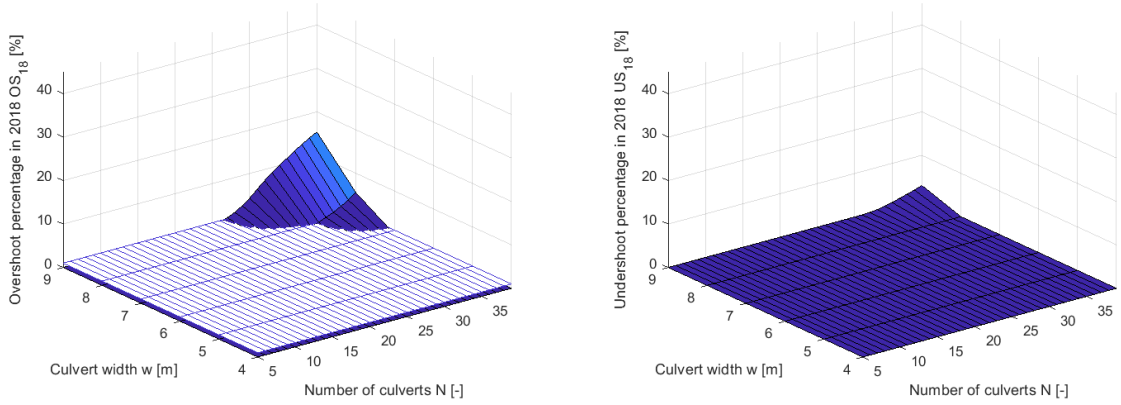

Figure 63: Over- and undershoot percentages for 2018 for different amounts of culverts and culvert heights and widths.

The overshoot requirement on the other hand, is exceeded at a combination of culvert width of 8 m and upward of 35 culverts and at *w* equal to 9 m and from 26 culverts onwards as is illustrated in Figure 63, where the overshoot plane intersects and surpasses the horizontal plane at $OS_{18} = 1$ %.

Regarding the monthly averaged tidal range of June and December 2018 in Figure 64, one sees that the desired value of *0.*40 m occurs at different configurations each month.

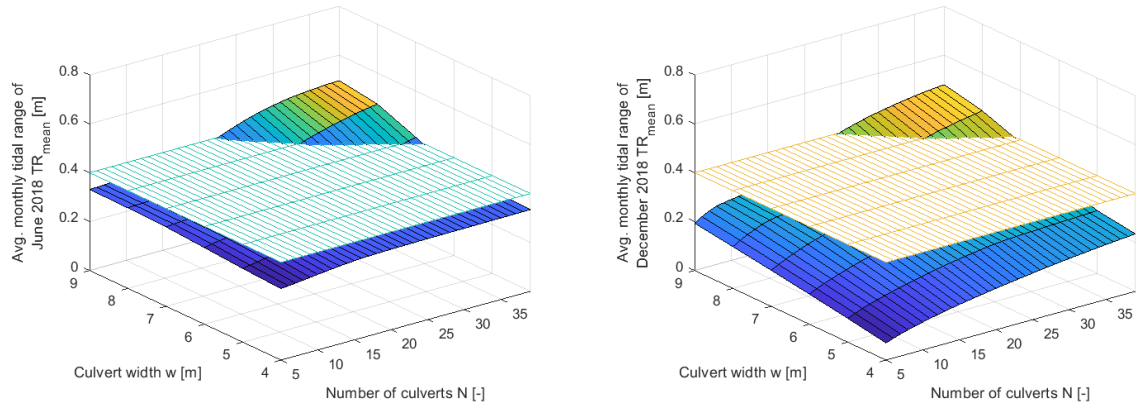

Figure 64: Monthly averaged tidal range of June 2018 and December 2018.

Besides, the desired monthly maximum tidal ranges occur also at different culvert configurations as can be seen in Figure 65. In order to obtain the desired values of the monthly averaged and monthly maximum tidal range each month, modulation of the turbines can decrease or increase the tidal range.

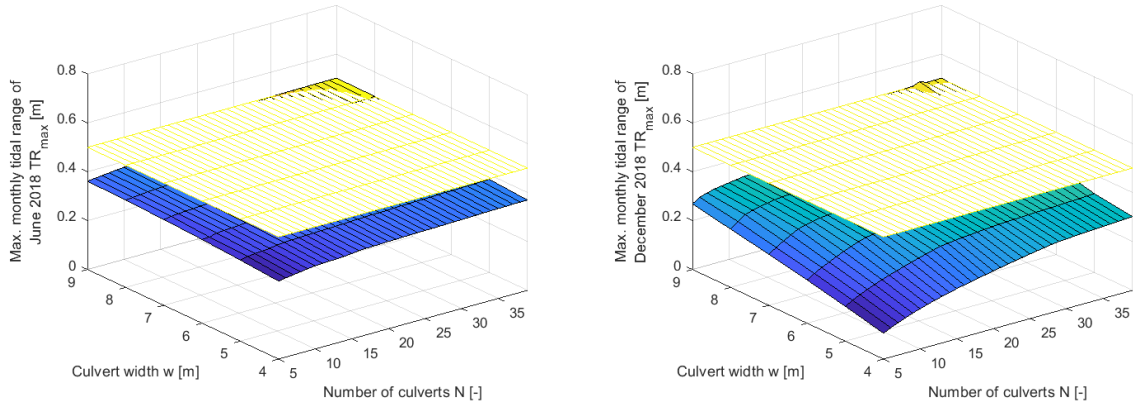

Figure 65: Monthly maximum tidal range of June 2018 and December 2018.

5.3.1 Discussion on the results

Considering the water management standards, one can see that the undershoot percentages are in compliance with the posed standards. The upper limiting water level is more frequently surpassed, which is subsequently reflected in the overshoot values per configuration. Exceeding the upper limiting water level merely takes place at cross-sectional areas of *64* and *81* m^2 with corresponding culvert numbers of respectively *35* and *26* and greater.

The advantage of the implementation of bidirectional turbines is that the flow through the culverts can be controlled continuously, as this is not the case when unidirectional turbines are installed. Regarding the other water management requirement, the tidal range is not in line with the over- and undershoot requirements. Therefore, can be concluded that additional water level modulation is required to achieve satisfying water management values at a specific culvert configuration while assuring a sufficient energy output. After analysing the culvert configurations appears that a bidirectional turbine configuration consisting of *24*

culvert measuring *9* m by *9* m. And thereby extracting a mean annual energy output of *116,90* GWh.

This configuration is therefore used to be economically reviewed and its feasibility is analysed.

6 Economics & feasibility

"A study of economics usually reveals
that the best time to buy anything is last year."
M. Allen

To investigate the economic feasibility of the chosen design of the tidal power plant Brouwersdam, a pre-existing calculation method provided by the Energy Centre the Netherlands (ECN) is used. In order to establish a truthful picture of the economic feasibility of the project, a collection of parameters need to be quantified. First, the investment costs of the tidal power plant design, existing of *24* culverts measuring *9* m by *9* m, are regarded.

6.1 Investment costs

The investment costs are split up in two categories: the civil structure costs and the turbine costs. The civil structure costs include the expenses of the preparation of the construction site, the excavation activities, construction and removal of temporary provisions.

6.1.1 Civil structure costs

To provide an insight into the investment costs of the tidal power plant, a cost estimation established by Mooyaart and van den Noortgaete (2010) will be used as a reference. The assumptions made in this cost estimate are:
- The amount of soil in the soil body includes *10* % loss due to settlement;
- Construction time is two years;
- The removal or adjustment of existing lead-up services is not accounted for;
- Real estate costs are not included;
- The band width is not determined.

Herein, the structure will be constructed according to the 'build in the dry' -construction principle. First, the asphalt layers providing protection of the dam and the asphalt of the roads is removed. A construction site at the Brouwersdam will be excavated and will be subsequently drained to prevent water from flooding in. The caissons, from the core of the dam can function as a water retaining wall, to guarantee the water safety during construction. The foundation for the culverts will then be placed, where after the culverts are constructed. On top of the culverts, room for machinery and gate locks is established. Followed by the removal of the caissons. Finally, a bottom protection will be placed and the whole construction site will be finished off (Mooyaart & van den Noortgaete, 2010). Figure 66 displays a schematical depiction of the applied construction method.

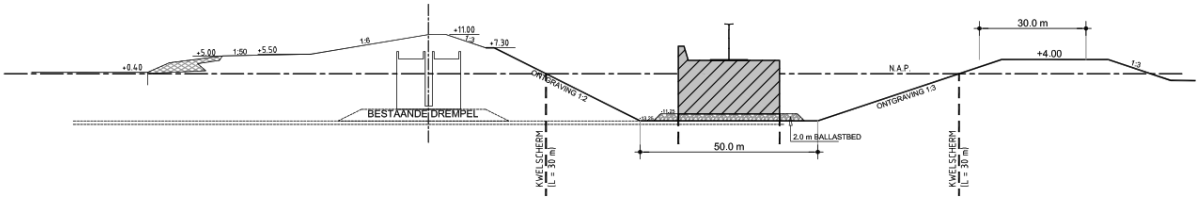

Figure 66: Example of a 'build in the dry' construction method (Mooyaart & van den Noortgaete, 2010).

This cost estimation is based on a tidal power plant design with a total width of *625* m and a culvert length of *50* m. Moreover, the number of culverts is assumed to be *86.* In order to establish a cost estimate for the configurations discussed in this document, the prices of the

cost items in the reference cost estimate are linearly scaled down to the price per meter dam width or price per culvert. An overview of the cost estimate is attached in Appendix 3.

6.1.2 Turbine costs

The costs of the turbines depend on their diameter and the installed capacity. The diameter of the turbine can be determined from the width and height of the culverts, which is *9* m. The installed capacity, or rated power, is the maximum power a turbine can extract from the flow. If greater wattages occur in the fluid, the turbine can only extract as much as the rated power. Available power is the power that can be extracted from the water. The difference between the available power in the fluid and the rated power is illustrated in Figure 67.

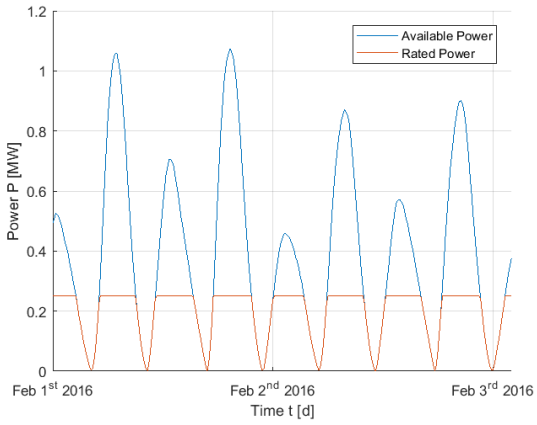

Figure 67: Available power signal and rated power curve with P_{rated} = 0.25 MW.

To determine the installed capacity, one needs to know the influence of the value of the rated power on the AEY. The histogram in Figure 68 depicts the occurrences of the wattages in the power signal and the system has a maximum power output of *2.7* MW.

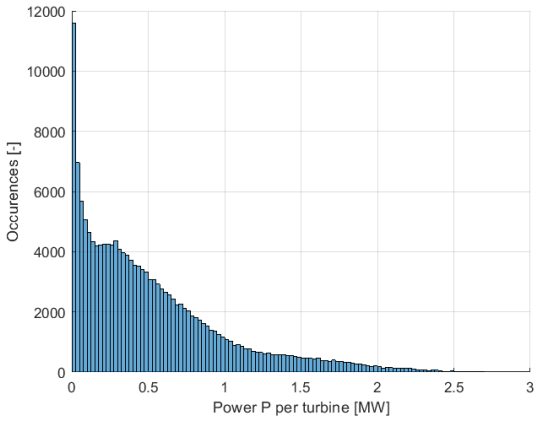

Figure 68: Histogram of occuring power values with bin width of 25 kW.

By integrating the rated power signal for different cut-off power values, the annual rated energy yield is determined. Figure 69 depicts the increase of annual rated energy yield as function of the installed capacity.

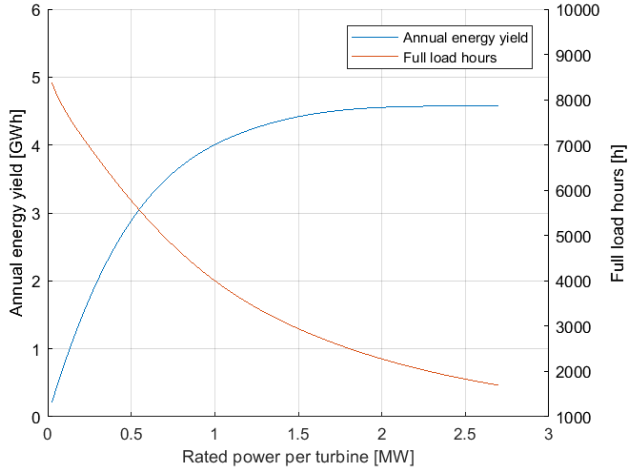

Figure 69: Annual energy yield per turbine and full load hours for varying rated power values.

Besides, the number of full load hours, which are also required in the ECN calculation method, is also determined according to the following relation.

$$FLH = \frac{E_{rated}}{P_{rated}}$$

The International Renewable Energy Agency (IRENA) states that the investment costs for large-hydropower projects typically range from a low of € *900* / kW to around € *3,100* / kW (IRENA, 2012). For this case, the average value of this range, € *2,000* / kW, is used to indicate the investment costs. Furthermore, Spengen & Reijneveld (2014) and Mooyaart & van den Noortgaete (2010) established cost estimates wherein the turbine costs are respectively *22* % and *25* % of the investment costs. Applying the most disadvantageous percentage to the investment costs results in linear relation between the installed capacity and the turbine costs, depicted in Figure 70 .

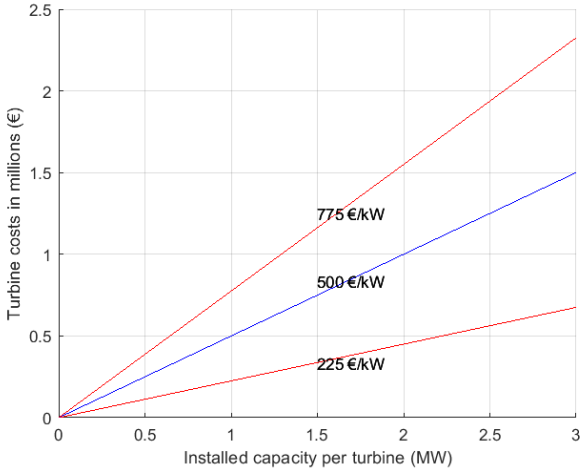

Figure 70: Relation between installed capacity of a turbine and its costs.

Looking at Figure 69 again, it can be seen that the AEY does not increase very much as the installed capacity increases. This decrease of the AEY-gradient sets in between *1* MW and *1.5* MW. Because of this, the installed capacity is *1.5* MW per turbine, which is *36* MW for

the total tidal barrage. This brings the total costs of the turbines to an amount of € *18,000,000*. Together with the costs for the civil structure, this results in a total investment costs value of € *153,662,674.49*.

To verify if the scaling of the used cost estimate of Mooyaart & van den Noortgaete is valid, the parameters of the Protide design are filled in in the scaled cost estimate and are compared to the investment costs for the Protide design calculated by Tidal Grevelingen Project (2018) in the market consultation document, which is € *130,000,000*. The scaled cost estimate method gives an investment cost for the Protide design of € *105,059,323.15*. The scaled cost estimate is approximately *19* % lower than the cost estimate of Tidal Grevelingen Project (2018). The cost estimate made in Tidal Grevelingen Project has a variation coefficient of +/- *23* %, and thus the established estimate falls within the set band width.

From this analysis can be concluded that the tidal power plant Brouwersdam has an installed capacity of *36* MW and a full load hour value of *2,945*.

6.2 Feasibility study

The conclusion that can be drawn from the analysis described in Section 6.1 is that the tidal power plant will be implemented with *24 1.5* MW turbines with a full load hour value of *2,945*.

A prediction on the development of the inflation executed by the Netherlands Bureau for Economic Policy Analysis (CPB) in 2016 results in an expected inflation value after 2021 of *1.7* %. Furthermore, Tidal Grevelingen Project (2018) uses the parameter values given in Table 14, which are also used in this feasibility study.

Table 14: Parameter values as stated in Tidal Grevelingen Project (2018).

Parameter	Unit	Value
Static maintenance costs	€/kW	2.5 % of investment costs
Market price of electricity	€/kWh	0.13 for years 1-15 0.049 for years 16-30
Loan interest rate	%	3.0
Needed return on equity	%	13.0
Equity share	%	30.0
Corporation tax	%	21.0
Economic lifespan	Years	30
Depreciation period	Years	30

Thereafter, the varying maintenance costs per kilowatt are assumed to be *0*, because assuming the static maintenance costs to be *2.5* % of the investment costs already is at the maximum value of the maintenance costs range (IRENA, 2012). The ECN subsidises the project by raising the market price of electricity to *0.13* €/kWh for the first *15* years (Tidal Grevelingen Project, 2018). Subsequently, no additional subsidies, e.g. construction grants and subsidies from environmental/political organisations, are taken into account in the feasibility study. Besides, as the considered economic lifespan is *30* years, the policy period is also assumed to be as long. From this, can be determined that the project is theoretically feasible when the loan period is higher than *10* years. To also establish some revenue, the

loan period is set to *15* years. This results in the following values used in the ECN feasibility method, depicted in Table 15.

Table 15: Parameter values used in the ECN business case analysis.

Parameter	Unit	Value
Input power	kW	36,000
Electric full load hours	h/year	2,945
Investment costs	€/kW	4,268.41
Static maintenance costs	€/kW	2.5 % of investment costs
Varying maintenance costs	€/kW	0
Market price of electricity	€/kWh	0.13 for years 1-15 0.049 for years 16-30
Investment subsidy caused by debt capital	€	0
Investment subsidy caused by equity	€	0
Inflation	%	1.7
Loan interest rate	%	3.0
Needed return on equity	%	13
Equity share	%	30
Corporation tax	%	21
Economic lifespan	Years	30
Loan period	Years	15
Depreciation period	Years	30
Policy period	Years	30

The calculation spreadsheet and the cash flow statement can be found in Appendix 4.
The values of the feasibility key numbers are given in the below mentioned table.

Table 16: Feasibility key numbers.

Key number	Unit	Value
Net Present Value	€	9,680,095
Internal Rate of Return	%	2.2
Payback Period	Years	15
Levelised Cost of Energy	€/kWh	0.058

From this, the conclusion can be drawn that the chosen configuration of tidal power plant Brouwersdam on the posed conditions is economically feasible.

7 Conclusion & discussion

"…Over de dam
Rijden we langs het water uit het zicht
Het glinstert in het laatste licht…''
Over de dam– Bløf

7.1 Conclusion

This master thesis is written to answer the research question: ''How could the bi-directional flow profile at the Brouwersdam be guided through the system in such a way that the water management is satisfied while ensuring critical factors like power generation and economic feasibility are suitably addressed?''.

From the results, the following main conclusions could be drawn:

- Implementing constrained flow devices allow the turbines to modulate the discharge and therefore can be used as water management tools.
- Installing bidirectional turbines will give full time possibility to control the discharge and subsequently the water level.
- Installing turbines in every culvert will improve the discharge control.
- Full time turbine modulation of the turbines is recommended.

The analysis on the different methods of hydropower in the literature study reflects that constrained flow is preferred. This choice is primarily based on the fact that the constrained flow technique has the ability to regulate the volume flow through the ducts, in contrast to confined free flow devices, where a by-pass flow occurs. Beyond that, constrained flow devices also have a higher theoretical power output than confined free flow methods.

Considering the results on the three chosen configurations, wherein the first configuration consists of unidirectionally equipped and unequipped culverts. The second configuration takes into account only unidirectional equipped culverts and no unequipped culverts, while the third case is set up with every culvert filled with bidirectional devices. From the invariant and multivariant analysis can be seen that the standards on water management in the first and second case are not met. This is a result of the unidirectional turbines being unable to perform water management in outflow. Thereby, unequipped culvert can also not contribute to the discharge modulating function of the tidal power plant. The bidirectional case, on the other hand, is able to permanently modulate the flow through the tidal barrage and has therefore a higher controllability, compared to the first two cases. To further investigate the controllability, two modulation methods are considered: Full time turbine modulation and intermittent turbine modulation. It appeared that full time turbine modulation is preferred over intermittent turbine modulation, because the discharge can be regulated over the full tidal range, while intermittent turbine modulation only sets in after the lake's water level surpasses a certain precautious water level. Although bidirectional turbines are preferred, it only solves the water management issue partially, as the monthly averaged and maximum tidal range values are too small.

After selecting a culvert configuration consisting of *24* culverts, measuring *9* m by *9* m, with *24* bidirectional turbines to be investigated economically. It can be concluded that this configuration is economically feasible assuming *24 1.5* MW turbines are installed, that the

energy's market price is € *0.13* per kilowatt hour for the first *15* years and € *0.049* per kilowatt hour for the second *15* years and that the loan period is *15* years. The payback period of this project is then *15* years and the net present value is calculated on € *9,680,095*. The levelised cost of energy is determined to be € *0.058*, while the internal rate of return is *2.2 %*.

7.2 Discussion

In this research assumptions to the Brouwersdam system are made to establish a usable model. Because of these assumptions, the determined values can deviate from reality.

Considering the invariant and multivariable analysis, no loss coefficient due to the presence of the turbines is assumed, as the specific type of turbine to implement is not yet known. Therefore, the discharge is overestimated and therefore also the energy output. The given extracted energy yield therefore displays a theoretical upper bound. The feasibility study accounts for an installed turbine capacity, from which the energy output is already lower than the energy yield estimated from the multivariable analysis. As long as the actual energy output lies between these bounds, the economic feasibility is secured, as the energy output is larger than the lower bound used in the feasibility study. The overestimated discharge also has its influence on the water management, as well as the rectangular basin assumption. With the overestimation of the discharge due to the decreased system loss coefficient, Lake Grevelingen drains and fills faster, and therefore, over- and undershoot and tidal ranges are overestimated as well. This is not an issue for the over- and undershoot, but desired tidal range values are reached earlier, which may not be the case in reality. The rectangular basin assumption influences the outcome of the water level variation. The rectangular basin assumption provides the water level variation to be directly proportional to the discharge. As the bathymetry of the lake provides a different basin shape, wherein the lake's banks are inclined, and therefore the water level variation is otherwise related to the discharge. Because the lake's surface area is determined at the current still water level, the basin, when the water level is lower than the current still water level, will fill or drain faster, while when the water level is higher than the current water level, the basin will fill or drain slower. It is expected that the absence of turbines loss coefficient has a larger influence on the system than the rectangular basin assumption, because the range wherein the tidal variation takes place is rather small compared to the lake surface dimensions.

Regarding the mean annual energy yields of the unidirectional and bidirectional cases of the multivariable analysis. The unidirectional case has a larger annual energy output than the bidirectional case for the same N,w-values, which is remarkable because the bidirectional case also extracts energy in outflow conditions. Considering the over- and undershoot and tidal range of the unidirectional case, one can see that these values are excessively exceeded and therefore higher hydraulic head values occur, resulting in higher energy yields. Actually, these hydraulic head values would not occur if the water level did not exceed the water management requirements so excessively and thereupon the energy yield would be lower.

Considering the economics, the economic feasibility study does not take into account any other subsidies or grants other than the SDE+ subsidy. Additional grants will make for a more beneficial business case. It is expected that because of the environment improving function of the tidal barrage, additional grants will be supplied. On the other hand, a large variety in the turbine costs is present, so the probability of the turbines being more expensive

than estimated is present. Therefore, performing a more elaborate sensitivity study and a multiple scenario analysis in the future is recommended.

7.3 Future work

Because the water management requirements in this thesis are partially met, i.e. the over- and undershoot standard is achieved, but the desired tidal range for the chosen bidirectional configuration of *24* culverts, measuring *9* m by *9* m, is too small. Therefore, adding an algorithm that accounts for the adjustments of the degree of reaction for the sake of the monthly averaged and monthly maximum tidal range, while ensuring the over- and undershoot standard is achieved simultaneously, is highly recommended and will give a more reliable energy yield. Furthermore, adding additional layers of resolution to the model, such as accounting for the lake's bathymetry, the expected sea level rise in the future and the effect of the turbines on the discharge, will result in a more trustworthy image with respect to water management and power generation. Because the economic feasibility of the project is dependent on a large number of parameters, which are also difficult to predict in the future, it is recommended to perform a more elaborate sensitivity study and a multiple scenario analysis to establish a more trustworthy image.

A subject that is not considered in this master thesis is the ecology aspect. The implementation of empty culverts already would be beneficial for the passage of fish and aquatic mammals, but this is not advised for water management reasons. Therefore, placing gate locks in the empty culvert could offer a solution, as these can close off a culvert and are easier to avoid by passing animals than a rotating constrained flow turbine. Also, installing fish friendly turbines, which are currently in development, can contribute to the ecology factor. Besides preventing animals from contact with hazardous parts of the tidal power plant, also the influence of the reconnection between the North sea and the lake on the morphology needs to be investigated, as this can harm the species around the lake indirectly, as negative consequences on tidal and mud flats, which are used as mating and resting places, can occur due to the opening in the Brouwersdam.

Finally, one can investigate another form of water management, in which 'Active' turbine modulation will be applied instead of the 'Passive' modulation, as described in this thesis. Active turbine modulation gives the turbines the additional ability to function as a pump and add energy into the flow to increase the flow rate rather than only extracting energy from the flow. Certainly, with the eye on the sea level rise, whereby it will be harder to drain Lake Grevelingen due to the higher water level in the North Sea, active turbine modulation has potential.

References

Bezuyen, K., Stive, M., Vaes, G., Vrijling, J., & Zitman, T. (2011). *Inleiding Waterbouwkunde.* Delft: VSSD.

Boon, M., & Roest, F. (2008). *Notitie civiele aspecten doorlaatmiddel Brouwersdam.* Ministerie van Verkeer en Waterstaat, Rijkswaterstaat.

Centraal Planbureau. (2016). *Middellange-termijnverkenning 2018-2021.* Den Haag: Centraal Planbureau.

Dixon, S. (1998). *Fluid Mechanics, Thermodynamics of Turbomachinery.* Oxford: Butterworth-Heinemann.

Elger, D., Williams, B., Crowe, C., & Roberson, J. (2014). *Engineering Fluid Mechanics.* John Wiley & Sons.

European Marine Energy Centre. (n.d.). *Tidal Devices*. Retrieved from http://www.emec.org.uk/marine-energy/tidal-devices/

Garrett, C., & Cummins, P. (2004). *Generating Power from Tidal Currents.* Journal of Waterway, Port, Coastal, and Ocean Engineering, Vol. 130, No. 3.

Getij Grevelingen. (2018). Artist impression Getijdencentrale Brouwersdam [digital image]. Retrieved from https://www.getijgrevelingen.nl/project

IRENA. (2012). *Renewable Energy Technologies: Cost Analyis Series.*

Leopold, M., & Scholl, M. (2018). *Monitoring getijdenturbines Oosterscheldekering. Jaarrapportage 2017.* Wageningen University & Research centre, Wageningen Marine Research, Wageningen.

Maynard, M. (2018, August 18). Tidal energy: the silent giants of the Pentland Firth. Retrieved from https://geographical.co.uk/nature/energy/item/2888-pentland-power

Meijnen, R., & Arnold, J. (2015). *TPP-Brouwersdam: Conceptual Design and comparison of Two Propellor Turbine Configurations.*

Mooyaart, L., & van den Noortgaete, T. (2010). *Getijdencentrale in de Brouwersdam Variantenstudie.* Royal Haskoning, Rotterdam.

Open Topografie Nederland. (2018, November 21). Blad 42-Oost: Zierikzee & Blad 43-West: Overflakkee [digital image]. Retrieved from Open Topo: https://www.opentopo.nl/

Ragheb, M., & Ragheb, A. (2011). *Wind Turbines Theory - The Betz Equation and Optimal Rotor Tip Speed Ratio.* University of Illinois, Department of Nuclear, Plasma and Radiological Engineering and Department of Aerospace Engineering, Urbana-Champaign.

Renewables First. (2015). *What is the physical size of hydropower systems?* Retrieved from https://www.renewablesfirst.co.uk/hydropower/hydropower-learning-centre/what-is-the-physical-size-of-a-hydro-system/

Rijkswaterstaat. (1971). *Brouwersdam - Overzicht en Dwarsprofielen.*

Rijkswaterstaat. (2019, January 4). *Waterinfo.* Retrieved from https://waterinfo.rws.nl/#!/nav/index/

Rijkswaterstaat. (n.d.). *Hoogwater*. Retrieved from https://www.rijkswaterstaat.nl/water/waterbeheer/bescherming-tegen-het-water/hoogwater/index.aspx

Roberts, J., & Mosey, G. (2013). *Feasibility Study of Economics and Performance of Wind Turbine Generators at the Newport Indiana Chemical Depot Site.* National Renewable Energy Laboratory, Environmental Protection Agency.

Spengen, J. v., Reijneveld, J., Wit, M., & Tieleman, O. (2014). *Civil Design of a Tidal Power Plant Case Brouwersdam.*

Tethys. (2012, June 27). *La Rance Tidal Barrage*. Retrieved from https://tethys.pnnl.gov/annex-iv-sites/la-rance-tidal-barrage

Tidal Grevelingen Project. (2018). *Market consultation about a flood barrier variant with tidal power plant.*

Vrijling, J., & Verlaan, J. (2015). *Financial Engineering.* Delft University of Technology, Faculty of Civil Engineering and Geosciences.

Vrijling, J., van Duivendijk, J., & Jonkman, S. (2008). *Getijcentrale in de Brouwersdam.* Delft University of Technology, Faculty of Civil Engineering and Geosciences.

White, F. (2011). *Fluid Mechanics.* New York: McGraw-Hill.

Appendices

Appendix 1

Tidal ranges of invariant cases 1,2 & 3

Case 1a – *18* culverts, *8* m by *8* m, *11* of *18* equipped with unmodulated unidirectional turbines

Monthly averaged and maximum tidal ranges

	Monthly averaged tidal range $\overline{T_r}$ [m]			Monthly maximum tidal range $T_{r,max}$ [m]		
	2016	2017	2018	2016	2017	2018
January	0.45	0.45	0.45	0.53	0.54	0.54
February	0.49	0.49	0.49	0.62	0.62	0.58
March	0.58	0.56	0.56	0.94	0.68	0.68
April	0.61	0.61	0.59	0.71	0.70	0.71
May	0.59	0.60	0.59	0.68	0.68	0.67
June	0.53	0.55	0.54	0.65	0.68	0.67
July	0.47	0.48	0.48	0.56	0.64	0.63
August	0.44	0.44	0.45	0.55	0.49	0.56
September	0.44	0.44	0.44	0.54	0.53	0.50
October	0.44	0.44	0.44	0.52	0.52	0.64
November	0.44	0.44	0.44	0.51	0.50	0.50
December	0.45	0.45	0.44	0.52	0.52	0.50

Case 1b – 18 culverts, 8 m by 8 m, 11 of 18 equipped with modulated unidirectional turbines

Monthly averaged and maximum tidal ranges

	Monthly averaged tidal range $\overline{T_r}$ [m]			Monthly maximum tidal range $T_{r,max}$ [m]		
	2016	2017	2018	2016	2017	2018
January	0.45	0.45	0.45	0.56	0.57	0.53
February	0.51	0.50	0.50	0.64	0.64	0.60
March	0.59	0.57	0.57	0.94	0.68	0.69
April	0.61	0.61	0.60	0.71	0.70	0.71
May	0.60	0.61	0.59	0.68	0.68	0.67
June	0.55	0.56	0.55	0.65	0.69	0.68
July	0.48	0.49	0.49	0.58	0.65	0.65
August	0.44	0.44	0.45	0.53	0.52	0.58
September	0.42	0.41	0.42	0.51	0.51	0.50
October	0.42	0.41	0.41	0.49	0.49	0.48
November	0.42	0.42	0.41	0.49	0.48	0.48
December	0.43	0.43	0.43	0.51	0.50	0.52

Case 2a – *18* culverts, *8* m by *8* m, each culvert equipped with unmodulated unidirectional turbines

Monthly averaged and maximum tidal ranges

	Monthly averaged tidal range $\overline{T_r}$ [m]			Monthly maximum tidal range $T_{r,max}$ [m]		
	2016	2017	2018	2016	2017	2018
January	0.61	0.61	0.63	0.79	0.79	0.72
February	0.71	0.70	0.71	0.87	0.87	1.03
March	0.80	0.79	0.79	0.95	0.93	0.92
April	0.84	0.84	0.83	0.96	0.94	0.95
May	0.83	0.84	0.82	0.94	0.93	0.90
June	0.77	0.79	0.78	0.89	0.94	0.92
July	0.67	0.70	0.70	0.79	0.97	1.02
August	0.59	0.58	0.60	0.94	0.88	0.91
September	0.52	0.50	0.52	0.62	0.61	0.86
October	0.49	0.46	0.47	0.55	0.58	0.59
November	0.49	0.49	0.47	0.57	0.57	0.58
December	0.54	0.55	0.54	0.64	0.62	0.71

Case 2b – *18* culverts, *8* m by *8* m, each culvert equipped with modulated unidirectional turbines

Monthly averaged and maximum tidal ranges

	Monthly averaged tidal range $\overline{T_r}$ [m]			Monthly maximum tidal range $T_{r,max}$ [m]		
	2016	2017	2018	2016	2017	2018
January	0.45	0.45	0.45	0.52	0.51	0.49
February	0.49	0.48	0.49	0.54	0.54	0.54
March	0.52	0.51	0.51	0.56	0.55	0.55
April	0.53	0.53	0.52	0.56	0.56	0.55
May	0.52	0.53	0.52	0.55	0.56	0.55
June	0.50	0.51	0.50	0.55	0.54	0.54
July	0.47	0.48	0.47	0.51	0.52	0.53
August	0.43	0.43	0.44	0.49	0.50	0.51
September	0.40	0.39	0.40	0.46	0.45	0.48
October	0.39	0.38	0.38	0.43	0.44	0.44
November	0.39	0.39	0.38	0.44	0.44	0.43
December	0.41	0.42	0.41	0.47	0.46	0.48

Case 3a – *18* culverts, *8* m by *8* m, each culvert equipped with unmodulated bidirectional turbines

Monthly averaged and maximum tidal ranges

	Monthly averaged tidal range $\overline{T_r}$ [m]			Monthly maximum tidal range $T_{r,max}$ [m]		
	2016	2017	2018	2016	2017	2018
January	0.31	0.31	0.31	0.40	0.35	0.37
February	0.31	0.31	0.31	0.35	0.35	0.36
March	0.32	0.31	0.31	0.35	0.35	0.37
April	0.33	0.32	0.32	0.37	0.36	0.36
May	0.32	0.32	0.32	0.35	0.36	0.35
June	0.31	0.32	0.31	0.36	0.36	0.36
July	0.31	0.31	0.31	0.37	0.35	0.36
August	0.31	0.31	0.31	0.37	0.35	0.35
September	0.31	0.30	0.31	0.37	0.36	0.35
October	0.31	0.30	0.30	0.35	0.35	0.35
November	0.31	0.31	0.30	0.35	0.35	0.35
December	0.31	0.31	0.31	0.34	0.35	0.35

Case 3b – *18* culverts, *8* m by *8* m, each culvert equipped with modulated bidirectional turbines

Monthly averaged and maximum tidal ranges

	Monthly averaged tidal range $\overline{T_r}$ [m]			Monthly maximum tidal range $T_{r,max}$ [m]		
	2016	2017	2018	2016	2017	2018
January	0.29	0.29	0.29	0.40	0.34	0.35
February	0.30	0.30	0.30	0.34	0.34	0.35
March	0.32	0.31	0.31	0.38	0.37	0.37
April	0.33	0.33	0.32	0.38	0.37	0.37
May	0.32	0.33	0.32	0.37	0.37	0.36
June	0.31	0.31	0.31	0.35	0.36	0.36
July	0.30	0.30	0.30	0.35	0.34	0.35
August	0.29	0.28	0.29	0.35	0.33	0.34
September	0.28	0.27	0.28	0.33	0.33	0.33
October	0.27	0.27	0.27	0.32	0.32	0.32
November	0.28	0.27	0.27	0.31	0.31	0.31
December	0.28	0.28	0.28	0.33	0.32	0.33

Appendix 2

Energy output of multivariable analysis of configuration with unequipped culverts and bidirectional turbines

Mean Annual Energy yields for different values of *N*, *w* and *M*.

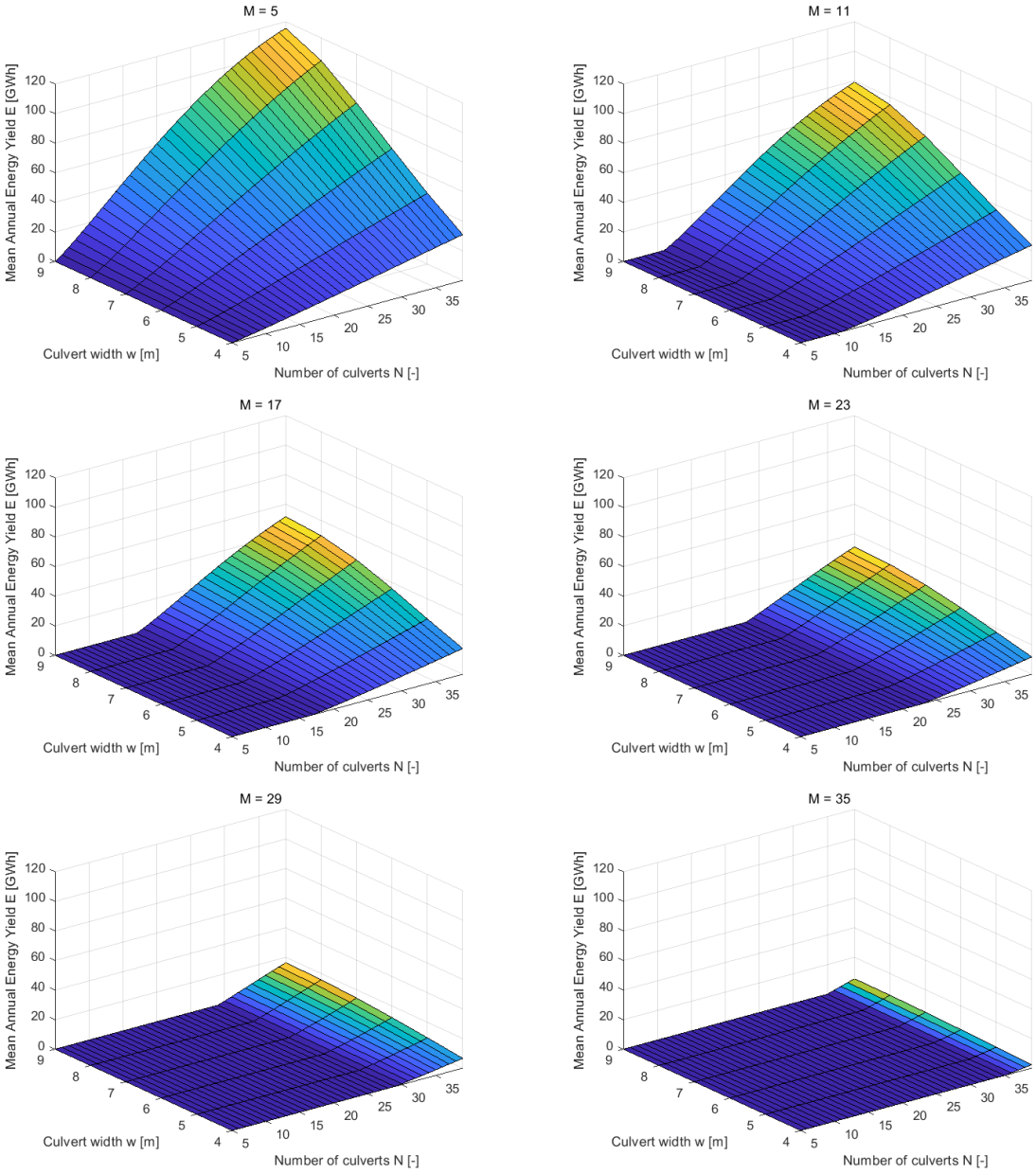

Appendix 3

Cost Estimate

Mooyaart & van den Noortgaete (2010)		
N	106	
W	7.5	m
W_tot	800	m

Configuration coming from multivariable analysis		
N	24	
W	9	m
W_tot	241	m

	Description	Unit	Quantity	Unit price [€/Quantity]	Price [€]	Unit	Quantity used per meter dam	Quantity used per culvert	Quantity used independent of N or w	Unit price [€/Quantity]	Price per culvert [€/culvert]	Cost items independent of W and N [€]	total amount of Quantity	Price [€]
	Construction of temporary provision													
	Constructing soil body for prov. road N57 (A = 144 m2, L = 900 m)	m3	142,560.00	15.00	2,138,400.00	m3/m	178.20			15.00			42,946.20	644,193.00
	Applying coating soil body (L = 900 m, B = 15 m, D = 0.5 m)	m2	6,750.00	20.00	135,000.00	m2/m	8.44			20.00			2,033.44	40,668.75
	Construction of temporary road (B = 10.5 m, L = 900 m)	m2	9,450.00	40.00	378,000.00	m2/m	11.81			40.00			2,846.81	113,872.50
	Removal of existing top layer (B = 27.3 m, L = 812.5m)	m2	22,181.00	25.00	554,525.00	m2/m	27.73			25.00			6,682.03	167,050.66
	Placing temporary sheet piles type AZ 26 (L = 1000 m, D = 15 m)	m2	15,000.00	20.00	300,000.00	m2/m	18.75			20.00			4,518.75	90,375.00
	Excavation of the construction site (A = 1400 m2, L = 812.5 m)	m3	1,137,500.00	5.00	5,687,500.00	m3/m	1,421.88			5.00			342,671.88	1,713,359.38
	Installation of the drainage installation	post	1.00	1,000,000.00	1,000,000.00	post/m	1.00		1.00			1,000,000.00	1.00	1,000,000.00
	Draining of the construction site (A = 600 m2, L = 812.5 m, 2 yrs)	m3	487,500.00	7.00	3,412,500.00	m3/m	609.38			7.00			146,859.38	1,028,015.63
	Placement of unpermeable layer (D = 1 m) by jet grouting	m3	40,000.00	700.00	28,000,000.00	m3/m	50.00			700.00			12,050.00	8,435,000.00
	Total temporary provision costs				*13,605,925.00*									13,232,534.91
	Construction of tidal power plant													
	Construction of sill (B = 35 m, L = 812.5 m, D = 2.75 m)	m2	28,438.00	250.00	7,109,500.00	m2/m	35.55			250.00			8,566.95	2,141,736.88
	Placement of concrete for turbines	m3	128,540.00	650.00	83,551,000.00	m3/m	160.68			650.00			38,722.68	25,169,738.75
	Fill up with sand	m3	116,600.00	15.00	1,749,000.00	m3/m	145.75			15.00			35,125.75	526,886.25
	Installation of turbines	eur	1.00	135,000,000.00	135,000,000.00	eur/culvert		1.00			750,000.00	*	24.00	18,000,000.00
	Construction of road on concrete structure (L = 812.5 m, B = 10.5 m)	m2	8,531.00	50.00	426,550.00	m2/m	10.66			50.00			2,569.96	128,498.19
	Connecting dam to concrete structure (A = 228 m2, L = 100 m)	m3	22,800.00	25.00	570,000.00	m3/m	28.50			25.00			6,868.50	171,712.50
	Connecting dam coating to concrete structure (B = 82 m, L = 100 m)	m2	8,200.00	50.00	410,000.00	m2/m	10.25			50.00			2,470.25	123,512.50
	Placement of bottom protection (D = 1 m)	m2	81,250.00	35.00	2,843,750.00	m2/m	101.56			35.00			24,476.56	856,679.69
	Maintainance of sheet piles (2 yrs)	ton	2,328.00	720.00	1,676,160.00	ton/m	2.91			720.00			701.31	504,943.20
	Total construction of tidal power plant costs				*233,335,960.00*									47,623,707.95
	Removal of temprary provision and old dam body													
	Removing sheetpiles type AZ 26	m2	15,000.00	15.00	225,000.00	m2/m	18.75			15.00			4,518.75	67,781.25
	Removal of left over top layer (B = 95 m, L = 812.5 m)	m2	77,188.00	25.00	1,929,700.00	m2/m	96.49			25.00			23,252.89	581,322.13
	Excavation of the dam	m3	9,562,500.00	5.00	47,812,500.00	m3/m	11,953.13			5.00			2,880,703.13	14,403,515.63
	Excavation of temporary dam	m3	142,560.00	5.00	712,800.00	m3/m	178.20			5.00			42,946.20	214,731.00
	Wet removal of caissons (S = 18x812.5 m, h = 16.2 m)	eur	800.00	12,500.00	10,000,000.00	eur/m	1.00			125,000.00			241.00	3,012,500.00
	Total removal of temporary provision and old dam body costs				*60,680,000.00*									18,279,850.00
Direct Costs						***Direct Costs***								
	Subtotal Direct Costs				*307,621,885.00*		**Subtotal Direct Costs**							*79,136,092.86*
	Further detailling		10 %	307,621,885.00	30,762,188.50		Further detailling			10 %			79,136,092.86	7,913,609.29
Total Direct Costs					**338,384,073.50**	*Total Direct Costs*								**87,049,702.14**
Indirect Costs						***Indirect Costs***								
	One-off costs		2 %	338,384,073.50	6,767,681.47		One-off costs			2 %			87,049,702.14	1,740,994.04
	Construction site costs		5 %	338,384,073.50	16,919,203.68		Construction site costs			5 %			87,049,702.14	4,352,485.11
	Execution costs		4 %	338,384,073.50	13,535,362.94		Execution costs			4 %			87,049,702.14	3,481,988.09
	General costs		4 %	338,384,073.50	13,535,362.94		General costs			4 %			87,049,702.14	3,481,988.09
	Profit and risk		10 %	338,384,073.50	33,838,407.35		Profit and risk			10 %			87,049,702.14	8,704,970.21
	Subtotal Indirect Costs				84,596,018.38		**Subtotal Indirect Costs**							21,762,425.54
Total Indirect Costs					**84,596,018.38**	*Total Indirect Costs*								**21,762,425.54**
Total Direct and Indirect Costs					**422,980,091.88**	*Total Direct and Indirect Costs*								**108,812,127.68**
	Unforeseen Costs		10 %	422,980,091.88	42,298,009.19		Unforeseen Costs			10 %			108,812,127.68	10,881,212.77
Total Construction Costs					***465,278,101.06***	***Total Construction Costs***								***119,693,340.45***
	Real estate						**Real estate**							
	Real estate		1	0	0		Real estate			1			0	0
	Engineering						**Engineering**							
	Engineering, administration and supervision		1	15,000,000.00	15,000,000.00		Engineering, administration and supervision			1			15,000,000.00	15,000,000.00
	Additional Costs						**Additional Costs**							
	Additional Costs		1	5,000,000.00	5,000,000.00		Additional Costs			1			5,000,000.00	5,000,000.00
	Total Basis estimate				485,278,101.06		Total Basis estimate							139,693,340.45
	Project unforeseen						Project unforeseen							
	Project unforeseen		10 %	485,278,101.06	48,527,810.11		Project unforeseen			10 %			139,693,340.45	13,969,334.04
Total Investment Costs					***533,805,911.17***	***Total Investment Costs***								***153,662,674.49***

* Costs of the turbines are not determined according to the cost estimate by Mooyaart en van den Noortgaete.

Appendix 4

ECN Feasibility calculation method

Berekening basisbedragen: SDE+ 2018

Waterkracht, valhoogte ≥ 50 cm, renovatie

BASISBEDRAG	Waarde	Eenheid	Toelichting	
Elektriciteit, warmte of groen gas	**0.058**	Euro/kWh	*Indien een basisbedrag wordt ingevuld in rij 40, toont deze waarde de onrendabele top.*	LCoE

CONVERSIEFACTOREN	Waarde	Eenheid	Toelichting
Verbrandingswaarde methaan (onderwaarde)	35.80	MJ/Nm3	
Verbrandingswaarde hernieuwbaar gas (onderwaarde)	31.65	MJ/Nm3	
Verbrandingswaarde hernieuwbaar gas (bovenwaarde)	35.17	MJ/Nm3	
kWh naar MJ	3.6	MJ/kWh	

INPUTVARIABELEN	Waarde	Eenheid	Toelichting
Inputvermogen	36000	kW_input	
Gaat het om een installatie voor hernieuwbaar gas?			
Methaangehalte hernieuwbaar gas voor gaszuivering			
Vermogen hernieuwbaargasproductie (voor zuivering)	-	Nm3/uur	
Outputvermogen (thermisch of hernieuwbaar gas)		kWth_output	
Outputvermogen (hernieuwbaar gas)	-	Nm3/uur	
Outputvermogen (elektrisch)	36000	kWe	
Vollasturen levering warmte of hernieuwbaar gas		uur/jaar	
Vollasturen levering elektriciteit	2945	uur/jaar	
Max. elektrisch rendement	100%		
Elektrisch rendement	100%		
Thermisch rendement of rendement gasproductie	0%		
Elektriciteitsderving bij warmtelevering		elektriciteit : warmte	
Investeringskosten	4268.41	Euro/kWinput	
		Euro/kWoutput	
Totale investeringskosten	153.66	Euro (miljoen)	*This value is depicted for information ,but is not used in the calculation*
Vaste O&M-kosten	106.71	Euro/kWinput	*2.5 % of the investment costs (Source: Tidal Grevelingen Project (2018))*
		Euro/kWoutput	
Totale jaarlijkse vaste O&M-kosten	3,842	Euro (duizend)	*This value is depicted for information ,but is not used in the calculation*
Variabele O&M-kosten (incl. contractkosten)	0.00	Euro/kWh_output	
Energie-inhoud brandstof	-	GJ/ton	
Biomassadoorzet	-	ton/jaar	
Netto brandstofprijs (aan de poort, incl. risico-opslag)		Euro/ton	
Marktprijs warmte of hernieuwbaar gas (reëel)		Euro/kWh	
Marktprijs elektriciteit (reëel)	0.130	Euro/kWh for years 1-15	Source: Tidal Grevelingen Project (2018)
	0.049	Euro/kWh for years 16-30	Source: Tidal Grevelingen Project (2018)
Basisbedrag (nominaal)		Euro/kWh	
Warmtekrachtverhouding in SDE-beschikking			
Investeringssubsidie t.g.v. vreemd vermogen (NCW)	0	Euro	
Investeringssubsidie t.g.v. eigen vermogen (NCW)	0	Euro	
Inflatie	1.7%		Source: Centraal Planbureau (2016)
Rente lening	3.0%		Source: Tidal Grevelingen Project (2018)
Vereiste return on equity	13.0%		Source: Tidal Grevelingen Project (2018)
Equity share in investering incl. EIA effect	30%		Source: Tidal Grevelingen Project (2018)
Debt share in investering incl. EIA effect	70%		
Vennootschapsbelasting	21.0%		Source: Tidal Grevelingen Project (2018)
Economische levensduur	30	jaar	Source: Tidal Grevelingen Project (2018)
Termijn lening	15	Jaar	
Afschrijvingstermijn	30	Jaar	Source: Tidal Grevelingen Project (2018)
Beleidsperiode	30	Jaar	

Onregelmatige cashflow	X		Toelichting

Tabel: Nominale kasstroom (positieve bedragen = gunstig voor de producent)

Positieve bedragen = gunstig voor de producent		**0**	**1**	**2**	**3**	**4**	**5**	**6**	**7**	**8**	**9**	**10**	**11**	**12**	**13**	**14**	**15**	**16**	**17**	**18**	**19**	**20**	**21**	**22**	**23**	**24**	**25**	**26**	**27**	**28**	**29**	**30**
Inflatie			*1.00*	*1.02*	*1.03*	*1.05*	*1.07*	*1.09*	*1.11*	*1.13*	*1.14*	*1.16*	*1.18*	*1.20*	*1.22*	*1.25*	*1.27*	*1.29*	*1.31*	*1.33*	*1.35*	*1.38*	*1.40*	*1.42*	*1.45*	*1.47*	*1.50*	*1.52*	*1.55*	*1.58*	*1.60*	*1.63*
Investering	Euro	-153,662,674																														
Afzet elektriciteit	kWh		106,020,000	106,020,000	106,020,000	106,020,000	106,020,000	106,020,000	106,020,000	106,020,000	106,020,000	106,020,000	106,020,000	106,020,000	106,020,000	106,020,000	106,020,000	106,020,000	106,020,000	106,020,000	106,020,000	106,020,000	106,020,000	106,020,000	106,020,000	106,020,000	106,020,000	106,020,000	106,020,000	106,020,000	106,020,000	106,020,000
Afzet warmte	kWh (LHV)		-	-	-	-	-	-	-	-	-	-	-	-	-	-	-	-	-	-	-	-	-	-	-	-	-	-	-	-	-	-
Afzet herniewbaar gas	kWh (HHV)		-	-	-	-	-	-	-	-	-	-	-	-	-	-	-	-	-	-	-	-	-	-	-	-	-	-	-	-	-	-
Afzet duurzame energie	kWh		106,020,000	106,020,000	106,020,000	106,020,000	106,020,000	106,020,000	106,020,000	106,020,000	106,020,000	106,020,000	106,020,000	106,020,000	106,020,000	106,020,000	106,020,000	106,020,000	106,020,000	106,020,000	106,020,000	106,020,000	106,020,000	106,020,000	106,020,000	106,020,000	106,020,000	106,020,000	106,020,000	106,020,000	106,020,000	106,020,000
Operationele kosten	Euro		-3,841,567	-3,906,873	-3,973,290	-4,040,836	-4,109,531	-4,179,393	-4,250,442	-4,322,700	-4,396,186	-4,470,921	-4,546,926	-4,624,224	-4,702,836	-4,782,784	-4,864,092	-4,946,781	-5,030,876	-5,116,401	-5,203,380	-5,291,838	-5,381,799	-5,473,289	-5,566,335	-5,660,963	-5,757,199	-5,855,072	-5,954,608	-6,055,836	-6,158,785	-6,263,485
Brandstofkosten	Euro		-	-	-	-	-	-	-	-	-	-	-	-	-	-	-	-	-	-	-	-	-	-	-	-	-	-	-	-	-	-
Marktwaarde elektriciteit	Euro/kWh		0.130	0.132	0.134	0.137	0.139	0.141	0.144	0.146	0.149	0.151	0.154	0.156	0.159	0.162	0.165	0.063	0.064	0.065	0.066	0.067	0.069	0.070	0.071	0.072	0.073	0.075	0.076	0.077	0.079	0.080
Marktwaarde warmte of hernieuwbaar gas	Euro/kWh		-	-	-	-	-	-	-	-	-	-	-	-	-	-	-	-	-	-	-	-	-	-	-	-	-	-	-	-	-	-
Correctiebedrag	Euro/kWh		0.130	0.132	0.134	0.137	0.139	0.141	0.144	0.146	0.149	0.151	0.154	0.156	0.159	0.162	0.165	0.063	0.064	0.065	0.066	0.067	0.069	0.070	0.071	0.072	0.073	0.075	0.076	0.077	0.079	0.080
Basisbedrag	Euro/kWh		-	-	-	-	-	-	-	-	-	-	-	-	-	-	-	-	-	-	-	-	-	-	-	-	-	-	-	-	-	-
SDE-vergoeding	Euro		-	-	-	-	-	-	-	-	-	-	-	-	-	-	-	-	-	-	-	-	-	-	-	-	-	-	-	-	-	-
Marktinkomsten	Euro		13,782,600	14,016,904	14,255,192	14,497,530	14,743,988	14,994,636	15,249,544	15,508,787	15,772,436	16,040,567	16,313,257	16,590,582	16,872,622	17,159,457	17,451,168	6,689,570	6,803,292	6,918,948	7,036,570	7,156,192	7,277,847	7,401,571	7,527,397	7,655,363	7,785,504	7,917,858	8,052,461	8,189,353	8,328,572	8,470,158
Inkomen totaal (nominaal)	Euro		13,782,600	14,016,904	14,255,192	14,497,530	14,743,988	14,994,636	15,249,544	15,508,787	15,772,436	16,040,567	16,313,257	16,590,582	16,872,622	17,159,457	17,451,168	6,689,570	6,803,292	6,918,948	7,036,570	7,156,192	7,277,847	7,401,571	7,527,397	7,655,363	7,785,504	7,917,858	8,052,461	8,189,353	8,328,572	8,470,158
Kosten totaal (nominaal)	Euro		-3,841,567	-3,906,873	-3,973,290	-4,040,836	-4,109,531	-4,179,393	-4,250,442	-4,322,700	-4,396,186	-4,470,921	-4,546,926	-4,624,224	-4,702,836	-4,782,784	-4,864,092	-4,946,781	-5,030,876	-5,116,401	-5,203,380	-5,291,838	-5,381,799	-5,473,289	-5,566,335	-5,660,963	-5,757,199	-5,855,072	-5,954,608	-6,055,836	-6,158,785	-6,263,485
Bruto inkomen (nominaal)	Euro		9,941,033	10,110,031	10,281,901	10,456,694	10,634,457	10,815,243	10,999,102	11,186,087	11,376,250	11,569,647	11,766,331	11,966,358	12,169,786	12,376,673	12,587,076	1,742,788	1,772,416	1,802,547	1,833,190	1,864,354	1,896,049	1,928,281	1,961,062	1,994,400	2,028,305	2,062,786	2,097,854	2,133,517	2,169,787	2,206,673
Afschrijving	Euro		-5,122,089	-5,122,089	-5,122,089	-5,122,089	-5,122,089	-5,122,089	-5,122,089	-5,122,089	-5,122,089	-5,122,089	-5,122,089	-5,122,089	-5,122,089	-5,122,089	-5,122,089	-5,122,089	-5,122,089	-5,122,089	-5,122,089	-5,122,089	-5,122,089	-5,122,089	-5,122,089	-5,122,089	-5,122,089	-5,122,089	-5,122,089	-5,122,089	-5,122,089	-5,122,089
Rente	Euro		-3,226,916	-3,053,416	-2,874,711	-2,690,644	-2,501,056	-2,305,780	-2,104,645	-1,897,477	-1,684,094	-1,464,309	-1,237,930	-1,004,760	-764,596	-517,226	-262,435	-	-	-	-	-	-	-	-	-	-	-	-	-	-	-	-
Aflossing	Euro		-5,783,342	-5,956,842	-6,135,547	-6,319,614	-6,509,202	-6,704,478	-6,905,612	-7,112,781	-7,326,164	-7,545,949	-7,772,327	-8,005,497	-8,245,662	-8,493,032	-8,747,823	-	-	-	-	-	-	-	-	-	-	-	-	-	-	-	-
Totale lasten lening	Euro		-9,010,258	-9,010,258	-9,010,258	-9,010,258	-9,010,258	-9,010,258	-9,010,258	-9,010,258	-9,010,258	-9,010,258	-9,010,258	-9,010,258	-9,010,258	-9,010,258	-9,010,258	-	-	-	-	-	-	-	-	-	-	-	-	-	-	-	-
Belastbaar inkomen	Euro		1,592,028	1,934,526	2,285,101	2,643,960	3,011,312	3,387,374	3,772,368	4,166,521	4,570,068	4,983,249	5,406,311	5,839,509	6,283,102	6,737,358	7,202,552	-3,379,301	-3,349,673	-3,319,542	-3,288,899	-3,257,735	-3,226,041	-3,193,808	-3,161,027	-3,127,689	-3,093,784	-3,059,303	-3,024,236	-2,988,572	-2,952,302	-2,915,416
Belasting bedrag	Euro		-334,326	-406,250	-479,871	-555,232	-632,376	-711,349	-792,197	-874,969	-959,714	-1,046,482	-1,135,325	-1,226,297	-1,319,451	-1,414,845	-1,512,536	709,653	703,431	697,104	690,669	684,124	677,469	670,700	663,816	656,815	649,695	642,454	635,089	627,600	619,983	612,237
Netto inkomen na belasting	Euro		596,450	693,523	791,772	891,204	991,824	1,093,637	1,196,647	1,300,860	1,406,279	1,512,907	1,620,748	1,729,804	1,840,077	1,951,570	2,064,282	2,452,442	2,475,847	2,499,651	2,523,859	2,548,479	2,573,517	2,598,981	2,624,878	2,651,215	2,678,000	2,705,240	2,732,943	2,761,117	2,789,770	2,818,911
Project cashflow	Euro	-153,662,674	9,606,707	9,703,780	9,802,030	9,901,462	10,002,082	10,103,895	10,206,905	10,311,118	10,416,536	10,523,164	10,631,005	10,740,061	10,850,335	10,961,828	11,074,540	2,452,442	2,475,847	2,499,651	2,523,859	2,548,479	2,573,517	2,598,981	2,624,878	2,651,215	2,678,000	2,705,240	2,732,943	2,761,117	2,789,770	2,818,911
Equity cashflow	Euro	-46,098,802	596,450	693,523	791,772	891,204	991,824	1,093,637	1,196,647	1,300,860	1,406,279	1,512,907	1,620,748	1,729,804	1,840,077	1,951,570	2,064,282	2,452,442	2,475,847	2,499,651	2,523,859	2,548,479	2,573,517	2,598,981	2,624,878	2,651,215	2,678,000	2,705,240	2,732,943	2,761,117	2,789,770	2,818,911
Subsidiebasis: energieproductie	kWh		106,020,000	106,020,000	106,020,000	106,020,000	106,020,000	106,020,000	106,020,000	106,020,000	106,020,000	106,020,000	106,020,000	106,020,000	106,020,000	106,020,000	106,020,000	106,020,000	106,020,000	106,020,000	106,020,000	106,020,000	106,020,000	106,020,000	106,020,000	106,020,000	106,020,000	106,020,000	106,020,000	106,020,000	106,020,000	106,020,000
Cumulatieve project cashflow	Euro		9,606,707	19,310,488	29,112,518	39,013,979	49,016,061	59,119,956	69,326,861	79,637,978	90,054,515	100,577,679	111,208,684	121,948,746	132,799,081	143,760,909	154,835,449	157,287,890	159,763,738	162,263,389	164,787,248	167,335,726	169,909,243	172,508,224	175,133,102	177,784,317	180,462,317	183,167,557	185,900,500	188,661,617	191,451,387	194,270,298

Tabel: Projectparameters

Verdisconteerde inkomsten (NPV)	Euro	9,680,095
Verdisconteerde energieafzet	kWh	627804450
Totale investering	Euro	153,662,674
DSCR (gemiddeld)		1.46
Projectrente (WACC)		5.6%
Projectrendement (IRR)		2.2%
Rendement op eigen vermogen (IRR)		1.4%
Aandeel lening	Euro	107,563,872
Aandeel equity	Euro	46,098,802
Warmtekrachtverhouding	E:W	
Samengesteld aantal vollasturen	Uur/jaar	2945
Terugverdientijd (PBP)	Jaar	15

Appendix 5

MATLAB code

```
%% ----- Case 3a - Flow through culverts equipped with bidirectional turbines------
%% ----- Optimal bidirectional turbine performance
clear all
clc
close all

%% Data import
% Import File from RWS
filename = 'WL_DATA_NS_2016_2018.csv';
WL_NS = dataimport(filename);
t = linspace(0,length(WL_NS)-1,length(WL_NS));

%Truncation of the North Sea level vector to start at through.
WL_NS = datatrunc(WL_NS);
t = linspace(0,length(WL_NS)-1,length(WL_NS));

%% General constants
rho = 1025;          % Density of salt water [kg/m^3]
g = 9.81;            % Gravitational acceleration [m/s^2]
nu = 10^-6;          % Kinematic viscosity [m^2/s]
delta_t = 60*10;     % Time step in data from RWS [min]
W = 8;               % Width of the Culvert [m]
H = 8;               % Height of the Culvert [m]
N = 18;              % Number of Culverts [-]
A = W*H;             % Cross-sectional area of culvert [m^2]
A_LG = 110e6;        % Surface area of Lake Grevelingen [m^2]

L = 49;              % Length of the culvert [m]
O = 2*(W+H);         % Wetted perimeter of duct [m]
D_h = 4*A/O;         % Hydraulic diameter [m]
epsilon = 0.3e-3;    % Roughness heigth concrete [m] (0.3-3 mm range)
K_C = 0.5;           % Inlet loss coefficient [-]
K_E = 1.0;           % Exit loss coefficient [-]
K_pfn = 0.0;         % Turbine loss coefficient [-]
eta_WTW = 0.9;

%% CASE 3a - Water level determination Lake Grevelingen - energy loss and turbines
%Determine Lake Grevelingen WL

% Initialisation
delta_h = zeros(length(WL_NS),1);
Q = zeros(length(WL_NS),1);
WL_LG = zeros(length(WL_NS),1);
C_sys = ones(length(WL_NS),6);
f = 2/3*ones(length(WL_NS),1);

% Initial water level value LG
WL_LG(1) = -0.20;

% Execution
for i = 1:5
    delta_h(1) = head(WL_NS(1),WL_LG(1));
    Q(1) = discharge(W,H,delta_h(1),C_sys(1,i),f(1));
    for n = 2:length(WL_NS)
        WL_LG(n) = waterlevel(WL_LG(n-1),N,Q(n-1),A_LG,delta_t);
        delta_h(n) = head(WL_NS(n),WL_LG(n));
        Q(n) = discharge(W,H,delta_h(n),C_sys(n,i),f(n));
    end
    U = Q/A;
    Re = abs(U)*D_h/nu;
    f_f = 0.25./(log10(epsilon./(3.7.*D_h)+(5.74./(Re.^0.9))).^2);
    C_sys(:,i+1) = syslosscoef(K_C,K_E,K_pfn,W,H,L,Re,epsilon);
end

% Insert Trendline
tr = trendline(t,WL_LG);

% Monthly averaged and maximum tidal range
TR = tidalrange(WL_LG);

% Percentage of overshoot and undershoot
OS = overshoot(WL_LG);
US = undershoot(WL_LG);

% Power generation
P = powergen(f,N,delta_h,Q);
P_mean = mean(P);
P_max = max(P);

% Energy yield
E = energy(P,delta_t); % Total energy yield in 3 years
E_mean = E/3; % Mean annual energy yield per year
```

```
%% ----- Case 3b - Flow through culverts equipped with bidirectional turbines------
%% ----- Modulated bidirectional turbine performance
clear all
clc
close all

%% Data import
% Import File from RWS
filename = 'WL_DATA_NS_2016_2018.csv';
WL_NS = dataimport(filename);
t = linspace(0,length(WL_NS)-1,length(WL_NS));

%Truncation of the North Sea level vector to start at through.
WL_NS = datatrunc(WL_NS);
% WL_NS = WL_NS(26784:26950);
t = linspace(0,length(WL_NS)-1,length(WL_NS));

%% General constants
rho = 1025;          % Density of salt water [kg/m^3]
g = 9.81;            % Gravitational acceleration [m/s^2]
nu = 10^-6;          % Kinematic viscosity [m^2/s]
delta_t = 60*10;     % Time step in data from RWS [min]
W = 8;               % Width of the Culvert [m]
H = 8;               % Height of the Culvert [m]
N = 18;              % Number of Culverts [-]
A = W*H;             % Cross-sectional area of culvert [m^2]
A_LG = 110e6;        % Surface area of Lake Grevelingen [m^2]

L = 49;              % Length of the culvert [m]
O = 2*(W+H);         % Wetted perimeter of duct [m]
D_h = 4*A/O;         % Hydraulic diameter [m]
epsilon = 0.3e-3;    % Roughness heigth concrete [m] (0.3-3 mm range)
K_C = 0.5;           % Inlet loss coefficient [-]
K_E = 1.0;           % Exit loss coefficient [-]
K_pfn = 0.0;         % Turbine loss coefficient [-]
eta_WTW = 0.9;

WL_max = 0.050;      % Upper limititing water level
WL_min = -0.45;      % Lower limiting water level


%% Case 3b - varying f
%Determine Lake Grevelingen WL

% Initialisation
delta_h = zeros(length(WL_NS),1);
Q = ones(length(WL_NS),1);
WL_LG = zeros(length(WL_NS),1);
C_sys = ones(length(WL_NS),6);
f = 2/3*ones(length(WL_NS),1);
ev = zeros(length(WL_NS),1);
U = zeros(length(WL_NS),1);
Re = zeros(length(WL_NS),1);
f_f = zeros(length(WL_NS),1);

WL_LG(1) = -0.20;
WL_LG_bound_plus = -0.045;
WL_LG_bound_min = -0.40;
% WL_LG_bound_plus = -0.2;
% WL_LG_bound_min = -0.2;


t_b = zeros(length(WL_NS),1);
m = zeros(length(WL_NS),1);
b = zeros(length(WL_NS),1);

% Execution
delta_h(1) = head(WL_NS(1),WL_LG(1));
for i = 1:5
    Q(1) = discharge(W,H,delta_h(1),C_sys(1,i),f(1));
    U(1) = Q(1)/A;
    Re(1) = abs(U(1))*D_h/nu;
    f_f(1) = 0.25./(log10(epsilon./(3.7.*D_h)+(5.74./(Re(1).^0.9))).^2);
    C_sys(1,i+1) = 1 + f_f(1).*L/D_h + K_C + K_E + K_pfn;
end
for n = 2:length(WL_NS)
    WL_LG(n) = waterlevel(WL_LG(n-1),N,Q(n-1),A_LG,delta_t);
    delta_h(n) = head(WL_NS(n),WL_LG(n));
        for i = 1:5
            Q(n) = discharge(W,H,delta_h(n),C_sys(n,i),f(n));
            U(n) = Q(n)/A;
            Re(n) = abs(U(n))*D_h/nu;
            f_f(n) = 0.25./(log10(epsilon./(3.7.*D_h)+(5.74./(Re(n).^0.9))).^2);
            C_sys(n,i+1) = 1 + f_f(n).*L/D_h + K_C + K_E + K_pfn;
            C_sys(n,1) = C_sys(n-1,6);
        end
```

```
    if WL_LG(n) >= WL_LG_bound_plus && delta_h(n) > 0
        t_b(n) = timetoupbound(WL_max, WL_LG(n-1), N, Q(n-1));
        m(n) = slope(f(n-1), t_b(n));
        b(n) = vertint(m(n), t(n-1), t_b(n),delta_t);
        f(n) = DOR(m(n), t(n-1), b(n),delta_t);
        if f(n) >= 1
            f(n) = 0.999999;
        end
    elseif WL_LG(n) <= WL_LG_bound_min && delta_h(n) < 0
        t_b(n) = timetolobound(WL_min, WL_LG(n-1), N, Q(n-1));
        m(n) = slope(f(n-1), t_b(n));
        b(n) = vertint(m(n), t(n-1), t_b(n),delta_t);
        f(n) = DOR(m(n), t(n-1), b(n),delta_t);
        if f(n) >= 1
            f(n) = 0.999999;
        end
    else
        f(n) = 2/3;
    end
    Q(n) = discharge(W,H,delta_h(n),C_sys(n,i),f(n));
    WL_LG(n) = waterlevel(WL_LG(n-1),N,Q(n-1),A_LG,delta_t);
end

% Insert Trendline
tr = trendline(t,WL_LG);

% Monthly averaged and maximum tidal range
TR = tidalrange(WL_LG);

% Percentage of overshoot and undershoot
OS = overshoot(WL_LG);
US = undershoot(WL_LG);

% Power generation
P = powergen(f,N,delta_h,Q);
P_mean = mean(P);
P_max = max(P);

% Energy yield
E = energy(P,delta_t); % Total energy yield in 3 years
E_mean = E/3; % Mean annual energy yield per year
```

```
%% ----- Case 2a - Flow through culverts equipped with unidirectional turbines------
%% ----- Optimal unidirectional turbine performance
clear all
clc
close all

%% Data import
% Import File from RWS
filename = 'WL_DATA_NS_2016_2018.csv';
WL_NS = dataimport(filename);
t = linspace(0,length(WL_NS)-1,length(WL_NS));

%Truncation of the North Sea level vector to start at through.
WL_NS = datatrunc(WL_NS);
t = linspace(0,length(WL_NS)-1,length(WL_NS));

%% General constants
rho = 1025;          % Density of salt water [kg/m^3]
g = 9.81;            % Gravitational acceleration [m/s^2]
nu = 10^-6;          % Kinematic viscosity [m^2/s]
delta_t = 60*10;     % Time step in data from RWS [min]
W = 8;               % Width of the Culvert [m]
H = 8;               % Height of the Culvert [m]
N = 18;              % Number of Culverts [-]
A = W*H;             % Cross-sectional area of culvert [m^2]
A_LG = 110e6;        % Surface area of Lake Grevelingen [m^2]

L = 49;              % Length of the culvert [m]
O = 2*(W+H);         % Wetted perimeter of duct [m]
D_h = 4*A/O;         % Hydraulic diameter [m]
epsilon = 0.3e-3;    % Roughness heigth concrete [m] (0.3-3 mm range)
K_C = 0.5;           % Inlet loss coefficient [-]
K_E = 1.0;           % Exit loss coefficient [-]
K_pfn = 0.0;         % Turbine loss coefficient [-]
eta_WTW = 0.9;

%% CASE 4a - Water level determination Lake Grevelingen - energy loss and turbines
%Determine Lake Grevelingen WL

% Initialisation
delta_h = zeros(length(WL_NS),1);
Q = zeros(length(WL_NS),1);
WL_LG = zeros(length(WL_NS),1);
C_sys = ones(length(WL_NS),6);
f = 2/3*ones(length(WL_NS),1);

% Initial water level value LG
WL_LG(1) = -0.20;

% Execution
for i = 1:5
    delta_h(1) = head(WL_NS(1),WL_LG(1));
    f(1) = inlet_outlet_f(delta_h(1));
    Q(1) = discharge(W,H,delta_h(1),C_sys(1,i),f(1));
    for n = 2:length(WL_NS)
        WL_LG(n) = waterlevel(WL_LG(n-1),N,Q(n-1),A_LG,delta_t);
        delta_h(n) = head(WL_NS(n),WL_LG(n));
        f(n) = inlet_outlet_f(delta_h(n));
        Q(n) = discharge(W,H,delta_h(n),C_sys(n,i),f(n));
    end
    U = Q/A;
    Re = abs(U)*D_h/nu;
    f_f = 0.25./(log10(epsilon./(3.7.*D_h)+(5.74./(Re.^0.9))).^2);
    C_sys(:,i+1) = syslosscoef(K_C,K_E,K_pfn,W,H,L,Re,epsilon);
end

% Insert Trendline
tr = trendline(t,WL_LG);

% Monthly averaged and maximum tidal range
TR = tidalrange(WL_LG);

% Percentage of overshoot and undershoot
OS = overshoot(WL_LG);
US = undershoot(WL_LG);

% Power generation
P = powergen(f,N,delta_h,Q);
P_mean = mean(P);
P_max = max(P);

% Energy yield
E = energy(P,delta_t); % Total energy yield in 3 years
E_mean = E/3; % Mean annual energy yield per year
```

```
%% ----- Case 2b - Flow through culverts equipped with unidirectional turbines------
%% ----- Modulated unidirectional turbine performance
clear all
clc
close all

%% Data import
% Import File from RWS
filename = 'WL_DATA_NS_2016_2018.csv';
WL_NS = dataimport(filename);
t = linspace(0,length(WL_NS)-1,length(WL_NS));

%Truncation of the North Sea level vector to start at through.
WL_NS = datatrunc(WL_NS);
t = linspace(0,length(WL_NS)-1,length(WL_NS));

%% General constants
rho = 1025;          % Density of salt water [kg/m^3]
g = 9.81;            % Gravitational acceleration [m/s^2]
nu = 10^-6;          % Kinematic viscosity [m^2/s]
delta_t = 60*10;     % Time step in data from RWS [min]
W = 8;               % Width of the Culvert [m]
H = 8;               % Height of the Culvert [m]
N = 18;              % Number of Culverts [-]
A = W*H;             % Cross-sectional area of culvert [m^2]
A_LG = 110e6;        % Surface area of Lake Grevelingen [m^2]

L = 49;              % Length of the culvert [m]
O = 2*(W+H);         % Wetted perimeter of duct [m]
D_h = 4*A/O;         % Hydraulic diameter [m]
epsilon = 0.3e-3;    % Roughness heigth concrete [m] (0.3-3 mm range)
K_C = 0.5;           % Inlet loss coefficient [-]
K_E = 1.0;           % Exit loss coefficient [-]
K_pfn = 0.0;         % Turbine loss coefficient [-]
eta_WTW = 0.9;

WL_max = 0.05;
WL_min = -0.45;

%% Case 4c - varying f
% Implementing variable degree of reaction f

%Determine Lake Grevelingen WL
% Initialisation
delta_h = zeros(length(WL_NS),1);
Q = ones(length(WL_NS),1);
WL_LG = zeros(length(WL_NS),1);
C_sys = ones(length(WL_NS),6);
f = 2/3*ones(length(WL_NS),1);
ev = zeros(length(WL_NS),1);
U = zeros(length(WL_NS),1);
Re = zeros(length(WL_NS),1);
f_f = zeros(length(WL_NS),1);

WL_LG(1) = -0.20;
WL_LG_bound_plus = 0.025;
WL_LG_bound_min = -0.23;

t_b = zeros(length(WL_NS),1);
m = zeros(length(WL_NS),1);
b = zeros(length(WL_NS),1);

% Execution
delta_h(1) = head(WL_NS(1),WL_LG(1));
for i = 1:5
    f(1) = inlet_outlet_f(delta_h(1));
    Q(1) = discharge(W,H,delta_h(1),C_sys(1,i),f(1));
    U(1) = Q(1)/A;
    Re(1) = abs(U(1))*D_h/nu;
    f_f(1) = 0.25./(log10(epsilon./(3.7.*D_h)+(5.74./(Re(1).^0.9))).^2);
    C_sys(1,i+1) = syslosscoef(K_C,K_E,K_pfn,W,H,L,Re(1),epsilon);
end
for n = 2:length(WL_NS)
    WL_LG(n) = waterlevel(WL_LG(n-1),N,Q(n-1),A_LG,delta_t);
    delta_h(n) = head(WL_NS(n),WL_LG(n));
        for i = 1:5
            f(n) = inlet_outlet_f(delta_h(n));
            Q(n) = discharge(W,H,delta_h(n),C_sys(n,i),f(n));
            U(n) = Q(n)/A;
            Re(n) = abs(U(n))*D_h/nu;
            f_f(n) = 0.25./(log10(epsilon./(3.7.*D_h)+(5.74./(Re(n).^0.9))).^2);
            C_sys(n,i+1) = syslosscoef(K_C,K_E,K_pfn,W,H,L,Re(n),epsilon);
            C_sys(n,1) = C_sys(n-1,6);
        end
        if WL_LG(n) >= WL_LG_bound_plus && delta_h(n) > 0
            t_b(n) = timetoupbound(WL_max, WL_LG(n-1), N, Q(n-1));
```

```
            m(n) = slope(f(n-1), t_b(n));
            b(n) = vertint(m(n), t(n-1), t_b(n),delta_t);
            f(n) = DOR(m(n), t(n-1), b(n),delta_t);
            if f(n) >= 1
                f(n) = 0.999999;
            end
        elseif  WL_LG(n) <= WL_LG_bound_min && delta_h(n) < 0
            t_b(n) = timetolobound(WL_min, WL_LG(n-1), N, Q(n-1));
            m(n) = slope(f(n-1), t_b(n));
            b(n) = vertint(m(n), t(n-1), t_b(n),delta_t);
            f(n) = DOR(m(n), t(n-1), b(n),delta_t);
            if f(n) >= 1
                f(n) = 0.999999;
            end
        else
            f(n) = inlet_outlet_f(delta_h(n));
        end
    Q(n) = discharge(W,H,delta_h(n),C_sys(n,i),f(n));
    WL_LG(n) = waterlevel(WL_LG(n-1),N,Q(n-1),A_LG,delta_t);
end

% Insert Trendline
tr = trendline(t,WL_LG);

% Monthly averaged and maximum tidal range
TR = tidalrange(WL_LG);

% Percentage of overshoot and undershoot
OS = overshoot(WL_LG);
US = undershoot(WL_LG);

% Power generation
P = powergen(f,N,delta_h,Q);
P_mean = mean(P);
P_max = max(P);

% Energy yield
E = energy(P,delta_t); % Total energy yield in 3 years
E_mean = E/3; % Mean annual energy yield per year
```

```
%% ----- Case 1a -Tidal Grevelingen Project proposal------
%% ----- Optimal turbine performance
clear all
clc
close all

%% Data import
% Import File from RWS
filename = 'WL_DATA_NS_2016_2018.csv';
WL_NS = dataimport(filename);
t = linspace(0,length(WL_NS)-1,length(WL_NS));

%Truncation of the North Sea level vector to start at through.
WL_NS = datatrunc(WL_NS);
t = linspace(0,length(WL_NS)-1,length(WL_NS));

%% General constants
rho = 1025;          % Density of salt water [kg/m^3]
g = 9.81;            % Gravitational acceleration [m/s^2]
nu = 10^-6;          % Kinematic viscosity [m^2/s]
delta_t = 60*10;     % Time step in data from RWS [min]
W = 8;               % Width of the Culvert [m]
H = 8;               % Height of the Culvert [m]
N = 18;              % Number of Culverts [-]
A = W*H;             % Cross-sectional area of culvert [m^2]
A_LG = 110e6;        % Surface area of Lake Grevelingen [m^2]

L = 49;              % Length of the culvert [m]
O = 2*(W+H);         % Wetted perimeter of duct [m]
D_h = 4*A/O;         % Hydraulic diameter [m]
epsilon = 0.3e-3;    % Roughness heigth concrete [m] (0.3-3 mm range)
K_C = 0.5;           % Inlet loss coefficient [-]
K_E = 1.0;           % Exit loss coefficient [-]
K_pfn = 0.0;         % Turbine loss coefficient [-]
eta_WTW = 0.9;

WL_max = 0.05;
WL_min = -0.45;

%% Case 5 _varying f
% Implementing variable degree of reaction f
%Determine Lake Grevelingen WL

% Initialisation
delta_h = zeros(length(WL_NS),1);
WL_LG = zeros(length(WL_NS),1);

Q_t = ones(length(WL_NS),1);
C_sys_t = ones(length(WL_NS),6);
f_t = 2/3*ones(length(WL_NS),1);
U_t = zeros(length(WL_NS),1);
Re_t = zeros(length(WL_NS),1);

M = 7;
Q_e = ones(length(WL_NS),1);
C_sys_e = ones(length(WL_NS),6);
f_e = zeros(length(WL_NS),1);
U_e = zeros(length(WL_NS),1);
Re_e = zeros(length(WL_NS),1);

WL_LG(1) = -0.20;
WL_LG_bound_plus = -0.13;
WL_LG_bound_min = -0.4;

t_b = zeros(length(WL_NS),1);
m = zeros(length(WL_NS),1);
b = zeros(length(WL_NS),1);

% Execution
delta_h(1) = head(WL_NS(1),WL_LG(1));
for i = 1:5
    f_t(1) = inlet_outlet_f78(delta_h(1));
    Q_t(1) = discharge(W,H,delta_h(1),C_sys_t(1,i),f_t(1));
    U_t(1) = Q_t(1)/A;
    Re_t(1) = abs(U_t(1))*D_h/nu;
    C_sys_t(1,i+1) = syslosscoef(K_C,K_E,K_pfn,W,H,L,Re_t(1),epsilon);
    Q_e(1) = discharge(W,H,delta_h(1),C_sys_e(1,i),f_e(1));
    U_e(1) = Q_e(1)/A;
    Re_e(1) = abs(U_e(1))*D_h/nu;
    C_sys_e(1,i+1) = syslosscoef(K_C,K_E,K_pfn,W,H,L,Re_e(1),epsilon);
end
for n = 2:length(WL_NS)
    WL_LG(n) = waterlevel78(WL_LG(n-1),N,M,Q_t(n-1),Q_e(n-1),A_LG,delta_t);
    delta_h(n) = head(WL_NS(n),WL_LG(n));
        for i = 1:5
            f_t(n) = inlet_outlet_f78(delta_h(n));
```

```
            Q_t(n) = discharge(W,H,delta_h(n),C_sys_t(n,i),f_t(n));
            U_t(n) = Q_t(n)/A;
            Re_t(n) = abs(U_t(n))*D_h/nu;
            C_sys_t(n,i+1) = syslosscoef(K_C,K_E,K_pfn,W,H,L,Re_t(n),epsilon);
            C_sys_t(n,1) = C_sys_t(n-1,6);
            Q_e(n) = discharge(W,H,delta_h(n),C_sys_e(n,i),f_e(n));
            U_e(n) = Q_e(n)/A;
            Re_e(n) = abs(U_e(n))*D_h/nu;
            C_sys_e(n,i+1) = syslosscoef(K_C,K_E,K_pfn,W,H,L,Re_e(n),epsilon);
            C_sys_e(n,1) = C_sys_e(n-1,6);
        end
    f_t(n) = inlet_outlet_f78(delta_h(n));
    Q_t(n) = discharge(W,H,delta_h(n),C_sys_t(n,i),f_t(n));
    WL_LG(n) = waterlevel78(WL_LG(n-1),N,M,Q_t(n-1),Q_e(n-1),A_LG,delta_t);
end

% Insert Trendline
tr = trendline(t,WL_LG);

% Monthly averaged and maximum tidal range
TR = tidalrange(WL_LG);

% Percentage of overshoot and undershoot
OS = overshoot(WL_LG);
US = undershoot(WL_LG);

% Power generation
P = powergen(f_t,N-M,delta_h,Q_t);
P_mean = mean(P);
P_max = max(P);

% Energy yield
E = energy(P,delta_t); % Total energy yield in 3 years
E_mean = E/3; % Mean annual energy yield per year
```

```
%% ----- Case 1b -Tidal Grevelingen Project proposal------
%% ----- Modulated turbine performance
clear all
clc
close all

%% Data import
% Import File from RWS
filename = 'WL_DATA_NS_2016_2018.csv';
WL_NS = dataimport(filename);
t = linspace(0,length(WL_NS)-1,length(WL_NS));

% Truncation of the North Sea level vector to start at through.
WL_NS = datatrunc(WL_NS);
t = linspace(0,length(WL_NS)-1,length(WL_NS));

%% General constants
rho = 1025;          % Density of salt water [kg/m^3]
g = 9.81;            % Gravitational acceleration [m/s^2]
nu = 10^-6;          % Kinematic viscosity [m^2/s]
delta_t = 60*10;     % Time step in data from RWS [min]
W = 8;               % Width of the Culvert [m]
H = 8;               % Height of the Culvert [m]
N = 18;              % Number of Culverts [-]
A = W*H;             % Cross-sectional area of culvert [m^2]
A_LG = 110e6;        % Surface area of Lake Grevelingen [m^2]

L = 49;              % Length of the culvert [m]
O = 2*(W+H);         % Wetted perimeter of duct [m]
D_h = 4*A/O;         % Hydraulic diameter [m]
epsilon = 0.3e-3;    % Roughness heigth concrete [m] (0.3-3 mm range)
K_C = 0.5;           % Inlet loss coefficient [-]
K_E = 1.0;           % Exit loss coefficient [-]
K_pfn = 0.0;         % Turbine loss coefficient [-]
eta_WTW = 0.9;

WL_max = 0.05;
WL_min = -0.45;

%% Case 5 _varying f
% Implementing variable degree of reaction f

%Determine Lake Grevelingen WL
% Initialisation
delta_h = zeros(length(WL_NS),1);
WL_LG = zeros(length(WL_NS),1);

Q_t = ones(length(WL_NS),1);
C_sys_t = ones(length(WL_NS),6);
f_t = 2/3*ones(length(WL_NS),1);
U_t = zeros(length(WL_NS),1);
Re_t = zeros(length(WL_NS),1);
f_f_t = zeros(length(WL_NS),1);

M = 7;
Q_e = ones(length(WL_NS),1);
C_sys_e = ones(length(WL_NS),6);
f_e = zeros(length(WL_NS),1);
U_e = zeros(length(WL_NS),1);
Re_e = zeros(length(WL_NS),1);
f_f_e = zeros(length(WL_NS),1);

WL_LG(1) = -0.2;
WL_LG_bound_plus = -0.14;
WL_LG_bound_min = -0.20; %minimum WL 0.005

t_b = zeros(length(WL_NS),1);
m = zeros(length(WL_NS),1);
b = zeros(length(WL_NS),1);


% Execution
delta_h(1) = head(WL_NS(1),WL_LG(1));
for i = 1:5
    f_t(1) = inlet_outlet_f78(delta_h(1));
    Q_t(1) = discharge(W,H,delta_h(1),C_sys_t(1,i),f_t(1));
    U_t(1) = Q_t(1)/A;
    Re_t(1) = abs(U_t(1))*D_h/nu;
    f_f_t(1) = 0.25./(log10(epsilon./(3.7.*D_h)+(5.74./(Re_t(1).^0.9))).^2);
    C_sys_t(1,i+1) = syslosscoef(K_C,K_E,K_pfn,W,H,L,Re_t(1),epsilon);
    Q_e(1) = discharge(W,H,delta_h(1),C_sys_e(1,i),f_e(1));
    U_e(1) = Q_e(1)/A;
    Re_e(1) = abs(U_e(1))*D_h/nu;
    f_f_e(1) = 0.25./(log10(epsilon./(3.7.*D_h)+(5.74./(Re_e(1).^0.9))).^2);
    C_sys_e(1,i+1) = syslosscoef(K_C,K_E,K_pfn,W,H,L,Re_e(1),epsilon);
end
```

```
for n = 2:length(WL_NS)
    WL_LG(n) = waterlevel78(WL_LG(n-1),N,M,Q_t(n-1),Q_e(n-1),A_LG,delta_t);
    delta_h(n) = head(WL_NS(n),WL_LG(n));
        for i = 1:5
            f_t(n) = inlet_outlet_f78(delta_h(n));
            Q_t(n) = discharge(W,H,delta_h(n),C_sys_t(n,i),f_t(n));
            U_t(n) = Q_t(n)/A;
            Re_t(n) = abs(U_t(n))*D_h/nu;
            f_f_t(n) = 0.25./(log10(epsilon./(3.7.*D_h)+(5.74./(Re_t(n).^0.9))).^2);
            C_sys_t(n,i+1) = syslosscoef(K_C,K_E,K_pfn,W,H,L,Re_t(n),epsilon);
            C_sys_t(n,1) = C_sys_t(n-1,6);
            Q_e(n) = discharge(W,H,delta_h(n),C_sys_e(n,i),f_e(n));
            U_e(n) = Q_e(n)/A;
            Re_e(n) = abs(U_e(n))*D_h/nu;
            f_f_e(n) = 0.25./(log10(epsilon./(3.7.*D_h)+(5.74./(Re_e(n).^0.9))).^2);
            C_sys_e(n,i+1) = syslosscoef(K_C,K_E,K_pfn,W,H,L,Re_e(n),epsilon);
            C_sys_e(n,1) = C_sys_e(n-1,6);
        end
        if WL_LG(n) > WL_LG_bound_plus && delta_h(n) > 0
            t_b(n) = timetoupbound78(WL_max, WL_LG(n-1), N, Q_t(n-1), M, Q_e(n-1));
            m(n) = slope(f_t(n-1), t_b(n));
            b(n) = vertint(m(n), t(n-1), t_b(n),delta_t);
            f_t(n) = DOR(m(n), t(n-1), b(n),delta_t);
            if f_t(n) >= 1
                f_t(n) = 0.999999;
            end
        elseif delta_h(n) < 0
                f_t(n) = 0;
        else
                f_t(n) = inlet_outlet_f78(delta_h(n));
        end
    Q_t(n) = discharge(W,H,delta_h(n),C_sys_t(n,i),f_t(n));
    WL_LG(n) = waterlevel78(WL_LG(n-1),N,M,Q_t(n-1),Q_e(n-1),A_LG,delta_t);
end

% Insert Trendline
tr = trendline(t,WL_LG);

% Monthly averaged and maximum tidal range
TR = tidalrange(WL_LG);

% Percentage of overshoot and undershoot
OS = overshoot(WL_LG);
US = undershoot(WL_LG);

% Power generation
P = powergen(f_t,N-M,delta_h,Q_t);
P_mean = mean(P);
P_max = max(P);

% Energy yield
E = energy(P,delta_t); % Total energy yield in 3 years
E_mean = E/3; % Mean annual energy yield per year
```

```
%% ----------------- Optimisation of Bidirectional turbine configuration -----------------
tic
clear all
clc
close all

%% Data import
% Import File from RWS
filename = 'WL_DATA_NS_2016_2018.csv';
WL_NS = dataimport(filename);
t = linspace(0,length(WL_NS)-1,length(WL_NS));

% Truncation of the North Sea level vector to start at through.
WL_NS = datatrunc(WL_NS);
t = linspace(0,length(WL_NS)-1,length(WL_NS));

%% General hydraulic constants
rho = 1025;                     % Density of salt water [kg/m^3]
g = 9.81;                       % Gravitational acceleration [m/s^2]
nu = 10^-6;                     % Kinematic viscosity [m^2/s]
delta_t = 60*10;                % Time step in data from RWS [min]
epsilon = 0.3e-3;               % Roughness height concrete [m] (0.3-3 mm range)
K_C = 0.5;                      % Loss coefficient of entrance [-]
K_E = 1.0;                      % Loss coefficient of exit [-]
K_pfn = 0.0;                    % Loss coefficient of turbine [-]

% Dimensional parameters
W = [4:1:9];                    % Width of the Culvert [m]
H = [4:1:9];                    % Height of the Culvert [m]
N = [5:1:39];                   % Number of Culverts [-]
W_wall = 1.0;                   % Width of wall [-]
A_c = W.*H;                     % Cross-sectional area of culvert [m^2]
A_LG = 110e6;                   % Surface area of Lake Grevelingen [m^2]
L = 49;                         % Length of culvert [m]
O = 2*(W+H);                    % Wetted perimeter of duct [m]
D_h = 4*A_c./O;                 % Hydraulic diameter [m]

WL_max = 0.05;                  % Max water level [m]
WL_min = -0.45;                 % Min water level [m]

%% Establishing Overview matrix (OVM)
% Determining values OVM Columns 1,2 and 3
OVM = zeros(length(N)*length(W),12);
OVM(:,1) = repmat(W',length(N),1);
VV = repmat(N(1):1:N(end),length(W),1);
OVM(:,2) = VV(:)';
OVM(:,3) = OVM(:,1).*OVM(:,2)+(OVM(:,2)+1)*W_wall;
WLLG_MAT = zeros(length(WL_NS),length(N)*length(W));

TR_matmean = zeros(length(W)*length(N), 36);
TR_matmax = zeros(length(W)*length(N), 36);

% Determine Lake Grevelingen WL
for xx = 1:length(N)
    for ii = 1:length(W)
% Initialisation
        delta_h = zeros(length(WL_NS),1);
        Q = ones(length(WL_NS),1);
        WL_LG = zeros(length(WL_NS),1);
        C_sys = ones(length(WL_NS),6);
        f = 2/3*ones(length(WL_NS),1);

        U = zeros(length(WL_NS),1);
        Re = zeros(length(WL_NS),1);
        f_f = zeros(length(WL_NS),1);

        WL_LG(1) = -0.20;
        WL_LG_bound_plus = -0.20;
        WL_LG_bound_min = -0.20;

        t_b = zeros(length(WL_NS),1);
        m = zeros(length(WL_NS),1);
        b = zeros(length(WL_NS),1);

% Execution
        delta_h(1) = head(WL_NS(1),WL_LG(1));
        for i = 1:5
            Q(1) = discharge(W(ii),H(ii),delta_h(1),C_sys(1,i),f(1));
            U(1) = Q(1)/A_c(ii);
            Re(1) = abs(U(1))*D_h(ii)/nu;
            f_f(1) = 0.25./(log10(epsilon./(3.7.*D_h(ii))+(5.74./(Re(1).^0.9))).^2);
            C_sys(1,i+1) = 1 + f_f(1).*L/D_h(ii) + K_C + K_E + K_pfn;
        end
        for n = 2:length(WL_NS)
            WL_LG(n) = waterlevel(WL_LG(n-1),N(xx),Q(n-1),A_LG,delta_t);
            delta_h(n) = head(WL_NS(n),WL_LG(n));
                for i = 1:5
                    Q(n) = discharge(W(ii),H(ii),delta_h(n),C_sys(n,i),f(n));
```

```
                    U(n) = Q(n)/A_c(ii);
                    Re(n) = abs(U(n))*D_h(ii)/nu;
                    f_f(n) = 0.25./(log10(epsilon./(3.7.*D_h(ii))+(5.74./(Re(n).^0.9))).^2);
                    C_sys(n,i+1) = 1 + f_f(n).*L/D_h(ii) + K_C + K_E + K_pfn;
                    C_sys(n,1) = C_sys(n-1,6);
                end
            if WL_LG(n) >= WL_LG_bound_plus && delta_h(n) > 0
                t_b(n) = timetoupbound(WL_max, WL_LG(n-1), N(xx), Q(n-1));
                m(n) = slope(f(n-1), t_b(n));
                b(n) = vertint(m(n), t(n-1), t_b(n),delta_t);
                f(n) = DOR(m(n), t(n-1), b(n),delta_t);
                if f(n) >= 1
                    f(n) = 0.999999;
                end
            elseif WL_LG(n) <= WL_LG_bound_min && delta_h(n) < 0
                t_b(n) = timetolobound(WL_min, WL_LG(n-1), N(xx), Q(n-1));
                m(n) = slope(f(n-1), t_b(n));
                b(n) = vertint(m(n), t(n-1), t_b(n),delta_t);
                f(n) = DOR(m(n), t(n-1), b(n),delta_t);
                if f(n) >= 1
                    f(n) = 0.999999;
                end
            else
                f(n) = 2/3;
            end
            Q(n) = discharge(W(ii),H(ii),delta_h(n),C_sys(n,i),f(n));
            WL_LG(n) = waterlevel(WL_LG(n-1),N(xx),Q(n-1),A_LG,delta_t);
        end
% Determining values for OVM Column 4 to 75
        RR = ii + length(W)*(xx-1);

% Percentage of overshoot and undershoot per year
        OS = overshoot(WL_LG);
        US = undershoot(WL_LG);
        OVM(RR,4) = OS(2,1);
        OVM(RR,5) = OS(2,2);
        OVM(RR,6) = OS(2,3);
        OVM(RR,7) = US(2,1);
        OVM(RR,8) = US(2,2);
        OVM(RR,9) = US(2,3);

% Power generation
        P = powergen(f,N(xx),delta_h,Q);
        P_mean = mean(P);
        P_max = max(P);

% Energy yield
        E = energy(P,delta_t);  % Total energy yield in 3 years
        E_mean = E/3;           % Mean annual energy yield per year

        OVM(RR,10) = P_mean;    % Mean power
        OVM(RR,11) = P_max;     % Max power
        OVM(RR,12) = E_mean;    % Mean annual energy yield

% Mean and maximum tidal range
        TR = tidalrange(WL_LG);
        TR_matmean(RR,:) = TR(2,:);
        TR_matmax(RR,:) = TR(3,:);
    end
end
OVM = [OVM TR_matmean TR_matmax];
timeElapsed = toc
```

```
%% ----------------- Optimisation of Unidirectional turbine configuration -----------------
tic
clear all
clc
close all

%% Data import
% Import File from RWS
filename = 'WL_DATA_NS_2016_2018.csv';
WL_NS = dataimport(filename);
t = linspace(0,length(WL_NS)-1,length(WL_NS));

% Truncation of the North Sea level vector to start at through.
WL_NS = datatrunc(WL_NS);
t = linspace(0,length(WL_NS)-1,length(WL_NS));

%% General hydraulic constants
rho = 1025;                     % Density of salt water [kg/m^3]
g = 9.81;                       % Gravitational acceleration [m/s^2]
nu = 10^-6;                     % Kinematic viscosity [m^2/s]
delta_t = 60*10;                % Time step in data from RWS [min]
epsilon = 0.3e-3;               % Roughness heigth concrete [m] (0.3-3 mm range)
K_C = 0.5;                      % Loss coefficient of entrance [-]
K_E = 1.0;                      % Loss coefficient of exit [-]
K_pfn = 0.0;                    % Loss coefficient of turbine [-]

% Dimensional parameters
W = [4:1:9];                    % Width of the Culvert [m]
H = [4:1:9];                    % Height of the Culvert [m]
N = [5:1:39];                   % Number of Culverts [-]
W_wall = 1.0;                   % Width of wall [-]
A_c = W.*H;                     % Cross-sectional area of culvert [m^2]
A_LG = 110e6;                   % Surface area of Lake Grevelingen [m^2]
L = 49;                         % Length of culvert [m]
O = 2*(W+H);                    % Wetted perimeter of duct [m]
D_h = 4*A_c./O;                 % Hydraulic diameter [m]

WL_max = 0.05;                  % Max water level [m]
WL_min = -0.45;                 % Min water level [m]

%% Establishing Overview matrix
% Determining values OVM Columns 1,2 and 3
OVM = zeros(length(N)*length(W),12);
OVM(:,1) = repmat(W',length(N),1);
VV = repmat(N(1):1:N(end),length(W),1);
OVM(:,2) = VV(:)';
OVM(:,3) = OVM(:,1).*OVM(:,2)+(OVM(:,2)+1)*W_wall;
WLLG_MAT = zeros(length(WL_NS),length(N)*length(W));

TR_matmean = zeros(length(W)*length(N), 36);
TR_matmax = zeros(length(W)*length(N), 36);

% Determine Lake Grevelingen WL
for xx = 1:length(N)
    for ii = 1:length(W)
% Initialisation
        delta_h = zeros(length(WL_NS),1);
        Q = ones(length(WL_NS),1);
        WL_LG = zeros(length(WL_NS),1);
        C_sys = ones(length(WL_NS),6);
        f = 2/3*ones(length(WL_NS),1);

        U = zeros(length(WL_NS),1);
        Re = zeros(length(WL_NS),1);
        f_f = zeros(length(WL_NS),1);

        WL_LG(1) = -0.20;
        WL_LG_bound_plus = -0.45;
        WL_LG_bound_min = -0.20;

        t_b = zeros(length(WL_NS),1);
        m = zeros(length(WL_NS),1);
        b = zeros(length(WL_NS),1);

% Execution
        delta_h(1) = head(WL_NS(1),WL_LG(1));
        for i = 1:5
            Q(1) = discharge(W(ii),H(ii),delta_h(1),C_sys(1,i),f(1));
            U(1) = Q(1)/A_c(ii);
            Re(1) = abs(U(1))*D_h(ii)/nu;
            f_f(1) = 0.25./(log10(epsilon./(3.7.*D_h(ii))+(5.74./(Re(1).^0.9))).^2);
            C_sys(1,i+1) = 1 + f_f(1).*L/D_h(ii) + K_C + K_E + K_pfn;
        end
        for n = 2:length(WL_NS)
            WL_LG(n) = waterlevel(WL_LG(n-1),N(xx),Q(n-1),A_LG,delta_t);
            delta_h(n) = head(WL_NS(n),WL_LG(n));
                for i = 1:5
                    Q(n) = discharge(W(ii),H(ii),delta_h(n),C_sys(n,i),f(n));
```

```
                    U(n) = Q(n)/A_c(ii);
                    Re(n) = abs(U(n))*D_h(ii)/nu;
                    f_f(n) = 0.25./(log10(epsilon./(3.7.*D_h(ii))+(5.74./(Re(n).^0.9))).^2);
                    C_sys(n,i+1) = 1 + f_f(n).*L/D_h(ii) + K_C + K_E + K_pfn;
                    C_sys(n,1) = C_sys(n-1,6);
                end
            if WL_LG(n) >= WL_LG_bound_plus && delta_h(n) > 0
                t_b(n) = timetoupbound(WL_max, WL_LG(n-1), N(xx), Q(n-1));
                m(n) = slope(f(n-1), t_b(n));
                b(n) = vertint(m(n), t(n-1), t_b(n),delta_t);
                f(n) = DOR(m(n), t(n-1), b(n),delta_t);
                if f(n) >= 1
                    f(n) = 0.999999;
                end
            elseif delta_h(n) < 0
                f(n) = 0;
            else
                f(n) = 2/3;
            end
            Q(n) = discharge(W(ii),H(ii),delta_h(n),C_sys(n,i),f(n));
            WL_LG(n) = waterlevel(WL_LG(n-1),N(xx),Q(n-1),A_LG,delta_t);
        end
% Determining values for OVM Column 4 to 75
        RR = ii + length(W)*(xx-1);

% Percentage of overshoot and undershoot
        OS = overshoot(WL_LG);
        US = undershoot(WL_LG);
        OVM(RR,4) = OS(2,1);
        OVM(RR,5) = OS(2,2);
        OVM(RR,6) = OS(2,3);
        OVM(RR,7) = US(2,1);
        OVM(RR,8) = US(2,2);
        OVM(RR,9) = US(2,3);

% Power Generation
        P = powergen(f,N(xx),delta_h,Q);
        P_mean = mean(P);
        P_max = max(P);

% Energy yield
        E = energy(P,delta_t);  % Total energy yield in 3 years
        E_mean = E/3;           % Mean annual energy yield per year

        OVM(RR,10) = P_mean;    % Mean power
        OVM(RR,11) = P_max;     % Max power
        OVM(RR,12) = E_mean;    % Mean annual energy yield

% Mean and maximum tidal range
        TR = tidalrange(WL_LG);
        TR_matmean(RR,:) = TR(2,:);
        TR_matmax(RR,:) = TR(3,:);
    end
end
OVM = [OVM TR_matmean TR_matmax];
timeElapsed = toc
```

```
%% ----------------- Optimisation of Bidirectional turbine configuration -----------------
tic
clear all
clc
close all

%% Data import
% Import File from RWS
filename = 'WL_DATA_NS_2016_2018.csv';
WL_NS = dataimport(filename);
t = linspace(0,length(WL_NS)-1,length(WL_NS));

% Truncation of the North Sea level vector to start at through.
WL_NS = datatrunc(WL_NS);
t = linspace(0,length(WL_NS)-1,length(WL_NS));

%% General hydraulic constants
rho = 1025;                     % Density of salt water [kg/m^3]
g = 9.81;                       % Gravitational acceleration [m/s^2]
nu = 10^-6;                     % Kinematic viscosity [m^2/s]
delta_t = 60*10;                % Time step in data from RWS [min]
epsilon = 0.3e-3;               % Roughness heigth concrete [m] (0.3-3 mm range)
K_C = 0.5;                      % Loss coefficient of entrance [-]
K_E = 1.0;                      % Loss coefficient of exit [-]
K_pfn = 0.0;                    % Loss coefficient of turbine [-]

% Dimensional parameters
W = [4:1:9];                    % Width of the Culvert [m]
H = [4:1:9];                    % Height of the Culvert [m]
N = [5:1:39];                   % Number of Culverts [-]
W_wall = 1.0;                   % Width of wall [-]
A_c = W.*H;                     % Cross-sectional area of culvert [m^2]
A_LG = 110e6;                   % Surface area of Lake Grevelingen [m^2]
L = 49;                         % Length of culvert [m]
O = 2*(W+H);                    % Wetted perimeter of duct [m]
D_h = 4*A_c./O;                 % Hydraulic diameter [m]

WL_max = 0.05;                  % Max water level [m]
WL_min = -0.45;                 % Min water level [m]

%% Establishing Overview matrix
% determining values OVM Columns 1,2 and 3
OVM = zeros(length(N)*length(W),12);
OVM(:,1) = repmat(W',length(N),1);
VV = repmat(N(1):1:N(end),length(W),1);
OVM(:,2) = VV(:)';
OVM(:,3) = OVM(:,1).*OVM(:,2)+(OVM(:,2)+1)*W_wall;
WLLG_MAT = zeros(length(WL_NS),length(N)*length(W));

TR_matmean = zeros(length(W)*length(N), 36);
TR_matmax = zeros(length(W)*length(N), 36);

%Determine Lake Grevelingen WL
for xx = 1:length(N)
    for ii = 1:length(W)
% Initialisation
        M = 5;
        if M > N(xx)
            M = N(xx);
        end

        delta_h = zeros(length(WL_NS),1);
        WL_LG = zeros(length(WL_NS),1);

        Q_t = ones(length(WL_NS),1);
        C_sys_t = ones(length(WL_NS),6);
        f_t = 2/3*ones(length(WL_NS),1);
        U_t = zeros(length(WL_NS),1);
        Re_t = zeros(length(WL_NS),1);
        f_f_t = zeros(length(WL_NS),1);

        Q_e = ones(length(WL_NS),1);
        C_sys_e = ones(length(WL_NS),6);
        f_e = zeros(length(WL_NS),1);
        U_e = zeros(length(WL_NS),1);
        Re_e = zeros(length(WL_NS),1);
        f_f_e = zeros(length(WL_NS),1);

        WL_LG(1) = -0.2;
        WL_LG_bound_plus = -0.20;
        WL_LG_bound_min = -0.20;

        t_b = zeros(length(WL_NS),1);
        m = zeros(length(WL_NS),1);
        b = zeros(length(WL_NS),1);

% Execution
        delta_h(1) = head(WL_NS(1),WL_LG(1));
```

```
        for i = 1:5
            f_t(1) = inlet_outlet_f78(delta_h(1));
            Q_t(1) = discharge(W(ii),H(ii),delta_h(1),C_sys_t(1,i),f_t(1));
            U_t(1) = Q_t(1)/A_c(ii);
            Re_t(1) = abs(U_t(1))*D_h(ii)/nu;
            f_f_t(1) = 0.25./(log10(epsilon./(3.7.*D_h(ii))+(5.74./(Re_t(1).^0.9))).^2);
            C_sys_t(1,i+1) = syslosscoef(K_C,K_E,K_pfn,W(ii),H(ii),L,Re_t(1),epsilon);
            Q_e(1) = discharge(W(ii),H(ii),delta_h(1),C_sys_e(1,i),f_e(1));
            U_e(1) = Q_e(1)/A_c(ii);
            Re_e(1) = abs(U_e(1))*D_h(ii)/nu;
            f_f_e(1) = 0.25./(log10(epsilon./(3.7.*D_h(ii))+(5.74./(Re_e(1).^0.9))).^2);
            C_sys_e(1,i+1) = syslosscoef(K_C,K_E,K_pfn,W(ii),H(ii),L,Re_e(1),epsilon);
        end
        for n = 2:length(WL_NS)
            WL_LG(n) = waterlevel78(WL_LG(n-1),N(xx),M,Q_t(n-1),Q_e(n-1),A_LG,delta_t);
            delta_h(n) = head(WL_NS(n),WL_LG(n));
                for i = 1:5
                    f_t(n) = inlet_outlet_f78(delta_h(n));
                    Q_t(n) = discharge(W(ii),H(ii),delta_h(n),C_sys_t(n,i),f_t(n));
                    U_t(n) = Q_t(n)/A_c(ii);
                    Re_t(n) = abs(U_t(n))*D_h(ii)/nu;
                    f_f_t(n) = 0.25./(log10(epsilon./(3.7.*D_h(ii))+(5.74./(Re_t(n).^0.9))).^2);
                    C_sys_t(n,i+1) = syslosscoef(K_C,K_E,K_pfn,W(ii),H(ii),L,Re_t(n),epsilon);
                    C_sys_t(n,1) = C_sys_t(n-1,6);
                    Q_e(n) = discharge(W(ii),H(ii),delta_h(n),C_sys_e(n,i),f_e(n));
                    U_e(n) = Q_e(n)/A_c(ii);
                    Re_e(n) = abs(U_e(n))*D_h(ii)/nu;
                    f_f_e(n) = 0.25./(log10(epsilon./(3.7.*D_h(ii))+(5.74./(Re_e(n).^0.9))).^2);
                    C_sys_e(n,i+1) = syslosscoef(K_C,K_E,K_pfn,W(ii),H(ii),L,Re_e(n),epsilon);
                    C_sys_e(n,1) = C_sys_e(n-1,6);
                end
                if WL_LG(n) > WL_LG_bound_plus && delta_h(n) > 0
                    t_b(n) = timetoupbound78(WL_max, WL_LG(n-1), N(xx), Q_t(n-1), M, Q_e(n-1));
                    m(n) = slope(f_t(n-1), t_b(n));
                    b(n) = vertint(m(n), t(n-1), t_b(n),delta_t);
                    f_t(n) = DOR(m(n), t(n-1), b(n),delta_t);
                    if f_t(n) >= 1
                        f_t(n) = 0.999999;
                    end
                elseif delta_h(n) < 0
                    f_t(n) = 0;
                else
                    f_t(n) = inlet_outlet_f78(delta_h(n));
                end
            Q_t(n) = discharge(W(ii),H(ii),delta_h(n),C_sys_t(n,i),f_t(n));
            WL_LG(n) = waterlevel78(WL_LG(n-1),N(xx),M,Q_t(n-1),Q_e(n-1),A_LG,delta_t);
        end
% Determining values for OVM Column 4 to 75
        RR = ii + length(W)*(xx-1);

% Percentage of overshoot and undershoot
        OS = overshoot(WL_LG);
        US = undershoot(WL_LG);
        OVM(RR,4) = OS(2,1);
        OVM(RR,5) = OS(2,2);
        OVM(RR,6) = OS(2,3);
        OVM(RR,7) = US(2,1);
        OVM(RR,8) = US(2,2);
        OVM(RR,9) = US(2,3);

% Power generation
        P = powergen(f_t,N(xx)-M,delta_h,Q_t);
        P_mean = mean(P);
        P_max = max(P);

% Energy yield
        E = energy(P,delta_t);  % Total energy yield in 3 years
        E_mean = E/3;           % Mean annual energy yield per year

        OVM(RR,10) = P_mean;    % Mean power
        OVM(RR,11) = P_max;     % Max power
        OVM(RR,12) = E_mean;    % Mean annual energy yield

% Mean and maximum tidal range
        TR = tidalrange(WL_LG);
        TR_matmean(RR,:) = TR(2,:);
        TR_matmax(RR,:) = TR(3,:);
    end
end
OVM = [OVM TR_matmean TR_matmax];
timeElapsed = toc
```

```
function WL_NS = datatrunc(WL_NS)
h_NS_trghs = -findpeaks(-WL_NS);
k = find(WL_NS == h_NS_trghs(1));
WL_NS = WL_NS(k(1):end);
end
```

```
function WL_NS = dataimport(filename)
h_NS_DATA = 0.01*flipud(csvread(filename)); % [m]
QQ = h_NS_DATA(1);
WL_NS = [QQ; h_NS_DATA];
end
```

```
function delta_h = head(WL_NS,WL_LG)
delta_h = WL_NS-WL_LG;
end
```

```
function f = inlet_outlet_f(delta_h)
if delta_h < 0
    f = 0;
else
    f = 2/3;
end
```

```
function Q = discharge(W,H,delta_h,C_sys,f)
A = W*H;
g = 9.81;
if delta_h < 0
    Q = -A*sqrt(2*g*abs(delta_h).*(1-f)./C_sys);
else
    Q = A*sqrt(2*g*delta_h.*(1-f)./C_sys);
end
```

```
function C_sys = syslosscoef(K_C,K_E,K_pfn,W,H,L,Re,epsilon)
A = W.*H;
O = 2*(W+H);
D_h = 4*A./O;

f_f = 0.25./(log10(epsilon./(3.7.*D_h)+(5.74./(Re.^0.9))).^2);
C_sys = 1 + f_f.*L/D_h + K_C + K_E + K_pfn;
end
```

```
function WL_LG = waterlevel(WL_LG,N,Q,A_LG,delta_t)
    WL_LG = WL_LG+N.*Q.*delta_t/A_LG;
end
```

```
function t_b = timetoupbound(WL_max, WL_LG, N, Q)
A_LG = 110e6;
t_b = (WL_max-WL_LG).*A_LG/(N*Q);
end
```

```
function t_b = timetolobound(WL_min, WL_LG, N, Q)
A_LG = 110e6;
t_b = ((WL_min-WL_LG).*A_LG/(N*Q));
end
```

```
function m = slope(f, t_b)
m = (1-f)./t_b;
end
```

```
function b = vertint(m, t, t_b, delta_t)
b = 1-m.*(t*delta_t+t_b);
end
```

```
function f = DOR(m, t, b, delta_t)
    f = m.*(t*delta_t+delta_t)+b;
end
```

```
function tr = trendline(timevector,WL_LG_vector)
omega_an = 2*pi()/(6*24*365);
A_mat = ones(length(WL_LG_vector),1);
B = sin(omega_an*timevector);
C = cos(omega_an*timevector);
mat = [A_mat, B', C'];
x_1 = mat\WL_LG_vector;
tr = x_1(1)+ x_1(2)*sin(omega_an*timevector) + x_1(3)*cos(omega_an*timevector);
end
```

```
function TR = tidalrange(WL_LG)
%% Initialisation
TR = zeros(3,36);
TR(1,:) = [0116 0216 0316 0416 0516 0616 0716 0816 0916 1016 1116 1216 0117 0217 0317 0417 0517 0617 0717
0817 0917 1017 1117 1217 0118 0218 0318 0418 0518 0618 0718 0818 0918 1018 1118 1218];
%% Datapoint division in months
jan16 = WL_LG(1:4390);
feb16 = WL_LG(4391:8566);
mar16 = WL_LG(8567:13030);
apr16 = WL_LG(13031:17350);
may16 = WL_LG(17351:21814);
jun16 = WL_LG(21815:26134);
jul16 = WL_LG(26135:30598);
aug16 = WL_LG(30599:35062);
sep16 = WL_LG(35063:39382);
oct16 = WL_LG(39383:43846);
nov16 = WL_LG(43847:48166);
dec16 = WL_LG(48167:52630);

jan17 = WL_LG(52631:57094);
feb17 = WL_LG(57095:61126);
mar17 = WL_LG(61127:65590);
apr17 = WL_LG(65591:69910);
may17 = WL_LG(69911:74374);
jun17 = WL_LG(74375:78694);
jul17 = WL_LG(78695:83158);
aug17 = WL_LG(83159:87622);
sep17 = WL_LG(87623:91942);
oct17 = WL_LG(91943:96406);
nov17 = WL_LG(96407:100726);
dec17 = WL_LG(100727:105190);

jan18 = WL_LG(105191:109654);
feb18 = WL_LG(109655:113686);
mar18 = WL_LG(113687:118150);
apr18 = WL_LG(118151:122470);
may18 = WL_LG(122471:126934);
jun18 = WL_LG(126935:131254);
jul18 = WL_LG(131255:135718);
aug18 = WL_LG(135719:140182);
sep18 = WL_LG(140183:144502);
oct18 = WL_LG(144503:148967);
nov18 = WL_LG(148967:153286);
dec18 = WL_LG(153287:157750);
%% Monthly average and monthly max tidal range - JAN 16
T_jan16 = findpeaks(jan16); D_jan16 = -findpeaks(-jan16);
if length(T_jan16)>length(D_jan16)
    T_jan16 = T_jan16(1:length(D_jan16));
elseif length(D_jan16)>length(T_jan16)
    D_jan16 = D_jan16(1:length(T_jan16));
else
    T_jan16 = T_jan16;
    D_jan16 = D_jan16;
end
TR_jan16 = zeros(length(T_jan16),1);
for ii = 1:length(T_jan16)
    TR_jan16(ii) = abs(T_jan16(ii))+abs(D_jan16(ii));
end
TR(2,1) = mean(TR_jan16); TR(3,1) = max(TR_jan16);
%% Monthly average and monthly max tidal range - FEB 16
T_feb16 = findpeaks(feb16); D_feb16 = -findpeaks(-feb16);
if length(T_feb16)>length(D_feb16)
    T_feb16 = T_feb16(1:length(D_feb16));
elseif length(D_feb16)>length(T_feb16)
    D_feb16 = D_feb16(1:length(T_feb16));
else
    T_feb16 = T_feb16;
```

```
    D_feb16 = D_feb16;
end
TR_feb16 = zeros(length(T_feb16),1);
for ii = 1:length(T_feb16)
    TR_feb16(ii) = abs(T_feb16(ii))+abs(D_feb16(ii));
end
TR(2,2) = mean(TR_feb16); TR(3,2) = max(TR_feb16);
%% Monthly average and monthly max tidal range - MAR 16
T_mar16 = findpeaks(mar16); D_mar16 = -findpeaks(-mar16);
if length(T_mar16)>length(D_mar16)
    T_mar16 = T_mar16(1:length(D_mar16));
elseif length(D_mar16)>length(T_mar16)
    D_mar16 = D_mar16(1:length(T_mar16));
else
    T_mar16 = T_mar16;
    D_mar16 = D_mar16;
end
TR_mar16 = zeros(length(T_mar16),1);
for ii = 1:length(T_mar16)
    TR_mar16(ii) = abs(T_mar16(ii))+abs(D_mar16(ii));
end
TR(2,3) = mean(TR_mar16); TR(3,3) = max(TR_mar16);
%% Monthly average and monthly max tidal range - APR 16
T_apr16 = findpeaks(apr16); D_apr16 = -findpeaks(-apr16);
if length(T_apr16)>length(D_apr16)
    T_apr16 = T_apr16(1:length(D_apr16));
elseif length(D_apr16)>length(T_apr16)
    D_apr16 = D_apr16(1:length(T_apr16));
else
    T_apr16 = T_apr16;
    D_apr16 = D_apr16;
end
TR_apr16 = zeros(length(T_apr16),1);
for ii = 1:length(T_apr16)
    TR_apr16(ii) = abs(T_apr16(ii))+abs(D_apr16(ii));
end
TR(2,4) = mean(TR_apr16); TR(3,4) = max(TR_apr16);
%% Monthly average and monthly max tidal range - MAY 16
T_may16 = findpeaks(may16); D_may16 = -findpeaks(-may16);
if length(T_may16)>length(D_may16)
    T_may16 = T_may16(1:length(D_may16));
elseif length(D_may16)>length(T_may16)
    D_may16 = D_may16(1:length(T_may16));
else
    T_may16 = T_may16;
    D_may16 = D_may16;
end
TR_may16 = zeros(length(T_may16),1);
for ii = 1:length(T_may16)
    TR_may16(ii) = abs(T_may16(ii))+abs(D_may16(ii));
end
TR(2,5) = mean(TR_may16); TR(3,5) = max(TR_may16);
%% Monthly average and monthly max tidal range - JUN 16
T_jun16 = findpeaks(jun16); D_jun16 = -findpeaks(-jun16);
if length(T_jun16)>length(D_jun16)
    T_jun16 = T_jun16(1:length(D_jun16));
elseif length(D_jun16)>length(T_jun16)
    D_jun16 = D_jun16(1:length(T_jun16));
else
    T_jun16 = T_jun16;
    D_jun16 = D_jun16;
end
TR_jun16 = zeros(length(T_jun16),1);
for ii = 1:length(T_jun16)
    TR_jun16(ii) = abs(T_jun16(ii))+abs(D_jun16(ii));
end
TR(2,6) = mean(TR_jun16); TR(3,6) = max(TR_jun16);
%% Monthly average and monthly max tidal range - JUL 16
T_jul16 = findpeaks(jul16); D_jul16 = -findpeaks(-jul16);
if length(T_jul16)>length(D_jul16)
    T_jul16 = T_jul16(1:length(D_jul16));
elseif length(D_jul16)>length(T_jul16)
    D_jul16 = D_jul16(1:length(T_jul16));
else
    T_jul16 = T_jul16;
    D_jul16 = D_jul16;
end
TR_jul16 = zeros(length(T_jul16),1);
for ii = 1:length(T_jul16)
    TR_jul16(ii) = abs(T_jul16(ii))+abs(D_jul16(ii));
end
TR(2,7) = mean(TR_jul16); TR(3,7) = max(TR_jul16);
%% Monthly average and monthly max tidal range - AUG 16
T_aug16 = findpeaks(aug16); D_aug16 = -findpeaks(-aug16);
if length(T_aug16)>length(D_aug16)
    T_aug16 = T_aug16(1:length(D_aug16));
elseif length(D_aug16)>length(T_aug16)
    D_aug16 = D_aug16(1:length(T_aug16));
```

```
else
    T_aug16 = T_aug16;
    D_aug16 = D_aug16;
end
TR_aug16 = zeros(length(T_aug16),1);
for ii = 1:length(T_aug16)
    TR_aug16(ii) = abs(T_aug16(ii))+abs(D_aug16(ii));
end
TR(2,8) = mean(TR_aug16); TR(3,8) = max(TR_aug16);
%% Monthly average and monthly max tidal range - SEP 16
T_sep16 = findpeaks(sep16); D_sep16 = -findpeaks(-sep16);
if length(T_sep16)>length(D_sep16)
    T_sep16 = T_sep16(1:length(D_sep16));
elseif length(D_sep16)>length(T_sep16)
    D_sep16 = D_sep16(1:length(T_sep16));
else
    T_sep16 = T_sep16;
    D_sep16 = D_sep16;
end
TR_sep16 = zeros(length(T_sep16),1);
for ii = 1:length(T_sep16)
    TR_sep16(ii) = abs(T_sep16(ii))+abs(D_sep16(ii));
end
TR(2,9) = mean(TR_sep16); TR(3,9) = max(TR_sep16);
%% Monthly average and monthly max tidal range - OCT 16
T_oct16 = findpeaks(oct16); D_oct16 = -findpeaks(-oct16);
if length(T_oct16)>length(D_oct16)
    T_oct16 = T_oct16(1:length(D_oct16));
elseif length(D_oct16)>length(T_oct16)
    D_oct16 = D_oct16(1:length(T_oct16));
else
    T_oct16 = T_oct16;
    D_oct16 = D_oct16;
end
TR_oct16 = zeros(length(T_oct16),1);
for ii = 1:length(T_oct16)
    TR_oct16(ii) = abs(T_oct16(ii))+abs(D_oct16(ii));
end
TR(2,10) = mean(TR_oct16); TR(3,10) = max(TR_oct16);
%% Monthly average and monthly max tidal range - NOV 16
T_nov16 = findpeaks(nov16); D_nov16 = -findpeaks(-nov16);
if length(T_nov16)>length(D_nov16)
    T_nov16 = T_nov16(1:length(D_nov16));
elseif length(D_nov16)>length(T_nov16)
    D_nov16 = D_nov16(1:length(T_nov16));
else
    T_nov16 = T_nov16;
    D_nov16 = D_nov16;
end
TR_nov16 = zeros(length(T_nov16),1);
for ii = 1:length(T_nov16)
    TR_nov16(ii) = abs(T_nov16(ii))+abs(D_nov16(ii));
end
TR(2,11) = mean(TR_nov16); TR(3,11) = max(TR_nov16);
%% Monthly average and monthly max tidal range - DEC 16
T_dec16 = findpeaks(dec16); D_dec16 = -findpeaks(-dec16);
if length(T_dec16)>length(D_dec16)
    T_dec16 = T_dec16(1:length(D_dec16));
elseif length(D_dec16)>length(T_dec16)
    D_dec16 = D_dec16(1:length(T_dec16));
else
    T_dec16 = T_dec16;
    D_dec16 = D_dec16;
end
TR_dec16 = zeros(length(T_dec16),1);
for ii = 1:length(T_dec16)
    TR_dec16(ii) = abs(T_dec16(ii))+abs(D_dec16(ii));
end
TR(2,12) = mean(TR_dec16); TR(3,12) = max(TR_dec16);
%% Monthly average and monthly max tidal range - JAN 17
T_jan17 = findpeaks(jan17); D_jan17 = -findpeaks(-jan17);
if length(T_jan17)>length(D_jan17)
    T_jan17 = T_jan17(1:length(D_jan17));
elseif length(D_jan17)>length(T_jan17)
    D_jan17 = D_jan17(1:length(T_jan17));
else
    T_jan17 = T_jan17;
    D_jan17 = D_jan17;
end
TR_jan17 = zeros(length(T_jan17),1);
for ii = 1:length(T_jan17)
    TR_jan17(ii) = abs(T_jan17(ii))+abs(D_jan17(ii));
end
TR(2,13) = mean(TR_jan17); TR(3,13) = max(TR_jan17);
%% Monthly average and monthly max tidal range - FEB 17
T_feb17 = findpeaks(feb17); D_feb17 = -findpeaks(-feb17);
if length(T_feb17)>length(D_feb17)
    T_feb17 = T_feb17(1:length(D_feb17));
```

```
elseif length(D_feb17)>length(T_feb17)
    D_feb17 = D_feb17(1:length(T_feb17));
else
    T_feb17 = T_feb17;
    D_feb17 = D_feb17;
end
TR_feb17 = zeros(length(T_feb17),1);
for ii = 1:length(T_feb17)
    TR_feb17(ii) = abs(T_feb17(ii))+abs(D_feb17(ii));
end
TR(2,14) = mean(TR_feb17); TR(3,14) = max(TR_feb17);
%% Monthly average and monthly max tidal range - MAR 17
T_mar17 = findpeaks(mar17); D_mar17 = -findpeaks(-mar17);
if length(T_mar17)>length(D_mar17)
    T_mar17 = T_mar17(1:length(D_mar17));
elseif length(D_mar17)>length(T_mar17)
    D_mar17 = D_mar17(1:length(T_mar17));
else
    T_mar17 = T_mar17;
    D_mar17 = D_mar17;
end
TR_mar17 = zeros(length(T_mar17),1);
for ii = 1:length(T_mar17)
    TR_mar17(ii) = abs(T_mar17(ii))+abs(D_mar17(ii));
end
TR(2,15) = mean(TR_mar17); TR(3,15) = max(TR_mar17);
%% Monthly average and monthly max tidal range - APR 17
T_apr17 = findpeaks(apr17); D_apr17 = -findpeaks(-apr17);
if length(T_apr17)>length(D_apr17)
    T_apr17 = T_apr17(1:length(D_apr17));
elseif length(D_apr17)>length(T_apr17)
    D_apr17 = D_apr17(1:length(T_apr17));
else
    T_apr17 = T_apr17;
    D_apr17 = D_apr17;
end
TR_apr17 = zeros(length(T_apr17),1);
for ii = 1:length(T_apr17)
    TR_apr17(ii) = abs(T_apr17(ii))+abs(D_apr17(ii));
end
TR(2,16) = mean(TR_apr17); TR(3,16) = max(TR_apr17);
%% Monthly average and monthly max tidal range - MAY 17
T_may17 = findpeaks(may17); D_may17 = -findpeaks(-may17);
if length(T_may17)>length(D_may17)
    T_may17 = T_may17(1:length(D_may17));
elseif length(D_may17)>length(T_may17)
    D_may17 = D_may17(1:length(T_may17));
else
    T_may17 = T_may17;
    D_may17 = D_may17;
end
TR_may17 = zeros(length(T_may17),1);
for ii = 1:length(T_may17)
    TR_may17(ii) = abs(T_may17(ii))+abs(D_may17(ii));
end
TR(2,17) = mean(TR_may17); TR(3,17) = max(TR_may17);
%% Monthly average and monthly max tidal range - JUN 17
T_jun17 = findpeaks(jun17); D_jun17 = -findpeaks(-jun17);
if length(T_jun17)>length(D_jun17)
    T_jun17 = T_jun17(1:length(D_jun17));
elseif length(D_jun17)>length(T_jun17)
    D_jun17 = D_jun17(1:length(T_jun17));
else
    T_jun17 = T_jun17;
    D_jun17 = D_jun17;
end
TR_jun17 = zeros(length(T_jun17),1);
for ii = 1:length(T_jun17)
    TR_jun17(ii) = abs(T_jun17(ii))+abs(D_jun17(ii));
end
TR(2,18) = mean(TR_jun17); TR(3,18) = max(TR_jun17);
%% Monthly average and monthly max tidal range - JUL 17
T_jul17 = findpeaks(jul17); D_jul17 = -findpeaks(-jul17);
if length(T_jul17)>length(D_jul17)
    T_jul17 = T_jul17(1:length(D_jul17));
elseif length(D_jul17)>length(T_jul17)
    D_jul17 = D_jul17(1:length(T_jul17));
else
    T_jul17 = T_jul17;
    D_jul17 = D_jul17;
end
TR_jul17 = zeros(length(T_jul17),1);
for ii = 1:length(T_jul17)
    TR_jul17(ii) = abs(T_jul17(ii))+abs(D_jul17(ii));
end
TR(2,19) = mean(TR_jul17); TR(3,19) = max(TR_jul17);
%% Monthly average and monthly max tidal range - AUG 17
T_aug17 = findpeaks(aug17); D_aug17 = -findpeaks(-aug17);
```

```
if length(T_aug17)>length(D_aug17)
    T_aug17 = T_aug17(1:length(D_aug17));
elseif length(D_aug17)>length(T_aug17)
    D_aug17 = D_aug17(1:length(T_aug17));
else
    T_aug17 = T_aug17;
    D_aug17 = D_aug17;
end
TR_aug17 = zeros(length(T_aug17),1);
for ii = 1:length(T_aug17)
    TR_aug17(ii) = abs(T_aug17(ii))+abs(D_aug17(ii));
end
TR(2,20) = mean(TR_aug17); TR(3,20) = max(TR_aug17);
%% Monthly average and monthly max tidal range - SEP 17
T_sep17 = findpeaks(sep17); D_sep17 = -findpeaks(-sep17);
if length(T_sep17)>length(D_sep17)
    T_sep17 = T_sep17(1:length(D_sep17));
elseif length(D_sep17)>length(T_sep17)
    D_sep17 = D_sep17(1:length(T_sep17));
else
    T_sep17 = T_sep17;
    D_sep17 = D_sep17;
end
TR_sep17 = zeros(length(T_sep17),1);
for ii = 1:length(T_sep17)
    TR_sep17(ii) = abs(T_sep17(ii))+abs(D_sep17(ii));
end
TR(2,21) = mean(TR_sep17); TR(3,21) = max(TR_sep17);
%% Monthly average and monthly max tidal range - OCT 17
T_oct17 = findpeaks(oct17); D_oct17 = -findpeaks(-oct17);
if length(T_oct17)>length(D_oct17)
    T_oct17 = T_oct17(1:length(D_oct17));
elseif length(D_oct17)>length(T_oct17)
    D_oct17 = D_oct17(1:length(T_oct17));
else
    T_oct17 = T_oct17;
    D_oct17 = D_oct17;
end
TR_oct17 = zeros(length(T_oct17),1);
for ii = 1:length(T_oct17)
    TR_oct17(ii) = abs(T_oct17(ii))+abs(D_oct17(ii));
end
TR(2,22) = mean(TR_oct17); TR(3,22) = max(TR_oct17);
%% Monthly average and monthly max tidal range - NOV 17
T_nov17 = findpeaks(nov17); D_nov17 = -findpeaks(-nov17);
if length(T_nov17)>length(D_nov17)
    T_nov17 = T_nov17(1:length(D_nov17));
elseif length(D_nov17)>length(T_nov17)
    D_nov17 = D_nov17(1:length(T_nov17));
else
    T_nov17 = T_nov17;
    D_nov17 = D_nov17;
end
TR_nov17 = zeros(length(T_nov17),1);
for ii = 1:length(T_nov17)
    TR_nov17(ii) = abs(T_nov17(ii))+abs(D_nov17(ii));
end
TR(2,23) = mean(TR_nov17); TR(3,23) = max(TR_nov17);
%% Monthly average and monthly max tidal range - DEC 17
T_dec17 = findpeaks(dec17); D_dec17 = -findpeaks(-dec17);
if length(T_dec17)>length(D_dec17)
    T_dec17 = T_dec17(1:length(D_dec17));
elseif length(D_dec17)>length(T_dec17)
    D_dec17 = D_dec17(1:length(T_dec17));
else
    T_dec17 = T_dec17;
    D_dec17 = D_dec17;
end
TR_dec17 = zeros(length(T_dec17),1);
for ii = 1:length(T_dec17)
    TR_dec17(ii) = abs(T_dec17(ii))+abs(D_dec17(ii));
end
TR(2,24) = mean(TR_dec17); TR(3,24) = max(TR_dec17);
%% Monthly average and monthly max tidal range - JAN 18
T_jan18 = findpeaks(jan18); D_jan18 = -findpeaks(-jan18);
if length(T_jan18)>length(D_jan18)
    T_jan18 = T_jan18(1:length(D_jan18));
elseif length(D_jan18)>length(T_jan18)
    D_jan18 = D_jan18(1:length(T_jan18));
else
    T_jan18 = T_jan18;
    D_jan18 = D_jan18;
end
TR_jan18 = zeros(length(T_jan18),1);
for ii = 1:length(T_jan18)
    TR_jan18(ii) = abs(T_jan18(ii))+abs(D_jan18(ii));
end
TR(2,25) = mean(TR_jan18); TR(3,25) = max(TR_jan18);
```

```
%% Monthly average and monthly max tidal range - FEB 18
T_feb18 = findpeaks(feb18); D_feb18 = -findpeaks(-feb18);
if length(T_feb18)>length(D_feb18)
    T_feb18 = T_feb18(1:length(D_feb18));
elseif length(D_feb18)>length(T_feb18)
    D_feb18 = D_feb18(1:length(T_feb18));
else
    T_feb18 = T_feb18;
    D_feb18 = D_feb18;
end
TR_feb18 = zeros(length(T_feb18),1);
for ii = 1:length(T_feb18)
    TR_feb18(ii) = abs(T_feb18(ii))+abs(D_feb18(ii));
end
TR(2,26) = mean(TR_feb18); TR(3,26) = max(TR_feb18);
%% Monthly average and monthly max tidal range - MAR 18
T_mar18 = findpeaks(mar18); D_mar18 = -findpeaks(-mar18);
if length(T_mar18)>length(D_mar18)
    T_mar18 = T_mar18(1:length(D_mar18));
elseif length(D_mar18)>length(T_mar18)
    D_mar18 = D_mar18(1:length(T_mar18));
else
    T_mar18 = T_mar18;
    D_mar18 = D_mar18;
end
TR_mar18 = zeros(length(T_mar18),1);
for ii = 1:length(T_mar18)
    TR_mar18(ii) = abs(T_mar18(ii))+abs(D_mar18(ii));
end
TR(2,27) = mean(TR_mar18); TR(3,27) = max(TR_mar18);
%% Monthly average and monthly max tidal range - APR 18
T_apr18 = findpeaks(apr18); D_apr18 = -findpeaks(-apr18);
if length(T_apr18)>length(D_apr18)
    T_apr18 = T_apr18(1:length(D_apr18));
elseif length(D_apr18)>length(T_apr18)
    D_apr18 = D_apr18(1:length(T_apr18));
else
    T_apr18 = T_apr18;
    D_apr18 = D_apr18;
end
TR_apr18 = zeros(length(T_apr18),1);
for ii = 1:length(T_apr18)
    TR_apr18(ii) = abs(T_apr18(ii))+abs(D_apr18(ii));
end
TR(2,28) = mean(TR_apr18); TR(3,28) = max(TR_apr18);
%% Monthly average and monthly max tidal range - MAY 18
T_may18 = findpeaks(may18); D_may18 = -findpeaks(-may18);
if length(T_may18)>length(D_may18)
    T_may18 = T_may18(1:length(D_may18));
elseif length(D_may18)>length(T_may18)
    D_may18 = D_may18(1:length(T_may18));
else
    T_may18 = T_may18;
    D_may18 = D_may18;
end
TR_may18 = zeros(length(T_may18),1);
for ii = 1:length(T_may18)
    TR_may18(ii) = abs(T_may18(ii))+abs(D_may18(ii));
end
TR(2,29) = mean(TR_may18); TR(3,29) = max(TR_may18);
%% Monthly average and monthly max tidal range - JUN 18
T_jun18 = findpeaks(jun18); D_jun18 = -findpeaks(-jun18);
if length(T_jun18)>length(D_jun18)
    T_jun18 = T_jun18(1:length(D_jun18));
elseif length(D_jun18)>length(T_jun18)
    D_jun18 = D_jun18(1:length(T_jun18));
else
    T_jun18 = T_jun18;
    D_jun18 = D_jun18;
end
TR_jun18 = zeros(length(T_jun18),1);
for ii = 1:length(T_jun18)
    TR_jun18(ii) = abs(T_jun18(ii))+abs(D_jun18(ii));
end
TR(2,30) = mean(TR_jun18); TR(3,30) = max(TR_jun18);
%% Monthly average and monthly max tidal range - JUL 18
T_jul18 = findpeaks(jul18); D_jul18 = -findpeaks(-jul18);
if length(T_jul18)>length(D_jul18)
    T_jul18 = T_jul18(1:length(D_jul18));
elseif length(D_jul18)>length(T_jul18)
    D_jul18 = D_jul18(1:length(T_jul18));
else
    T_jul18 = T_jul18;
    D_jul18 = D_jul18;
end
TR_jul18 = zeros(length(T_jul18),1);
for ii = 1:length(T_jul18)
    TR_jul18(ii) = abs(T_jul18(ii))+abs(D_jul18(ii));
```

```
end
TR(2,31) = mean(TR_jul18); TR(3,31) = max(TR_jul18);
%% Monthly average and monthly max tidal range - AUG 18
T_aug18 = findpeaks(aug18); D_aug18 = -findpeaks(-aug18);
if length(T_aug18)>length(D_aug18)
    T_aug18 = T_aug18(1:length(D_aug18));
elseif length(D_aug18)>length(T_aug18)
    D_aug18 = D_aug18(1:length(T_aug18));
else
    T_aug18 = T_aug18;
    D_aug18 = D_aug18;
end
TR_aug18 = zeros(length(T_aug18),1);
for ii = 1:length(T_aug18)
    TR_aug18(ii) = abs(T_aug18(ii))+abs(D_aug18(ii));
end
TR(2,32) = mean(TR_aug18); TR(3,32) = max(TR_aug18);
%% Monthly average and monthly max tidal range - SEP 18
T_sep18 = findpeaks(sep18); D_sep18 = -findpeaks(-sep18);
if length(T_sep18)>length(D_sep18)
    T_sep18 = T_sep18(1:length(D_sep18));
elseif length(D_sep18)>length(T_sep18)
    D_sep18 = D_sep18(1:length(T_sep18));
else
    T_sep18 = T_sep18;
    D_sep18 = D_sep18;
end
TR_sep18 = zeros(length(T_sep18),1);
for ii = 1:length(T_sep18)
    TR_sep18(ii) = abs(T_sep18(ii))+abs(D_sep18(ii));
end
TR(2,33) = mean(TR_sep18); TR(3,33) = max(TR_sep18);
%% Monthly average and monthly max tidal range - OCT 18
T_oct18 = findpeaks(oct18); D_oct18 = -findpeaks(-oct18);
if length(T_oct18)>length(D_oct18)
    T_oct18 = T_oct18(1:length(D_oct18));
elseif length(D_oct18)>length(T_oct18)
    D_oct18 = D_oct18(1:length(T_oct18));
else
    T_oct18 = T_oct18;
    D_oct18 = D_oct18;
end
TR_oct18 = zeros(length(T_oct18),1);
for ii = 1:length(T_oct18)
    TR_oct18(ii) = abs(T_oct18(ii))+abs(D_oct18(ii));
end
TR(2,34) = mean(TR_oct18); TR(3,34) = max(TR_oct18);
%% Monthly average and monthly max tidal range - NOV 18
T_nov18 = findpeaks(nov18); D_nov18 = -findpeaks(-nov18);
if length(T_nov18)>length(D_nov18)
    T_nov18 = T_nov18(1:length(D_nov18));
elseif length(D_nov18)>length(T_nov18)
    D_nov18 = D_nov18(1:length(T_nov18));
else
    T_nov18 = T_nov18;
    D_nov18 = D_nov18;
end
TR_nov18 = zeros(length(T_nov18),1);
for ii = 1:length(T_nov18)
    TR_nov18(ii) = abs(T_nov18(ii))+abs(D_nov18(ii));
end
TR(2,35) = mean(TR_nov18); TR(3,35) = max(TR_nov18);
%% Monthly average and monthly max tidal range - DEC 18
T_dec18 = findpeaks(dec18); D_dec18 = -findpeaks(-dec18);
if length(T_dec18)>length(D_dec18)
    T_dec18 = T_dec18(1:length(D_dec18));
elseif length(D_dec18)>length(T_dec18)
    D_dec18 = D_dec18(1:length(T_dec18));
else
    T_dec18 = T_dec18;
    D_dec18 = D_dec18;
end
TR_dec18 = zeros(length(T_dec18),1);
for ii = 1:length(T_dec18)
    TR_dec18(ii) = abs(T_dec18(ii))+abs(D_dec18(ii));
end
TR(2,36) = mean(TR_dec18); TR(3,36) = max(TR_dec18);
```

```
function OS = overshoot(WL_LG)
g16 = WL_LG(1:52630);
g17 = WL_LG(52631:105190);
g18 = WL_LG(105191:157750);

listplus = zeros(length(WL_LG),1);
OS = zeros(2,3);
```

```
OS(1,:) = [2016, 2017, 2018];
%% 2016
for n = 1:length(g16)
    if g16(n)>0.05
        listplus(n) = 1;
    else
        listplus(n) = 0;
    end
    OS(2,1) = sum(listplus==1)/length(g16)*100;
end
%% 2017
for m = 1:length(g17)
    if g17(m)>0.05
        listplus(m) = 1;
    else
        listplus(m) = 0;
    end
    OS(2,2) = sum(listplus==1)/length(g17)*100;
end
%% 2018
for s = 1:length(g18)
    if g18(s)>0.05
        listplus(s) = 1;
    else
        listplus(s) = 0;
    end
    OS(2,3) = sum(listplus==1)/length(g18)*100;
end
```

```
function US = undershoot(WL_LG)
g16 = WL_LG(1:52630);
g17 = WL_LG(52631:105190);
g18 = WL_LG(105191:157750);

listplus = zeros(length(WL_LG),1);
US = zeros(2,3);
US(1,:) = [2016, 2017, 2018];
%% 2016
for n = 1:length(g16)
    if g16(n)<-0.45
        listplus(n) = 1;
    else
        listplus(n) = 0;
    end
    US(2,1) = sum(listplus==1)/length(g16)*100;
end
%% 2017
for m = 1:length(g17)
    if g17(m)<-0.45
        listplus(m) = 1;
    else
        listplus(m) = 0;
    end
    US(2,2) = sum(listplus==1)/length(g17)*100;
end
%% 2018
for s = 1:length(g18)
    if g18(s)<-0.45
        listplus(s) = 1;
    else
        listplus(s) = 0;
    end
    US(2,3) = sum(listplus==1)/length(g18)*100;
end
```

```
function P = powergen(f,N,delta_h,Q)
g = 9.81; rho = 1025;
P = (rho*g/1000000)*N*f.*delta_h.*Q;%MW
end
```

```
function E = energy(P,delta_t)
E = trapz(P)/(3600*1000/delta_t);% GWh
end
```

```
function WL_LG = waterlevel78(WL_LG,N,M,Q_t,Q_e,A_LG,delta_t)
    WL_LG = WL_LG + ((N-M)*Q_t + M*Q_e).*delta_t/A_LG;
end
```

```
function f = inlet_outlet_f78(delta_h)
if delta_h < 0
    f = 0;
else
    f = 2/3;
end
```

```
function t_b = timetoupbound78(WL_max, WL_LG, N, Q_t, M, Q_e)
A_LG = 110e6;
t_b = (WL_max-WL_LG).*A_LG/((N-M)*Q_t+M*Q_e);
end
```

```
function t_b = timetolobound78(WL_min, WL_LG, N, Q_t, M, Q_e)
A_LG = 110e6;
t_b = ((WL_min-WL_LG).*A_LG/((N-M)*Q_t+M*Q_e));
end
```